

# **LED Light Control for use in Visible Light Communications**

A Degree Thesis

Submitted to the Faculty of the  
Escola Tècnica d'Enginyeria de Telecomunicació de  
Barcelona

Universitat Politècnica de Catalunya

by

**Carlos Labella**

In partial fulfilment  
of the requirements for the degree in  
**ELECTRONICS SYSTEM ENGINEERING**

**Advisor: Prof. Josep Paradells Aspas**

**Barcelona, May 2017**



## **Abstract**

This project describes the implementation of a custom LED driver based on the Texas Instruments TPS92641 integrated circuit. The main contribution of this project is to show how a generic driver for LED luminaires can obtain a data communication rate of up to 133 kbps when placed up to 3 meters away from the corresponding receiver. This document provides both an evaluation of the data converter, based on a MAX79356 modem designed for Power Line Communications, and the corresponding throughput evaluations when employing this chip for Visual Light Communication (VLC) purposes.

## **Resum**

L'objecte d'investigació d'aquest projecte és la implementació d'un controlador per lluminàries LED comercials basat en un circuit integrat TPS92641 de Texas Instruments. La principal contribució d'aquest estudi rau en demostrar que, fent ús d'un controlador genèric per lluminàries LED, és possible obtenir una comunicació de dades de fins a 133 kbps a una distància de 3 metres. L'estudi se centra en avaluar el comportament del convertidor i la realització de demostracions de rendiment. Entre d'altres, s'avalua l'ús del component MAX79356, un mòdem per a Power Line Communications, i es demostra com es pot emprar satisfactòriament per a comunicacions per llum visible (VLC).

## **Resumen**

El objeto de investigación de este proyecto es la implementación de un controlador basado en un circuito integrado TPS92641 de Texas Instruments para luminarias LED comerciales. La principal contribución de este proyecto es demostrar que, haciendo uso de un controlador genérico para luminarias LED, es posible obtener una tasa de transferencia de 133 kbps a una distancia de 3 metros. El estudio se centra en evaluar el comportamiento del convertidor y en la realización de demostraciones de rendimiento. Entre otros, se evalúa el uso del componente MAX79356, un modem para Power Line Communications (PLC) y se demuestra su uso satisfactorio en el campo de las comunicaciones por luz visible (VLC).

*I am grateful to, my father, Luis Manuel, for being a reference for me along my life, both in personal and professional fields, my mother, Maria, for making easier everyday task and encourage my academic career, my brothers, Daniel and Juan Luis, for their unconditional support and help in different stages of the project.*

*Especially, I thank my girlfriend, Gisela, for being able to show me the good side of things.*

*This project is so mine as your.*

*Agradezco, a mi padre, Luis Manuel, por haber sido una referencia para mí a lo largo de mi vida, tanto en el ámbito personal como profesional, a mi madre, María, por facilitarme tareas del día a día y la dedicación a los estudios, a mis hermanos, Daniel y Juan Luis, por su apoyo incondicional y su ayuda en varias etapas del proyecto.*

*De manera especial, agradezco a mi pareja, Gisela, por ser capaz de mostrarme el lado bueno de las cosas.*

*Este proyecto es tan mío como vuestro.*

## **Acknowledgements**

I thank my Thesis' advisor, Dr. Josep Paradells, his invaluable help along this project. Also, I thank Dr. Joaquim Oller, for his help in different stages of the development.



## Revision history and approval record

Revision	Date	Purpose
0	14/04/2017	Document creation
1	17/04/2017	Document revision
2	23/04/2017	Document revision
3	25/04/2017	Document revision
4	29/04/2017	Document revision
5	1/05/2017	Document revision
6	3/05/2017	Document revision
7	8/05/2017	Document revision
8	11/05/2017	Document revision
9	14/05/2017	Document revision

### DOCUMENT DISTRIBUTION LIST

Name	e-mail
Carlos Labella	Carlos.labella@alu-etsetb.upc.edu
Josep Paradells	josep.paradells@entel.upc.edu

Written by:		Reviewed and approved by:	
Date	14/04/2017	Date	15/05/2017
Name	Carlos Labella	Name	Josep Paradells
Position	Project Author	Position	Project Supervisor



## **Table of contents**

Abstract .....	2
Resum.....	3
Resumen .....	4
Acknowledgements .....	6
Revision history and approval record.....	8
Table of contents .....	10
List of Figures.....	12
List of Tables .....	16
1. Introduction.....	1
1.1. Statement of purpose .....	1
1.2. Requirements and specification.....	2
1.3. Methods and procedures .....	3
1.4. Work plan .....	3
1.5. Deviations from initial plan.....	4
2. State of the Art .....	6
2.1. White LED vs RGB LED .....	7
2.2. Buck converter control topologies.....	9
2.2.1. Voltage mode control.....	9
2.2.2. Current mode control.....	10
2.2.3. Hysteresis (ripple) control.....	10
3. Project development:.....	12
3.1. Buck converter for LED driver selection.....	12
3.2. TPS92641 specification .....	14
3.3. TPS92641EVM mods .....	14
3.4. Hands-on experience with TPS92641EVM.....	17
3.4.1. Bandwidth measurement.....	18
3.4.2. Commercial lamps compatibility test.....	24
4. Applications .....	26
4.1. Baseband Audio over VLC .....	26
4.1.1. LED driver control input adaption for baseband audio signal. ....	26
4.1.2. Baseband Audio over VLC receiver.....	29
4.1.3. Conclusions of implemented application.....	33
4.2. FM Audio over VLC .....	33

4.2.1.	Frequency modulation implementation .....	34
4.2.2.	Frequency demodulation implementation .....	37
4.2.2.1.	VLC receiver .....	37
4.2.3.	CD4046B configuration for FM demodulation .....	43
4.2.4.	Conclusions of implemented application.....	45
4.3.	OFDM VLC based system evaluation .....	46
4.3.1.	G3-PLC technology .....	46
4.3.2.	MAX79356 .....	47
4.3.2.1.	Simple MAC firmware evaluation.....	52
4.3.2.2.	Full MAC firmware.....	58
4.3.2.3.	Transparent UART firmware.....	59
4.4.	Custom modulation evaluation.....	59
4.4.1.	Custom modulation transmitter design.....	60
4.4.2.	Custom modulation receiver design.....	64
4.4.3.	Conclusions of implemented application.....	70
5.	Budget.....	71
5.1.	VLC LED driver .....	71
5.2.	VLC Receiver .....	72
5.3.	Baseband Audio VLC application .....	73
5.4.	FM Audio VLC application .....	74
5.5.	PLC VLC application .....	75
5.6.	Custom modulation application.....	76
5.7.	Summary of total human resource dedication and cost .....	77
6.	Conclusions and Future Work.....	78
	Bibliography.....	81
	Appendices.....	83
	Glossary .....	103

## **List of Figures**

Figure 1. Project scheduling Gantt diagram. ....	4
Figure 2. Visible spectrum wavelength distribution [4]. ....	7
Figure 3. Spectrum of a white LED showing blue light directly emitted by the GaN-based LED (peak at about 465 nm) and the more broadband Stokes-shifted light emitted by the Ce <sup>3+</sup> :YAG phosphor, which emits at roughly 500–700 nm [3]. ....	8
Figure 4. Typical color-filtered transmission spectrums illustrate how the RGB-LED spectrum has peaks for red, green and blue. ....	8
Figure 5. Simple schematic of buck converter [10]. ....	9
Figure 6. Voltage Model Control simplified description [10]. ....	10
Figure 7. Current Mode Control simplified description [10]. ....	10
Figure 8. Hysteresis control illustration [10]. ....	11
Figure 9. Hysteresis Control, simplified description [10]. ....	11
Figure 10. STEVAL-ILL066V1 board. ....	13
Figure 11. TPS92641EVM board. ....	13
Figure 12. TPS92641EVM Schematic. ....	16
Figure 13. TPS92641EVM AC response measurement connexion diagram. ....	18
Figure 14. TPS92641 AC Response with C <sub>comp</sub> = 470 nF. ....	18
Figure 15. TPS92641 AC response with C <sub>COMP</sub> = 470 nF (black) and C <sub>COMP</sub> = 100 nF (red). ....	20
Figure 16. TPS92641 AC response C <sub>comp</sub> = 470 nF (black), C <sub>comp</sub> = 100 nF (red), C <sub>comp</sub> = 1 nF (blue). ....	21
Figure 17. Oscilloscope screenshot with V <sub>in</sub> = 200 mV@100 kHz using Figure 13 equipment configuration AC-coupled. ....	22
Figure 18. Oscilloscope screenshot with V <sub>in</sub> = 200 mV@100 kHz using Figure 13 equipment configuration DC-coupled. ....	22
Figure 19. Oscilloscope screenshot with FFT representation of indirect LED current measurement through R <sub>CS</sub> . Marker “S” is placed at 96 kHz and marker “E” at 846 kHz. ....	23
Figure 20. Oscilloscope screenshot with FFT representation of indirect LED current measurement through R <sub>CS</sub> . Marker “S” is placed at 744 kHz and marker “E” at 945 kHz. ....	24
Figure 21. LED driver control input adaptation for audio signal. ....	26
Figure 22. Frequency response of control adaption design for audio signals. ....	27
Figure 23. LED driver control input adaptation for audio signal with prefiltering stage added, f <sub>c</sub> @200 Hz. ....	28
Figure 24. Frequency response of control adaption design for audio signals with no prefiltering (black line) and with it at f <sub>c</sub> @200Hz (red line). ....	28

Figure 25. TPS92641EVM with control adaption circuit (prototype board at bottom-left corner of the image).....	29
Figure 26. Photovoltaic cell used in this project AC response. ....	30
Figure 27. Audio over visible light receiver scheme. ....	30
Figure 28. Complete Baseband Audio over VLC system Frequency response. ....	31
Figure 29. Audio over visible light reception scheme with Twin-T Notch filter.....	31
Figure 30. Twin-T Notch filter, configuration implemented in Figure 29 , with center frequency at 100 Hz AC response. ....	32
Figure 31. Oscilloscope screenshot measuring fluorescent interference, CH1 received signal on photovoltaic cell, CH2 notch filter output. ....	32
Figure 32. Audio over visible light receiver prototype. ....	33
Figure 33. CD4046B internal block diagram. ....	34
Figure 34. CD4046B diagram for audio FM modulation. ....	35
Figure 35. Equipment configuration for FM application measurement.....	36
Figure 36. Oscilloscope screenshot, CH1 FM signal, CH2 led current measured through Rcs. ....	36
Figure 37. FM implementation and integrated with TPS92641EVM. ....	37
Figure 38. Left, OPT101 block diagram. Right, spectral responsivity. ....	38
Figure 39. OPT101 AC response with $R_{ext}=100\text{ k}\Omega$ . ....	38
Figure 40. Oscilloscope screenshot, CH1 LED driver control input signal, CH2 OPT101 output signal. ....	39
Figure 41. MAX9814 simplified block diagram. ....	39
Figure 42. VLC receiver diagram based and OPT101 and MAX9814. ....	40
Figure 43. PCB design preview image. ....	41
Figure 44. VLC receiver based on OPT101 and MAX9814 prototype. ....	41
Figure 45. Equipment configuration for receiver evaluation.....	42
Figure 46. Oscilloscope screenshot, CH1 LED driver control input signal, CH2 Light receiver output signal.....	42
Figure 47. FFT representation of received signal, Figure 46 CH2, Marker "S" is placed at 35 kHz, and "E" at 100 kHz.....	43
Figure 48. CD4046B diagram for audio FM demodulation. ....	44
Figure 49. FM audio through light system AC response.....	45
Figure 50. Left, VLC receiver prototype. Right, FM audio demodulation prototype.....	45
Figure 51. MAX79356 typical configuration.....	48
Figure 52. Transmitter diagram with minimum configuration based on MAX79356. ....	49
Figure 53. Receiver diagram with minimum configuration based on MAX79356. ....	50

Figure 54. Implemented MAX79356 based transmitter. ....	51
Figure 55. Implemented MAX79356 based receiver. ....	51
Figure 56. Devices configuration for evaluate Transmitter-Receiver system based on MAX79356.....	52
Figure 57. ZENO Simple Connect software main window. ....	53
Figure 58. ZENO Simple Connect software screenshot with both transmitter, right side of image, and receiver, left side of image, showing the highest transfer rate achieved. ....	55
Figure 59. Oscilloscope screenshot, CH1 LED driver signal input, CH2 Light receiver output. ....	57
Figure 60. FFT representation of PLC transmission signal at Figure 59. Marker “S” and “E” are placed at first carrier, 35 kHz and last carrier, 90 kHz. ....	57
Figure 61. First start of G3 “PLC connect” application screenshot. ....	58
Figure 62. G3 PLC Connect software screenshot after correctly receiving several packets from transmitter. ....	59
Figure 63. Custom modulation transmitter flow diagram. ....	61
Figure 64. 8 bit R2R ladder DAC converter diagram.....	62
Figure 65. PCB layout of implemented R2R ladder based DAC.....	62
Figure 66. Oscilloscope screenshot measuring R2R ladder based DAC output with the 4 different symbols generated.....	63
Figure 67. Oscilloscope screenshot with CH1 LED driver control input, CH2 Light receiver output. ....	63
Figure 68. TMS320f28027 transmitter based implementation with R2R ladder and TPS92641 LED driver.....	64
Figure 69. Oscilloscope screenshot, CH1 Received signal, CH2 comparator output, and cursors show the voltatge threshold and hysteresis. ....	65
Figure 70. Oscilloscope screenshot, CH1 received signal, CH2 comparator output for amplitude detection, cursor show the threshold configuration. ....	65
Figure 71. Custom modulation receiver flow diagram ....	66
Figure 72. Oscilloscope screenshot CH1 received signal, CH2 zero-crossing detector output. Between “S” and “E” cursors 0x3C byte is transmitted in 60 us. Red markers corresponds to: T1=5.4us, T2=3.4us T3=6.2us T4=8.4us.....	68
Figure 73. Oscilloscope screenshot, CH1 received signal, CH2 amplitude detector output. ....	69
Figure 74. TMS320f28027 recevier based implementation with VLC receiver designed in FM Audio over VLC application ....	70
Figure 75 The RIAA equalization curve for playback of vinyl records. The recording curve performs the inverse function, reducing low frequencies and boosting high frequencies [14]. ....	79

Figure 76 Capture sequence for Delta Mode Time-Stamp With Rising and Falling Edge Detect..... 102

## **List of Tables**

Table 1. Project task schedule table. ....	3
Table 2. Available colours with wavelength range, voltage drop, and material [3]. ....	6
Table 3. TPS92641EVM Electrical and Performance Specifications. ....	13
Table 4. Frequency mod involved components. ....	15
Table 5 Basic LED specification ....	17
Table 6. MAX79356 frequency bands standard supported. ....	46
Table 7. Maximum speed obtained in function of used modulation. ....	56
Table 8. Symbol codification table. ....	60
Table 9. Possible transitions with associated time values, being $T_1$ the time equivalent to half period symbol. ....	67
Table 10. VLC LED driver material cost. ....	71
Table 11. VLC LED driver distributed task time and estimated cost. ....	71
Table 12. VLC Receiver material cost. ....	72
Table 13. VLC Receiver distributed task time and estimated cost. ....	72
Table 14. Baseband Audio VLC application material cost. ....	73
Table 15. Baseband Audio VLC application distributed task time and estimated cost. ....	73
Table 16. FM Audio VLC application material cost. ....	74
Table 17. FM Audio VLC application distributed task time and estimated cost. ....	74
Table 18. PLC VLC application material cost. ....	75
Table 19. PLC VLC application distributed task time and estimated cost. ....	75
Table 20. Custom Modulation application material cost. ....	76
Table 21. Custom Modulation application distributed task time and estimated cost. ....	76
Table 22. Total human resource time dedication and estimated cost. ....	77



# **1. Introduction**

When we talk about data communication, its basic steps include the composition of the message, the encoding of the message, the usage of a medium or channel, the signal transmission, the signal reception, the correspondent decoding of the message and finally, the interpretation of the message by the receiver.

Such communication, indeed, can be carried out in a large amount of different ways. Nowadays' technologies such as Wi-Fi, Bluetooth, GSM, LoRa, ADSL, among many others, allow communications everybody is used to. The decision about which one to choose, shall be given by different factors such as the distance between the transmitter and the receiver, channel, message, etc.

This document focuses on a novel, different Visible Light Communication (VLC) technology. This type of communication as an early example was firstly employed by navy vessels, which used light reflectors to manage Morse code.

Recently, LED technology has replaced incandescent lamps by offering a greater energy efficiency and life time. LED luminaires have other properties that make them perfect for data communication. VLC can be efficiently implemented by such commercial LED luminaries. Because of the ubiquity of such elements, VLC appears as an interesting candidate for home and industrial data communications and, as of 2017, has great interest among the scientific community, where it is frequently mentioned and discussed in numerous R&D studies, papers and projects.

The rest of this document is structured as follows: Section 0 includes requirements, purpose and methods for this project. Section 2 contains information about the current state-of-the-art of VLC technology and some control methods for LED drivers. Next, Section 3 introduces the integrated circuits which are used in Section 4, which contains several implementations of prototypes and applications. Finally, Section 5 considers the cost of implementing each of these applications in a realistic manner. Section 6 concludes the document by stating several ideas for future developments.

## **1.1. Statement of purpose**

To accomplish the development of a driver for LED light control for use in VLC, the project's main goals are:

1. Operate the LED driver by following an analog signal at an AC frequency of 100 kHz.
2. Demonstrate that LED driver can support an OFDM modulation (1 - 100 kHz BW).
3. Make the whole system compatible with as many lamps types as possible for it to be applicable to real-life cases outside the laboratory.

## 1.2. Requirements and specification

Once established project main goals, project requirements and project specification are as follow.

Project requirements:

- 1 W to 100 W LED lamp support.

There are plenty of lamp types available in market. LED lamps are often made by a set of small LEDs in series. Normally, the number and type of LEDs determinates the voltage and power of the lamps. To support as many lights as possible, it is needed to have a big range in power requirement. 1 W to 100 W is enough to support 80% of lamps present in market.

- 7 V to 60 V input voltage support.

In the most frequent use case, lamps come with its own converter, so the idea is to do not deploy a custom one, and make possible to work with it.

- Analog modulation support.

A modulation is needed to employ light for communication purposes. On-Off-Keying is an easy one to implement by adding an external switch that turns on and off the LED, but also the one offering the lowest channel performance. Quadrature Phase-Shift Keying (QPSK), an analog modulation, is more difficult to implement, but in turn offers a better channel performance.

- 100:1 dimming ratio.

A good dimming ratio allows adjusting light intensity to different places or scenarios. With a 100:1 ratio, there are 100 possible brightness steps between the brightest and the darkest level.

In order to develop the project with the previous requirements, commercial parts are used and their specifications are:

- TPS92641 led driver IC.

This integrated circuit is a synchronous buck controller for precision dimming LED driver. It allows handling high power lamps with a voltage input range from 7 V to 85 V. Analog and digital dimming inputs are intended to be used as modulation control signals.

- MAX79356 PLC modem.

ZENO (MAX79356) is a programmable narrowband orthogonal frequency division multiplexing (OFDM)-based PLC modem system-on-chip (SoC) device that provides secured power line communication in a small package.

- Power supply.

All the above elements need a voltage/current source. Both power supplies types, one provided by LED manufacturer and one generic are employed in our tests. Other design parts operate with battery power.

### 1.3. Methods and procedures

This project is based on a previous one made at university. The previous project consisted in bidirectional visible light communication for a single LED lamp model, using OOK modulation. There was a need to update and re-design the hardware so a much wider range of LED lamps could be used as VLC transmitters and support analog modulations. The current project aims to achieve such design and even improve the throughput of the previous work.

### 1.4. Work plan

The planning of this project has been done on weekdays, with an average of 4 hours per day. The Table 1 shows the breakdown of tasks and duration grouped by work packages.

Nombre de tarea	Duración	Comienzo	Fin
<b>LED light control for use in VLC</b>	<b>163 días</b>	<b>vie 16/09/16</b>	<b>mar 02/05/17</b>
<b>WP1: VLC documentation research</b>	<b>9 días</b>	<b>vie 16/09/16</b>	<b>mié 28/09/16</b>
VLC documentation research	4 días	vie 16/09/16	mié 21/09/16
Compare and evaluate	5 días	jue 22/09/16	mié 28/09/16
<b>WP2: Hardware research for fulfill requirements</b>	<b>6 días</b>	<b>jue 29/09/16</b>	<b>jue 06/10/16</b>
Component research and select	6 días	jue 29/09/16	jue 06/10/16
<b>WP3: Hardware design and implementation</b>	<b>18 días</b>	<b>vie 07/10/16</b>	<b>mar 01/11/16</b>
Diagram design	9 días	vie 07/10/16	mié 19/10/16
Quick implementation	9 días	jue 20/10/16	mar 01/11/16
<b>WP4: Hardware Test</b>	<b>15 días</b>	<b>mié 02/11/16</b>	<b>mar 22/11/16</b>
Evaluate AC modulation	8 días	mié 02/11/16	vie 11/11/16
Evaluate voltage rating	5 días	lun 14/11/16	vie 18/11/16
Document results	2 días	lun 21/11/16	mar 22/11/16
<b>WP5: Project critical review</b>	<b>2 días</b>	<b>mié 23/11/16</b>	<b>jue 24/11/16</b>
Project critical review	2 días	mié 23/11/16	jue 24/11/16
<b>WP6: Baseband audio transmission demonstration</b>	<b>9 días</b>	<b>vie 25/11/16</b>	<b>mié 07/12/16</b>
Adapt LED driver input for audio	3 días	vie 25/11/16	mar 29/11/16
Build light receiver	4 días	mié 30/11/16	lun 05/12/16
Evaluate results	2 días	mar 06/12/16	mié 07/12/16
<b>WP7: Audio transmission using FM demonstration</b>	<b>12 días</b>	<b>jue 08/12/16</b>	<b>vie 23/12/16</b>
Think FM implementation	3 días	jue 08/12/16	lun 12/12/16
Tx hardware design	4 días	mar 13/12/16	vie 16/12/16
Rx hardware design	4 días	lun 19/12/16	jue 22/12/16
Evaluate results	1 día	vie 23/12/16	vie 23/12/16
<b>WP8: OFDM based communication demonstration</b>	<b>35 días</b>	<b>lun 26/12/16</b>	<b>vie 10/02/17</b>
Search OFDM comercial parts	10 días	lun 26/12/16	vie 06/01/17
Tx hardware design	10 días	lun 09/01/17	vie 20/01/17
Rx Hardware design	10 días	lun 23/01/17	vie 03/02/17
Evaluate results	5 días	lun 06/02/17	vie 10/02/17
<b>WP9: Custom modulation communication demonstration</b>	<b>35 días</b>	<b>lun 13/02/17</b>	<b>vie 31/03/17</b>
Search controller for custom modulation	5 días	lun 13/02/17	vie 17/02/17
Tx hardware and software design	14 días	lun 20/02/17	jue 09/03/17
Rx hardware and software design	12 días	vie 10/03/17	lun 27/03/17
Evaluate results	4 días	mar 28/03/17	vie 31/03/17
<b>WP10: Final report</b>	<b>22 días</b>	<b>lun 03/04/17</b>	<b>mar 02/05/17</b>
Think document structure	4 días	lun 03/04/17	jue 06/04/17
Transcribe text	12 días	vie 07/04/17	lun 24/04/17
Presentation design	6 días	mar 25/04/17	mar 02/05/17

Table 1. Project task schedule table.

Figure 1 shows the project scheduling Gantt diagram.

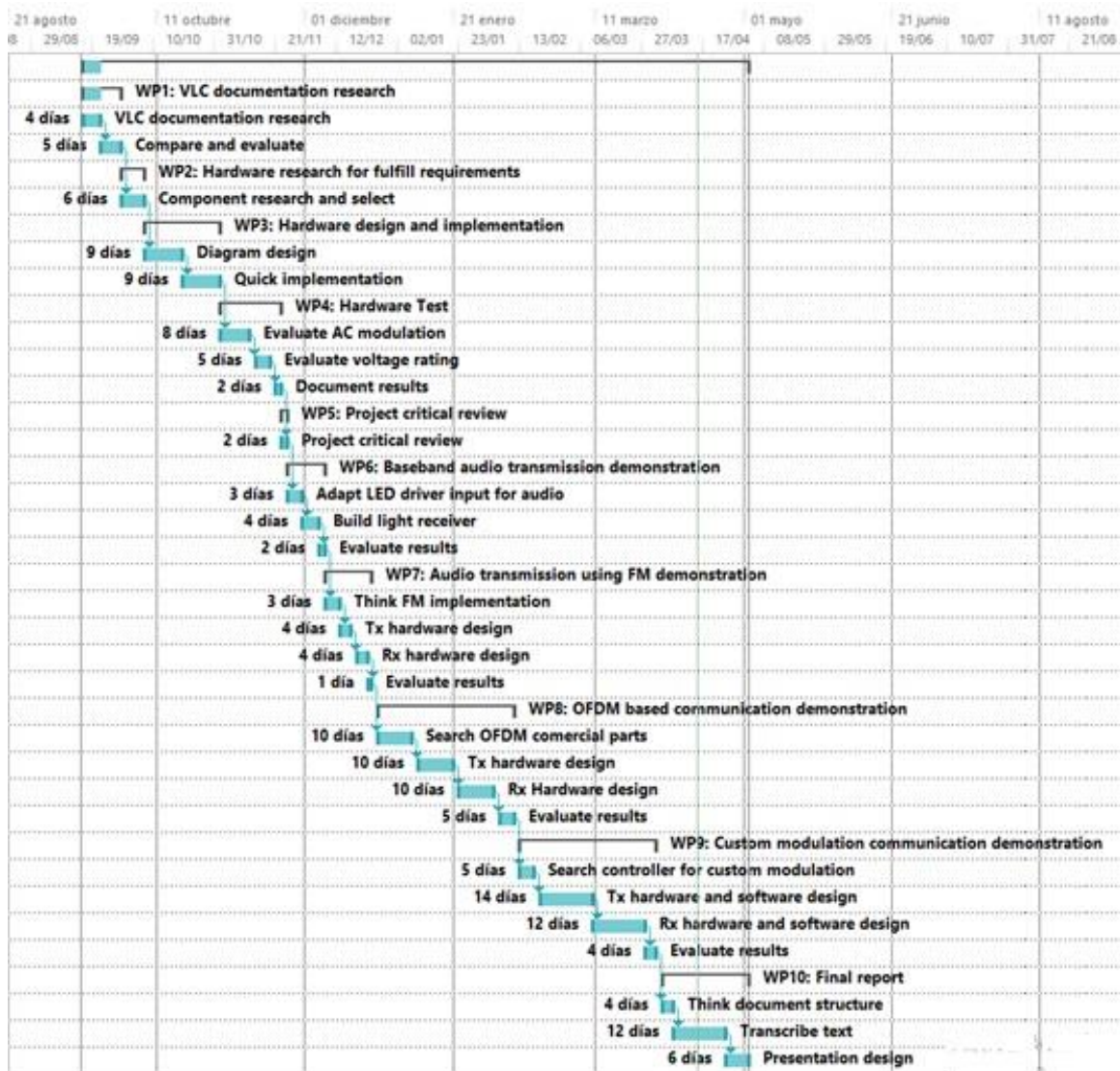


Figure 1. Project scheduling Gantt diagram.

### 1.5. Deviations from initial plan

The initial objectives of the project included the implementation, evaluation and demonstration of an On-Off Keying modulation (OOK), and the full implementation of a transmission/reception OFDM-based system.

OOK modulation performance was already studied in a previous project so this project focused on the evaluation of analog modulations. Such modulations were expected to provide better performance.

First, there was a need for theoretical study of the project. After such stage, some materials were required and they had to be tested at a hardware-level to establish an initial performance baseline.

By February 2017, one month later than the schedule because of the complexity of the task, a communication system based on OFDM was completed. Such system provides good performance, much better than OOK. According to the project's objectives, a demonstration is performed to quantify such improvement.

## 2. State of the Art

For a project like this, an initial comprehensive background review of the literature is required. There are many investigations carried out on VLC. Recent research articles published show transfer rates of 2.5 Gbps based on OOK modulation (12 meters distance) [1] or 9 Gbps 64 QAM-OFDM based link (5 meters distance) [2]. However, both previous articles make use of a laser diode as light source, given its higher intrinsic bandwidth. Such hardware is intrinsically different than the one employed in this project, which targets commercial and home systems.

Belonging to the material which LEDs are made, low-cost commercial white LEDs are often composed by the base of a blue diode LED with a phosphorus layer that complements chromatic radiation, which results in a perception of white colour for the human eye. Table 2 shows the different characteristics, such as wavelength radiation, voltage drop or bandwidth, which define LED bands. LED bandwidth specification depends mostly on the semiconductor material used.

	<b>Color</b>	<b>Wavelength [nm]</b>	<b>Voltage drop [ΔV]</b>	<b>Semiconductor material</b>
	<u>Red</u>	$610 < \lambda < 760$	$1.63 < \Delta V < 2.03$	<u>Aluminium gallium arsenide (AlGaAs)</u> <u>Gallium arsenide phosphide (GaAsP)</u> <u>Aluminium gallium indium phosphide (AlGaInP)</u> <u>Gallium(III) phosphide (GaP)</u>
	<u>Yellow</u>	$570 < \lambda < 590$	$2.10 < \Delta V < 2.18$	<u>Gallium arsenide phosphide (GaAsP)</u> <u>Aluminium gallium indium phosphide (AlGaInP)</u> <u>Gallium(III) phosphide (GaP)</u>
	<u>Green</u>	$500 < \lambda < 570$	$1.9^{[26]} < \Delta V < 4.0$	<b>Traditional green:</b> <u>Gallium(III) phosphide (GaP)</u> <u>Aluminium gallium indium phosphide (AlGaInP)</u> <u>Aluminium gallium phosphide (AlGaP)</u> <b>Pure green:</b> <u>Indium gallium nitride (InGaN) / Gallium(III) nitride (GaN)</u>
	<u>Blue</u>	$450 < \lambda < 500$	$2.48 < \Delta V < 3.7$	<u>Zinc selenide (ZnSe)</u> <u>Indium gallium nitride (InGaN)</u> <u>Silicon carbide (SiC) as substrate</u> <u>Silicon (Si) as substrate—under development</u>
	White	Broad spectrum	$2.8 < \Delta V < 4.2$	<b>Cool / Pure White:</b> Blue/UV diode with yellow phosphor <b>Warm White:</b> Blue diode with orange phosphor

*Table 2. Available colours with wavelength range, voltage drop, and material [3].*

Experiments in the previously cited articles make use of 1 to 8 W LED. The current project aims to use commercial luminaires in the range of 10 to 100 W, so we focus on obtaining a kbps transfer rate which, differently to the mentioned research articles, requires the use of fast DC-DC converters for handling such power.

A splitting of the internal structure of the hardware employed in this project shows a closed loop DC-DC converter. For control purposes, it accepts a Pulse Width Modulation (PWM) modulation, based on the error obtained with respect control signal, which acts directly on the dynamics of the converter. Then, the own control of the converter can be used to perform analog modulations and unify the power supply of the LED and control for VLC.

Buck converters are often placed inside commercial lamps for mains voltage conversion. As the required voltage for the LEDs, it exists a wide variety of configurations from 3 V to 100 V. Due to possible variations in the nominal voltage of the LED during the fabrication process, a converter is commonly included which operates in constant current mode to mitigate this issue.

## 2.1. White LED vs RGB LED

The white LED is the most used for replacement of incandescent lamps. It is largely produced because of its low cost. Figure 3 shows LED spectral radiation.

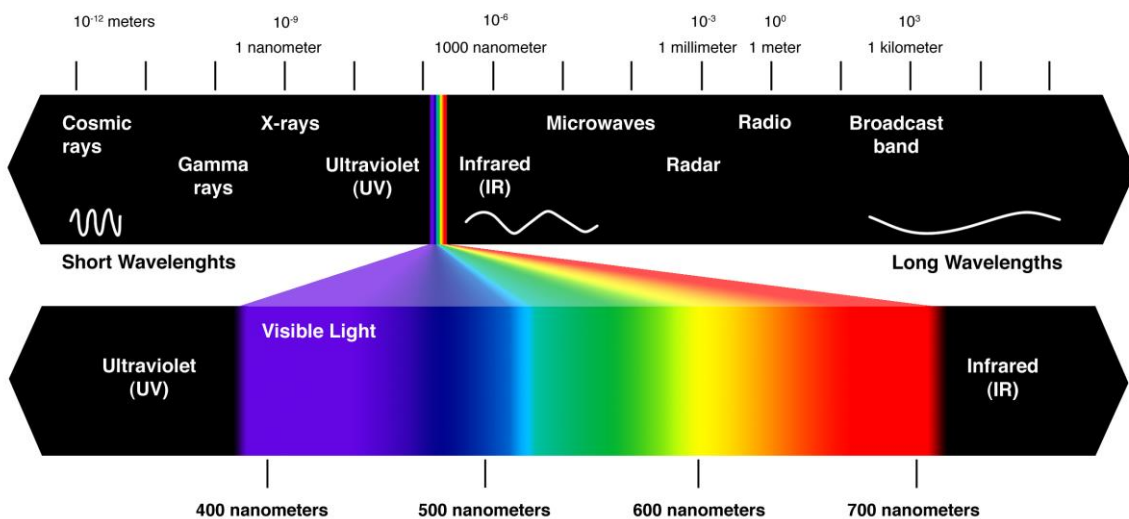


Figure 2. Visible spectrum wavelength distribution [4].

As shown in the Figure 3, there is a more selective radiation environment belonging to the blue wavelength, and a more dispersed for the rest wavelengths. To generate white colour such as the employed in this project, there are two methods: RGB and the “Phosphor method”. The latter method features better white quality by combining only the blue wavelength with yellow phosphor coating and also less complexity.

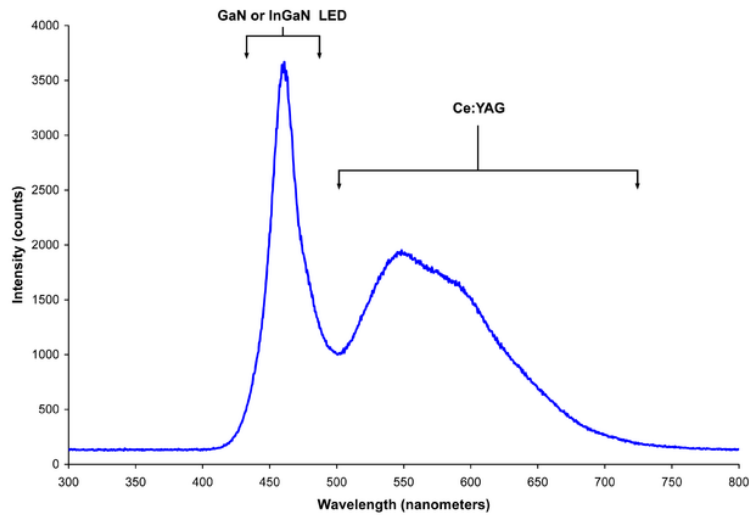


Figure 3. Spectrum of a white LED showing blue light directly emitted by the GaN-based LED (peak at about 465 nm) and the more broadband Stokes-shifted light emitted by the Ce<sup>3+</sup>:YAG phosphor, which emits at roughly 500–700 nm [3].

The RGB LED’s spectral response is represented in Figure 4. Due to the human nature of the eye, the addition of red green and blue components with the same intensity does not give as a result a pure white, so it must be normalized with the human eye response.

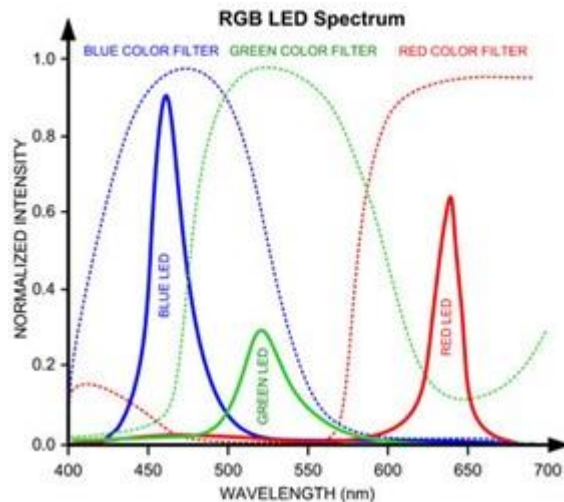


Figure 4. Typical color-filtered transmission spectrums illustrate how the RGB-LED spectrum has peaks for red, green and blue.

Experiments carried out in [7] show a bandwidth of 2 MHz for a generic white LED and 10 MHz for a red LED. In turn, in [6] bandwidths around 5-12 MHz are achieved using different manufacturers LEDs. As said before, bandwidth specification depends on LED semiconductor material, being phosphor the one offering less bandwidth.

OOK modulation allows directly relating bandwidth to bit-rate. Thus, in the case of white LED, data rate of 4 Mbps is possible without making use of optical filtering. Adding optical

filtering, so only the blue associated wavelengths arrive to receiver, could be possible to reach 20 Mbps.

Using a RGB LED as a transmitter element of VLC could be possible to reach OOK-modulated transfer rates of 20 Mbps without the need for additional optical filters, and up to 60 Mbps when employing them for independent colour transmission.

On the other hand, RGB LED is more complex and expensive, so they are not usually considered as the replacement of incandescent lamps.

## 2.2. Buck converter control topologies

For handling high power LED lamps, different configurations based on DC-DC converters can be used. Buck converter allows an easy implementation using few components, with its associated low size and cost. They also offer high efficiency, about 90 %, and large line voltage variation tolerance.

Figure 5 shows a DC/DC buck conversion that converts DC voltage denoted  $V_{IN}$  by time-division switching and smoothing the output by means an LC filter.

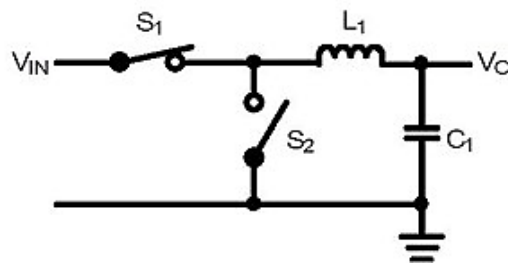


Figure 5. Simple schematic of buck converter [10].

DC/DC converters switches DC to AC, smooths it and reconverts to DC. In terms of PWM, if  $V_{IN}$  is 10V, for  $S1=ON/S2=OFF$  for 25% and  $S1=OFF/S2=ON$  for the rest,  $V_o$  will be 25%, or 2.5V.

For Buck topology, several control types are possible. They are listed in the following subsections.

### 2.2.1. Voltage mode control

Voltage mode control (Figure 6) represents the most basic method, in which only the output voltage is returned through a feedback loop. The differential voltage, which is obtained to compare the output voltage with the reference voltage by an error amp, is compared with triangular waves by a PWM generator. As a result, the pulse width of the PWM signal is determined to control the output voltage. Advantages of this method are its relative simplicity based on the use of a feedback loop consisting solely of voltages, the ability to control shorter on-time, and high noise tolerance. Possible drawbacks are the complexity of the phase compensation circuit and a cumbersome design process.

### • Voltage mode control

- ✓ A voltage-only feedback loop makes control simple
- ✓ The ability to control shorter on-time
- ✓ High noise tolerance
- ✓ Complex phase compensation circuitry

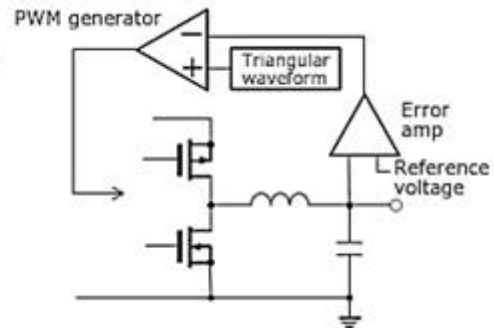


Figure 6. Voltage Model Control simplified description [10].

### 2.2.2. Current mode control

The current mode control in Figure 7 is a modification of voltage mode control, where the inductor current in the circuit is used instead of the triangular waveforms used previously. Since the current mode has two types of feedback loops: voltage loop and current loop, the control is relatively complex. However, the current mode is simpler from the design point of view and presents highly stable feedback loop and a faster load transient response than the voltage control approach. In turn, a drawback is low-noise tolerance due to the high sensitivity of current detection

### • Current mode control

- ✓ Modified voltage mode control
- ✓ Detects and uses circuit inductor current instead of triangular waves
- ✓ High stability of the feedback loop
- ✓ Substantially simplified phase compensation circuit design
- ✓ Faster load transient response than voltage mode
- ✓ Noise to current detection feedback loop must be addressed

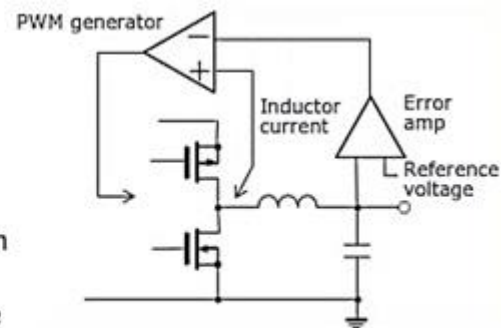


Figure 7. Current Mode Control simplified description [10].

### 2.2.3. Hysteresis (ripple) control

The hysteresis control method, also known as ripple control and shown in Figure 8 and Figure 9, was developed to meet the power requirements of even faster load transient response of load elements, such as the CPU and FPGA. When detecting that the output voltage has exceeded or fallen below a set threshold level, the comparator directly turns the switch on/off.

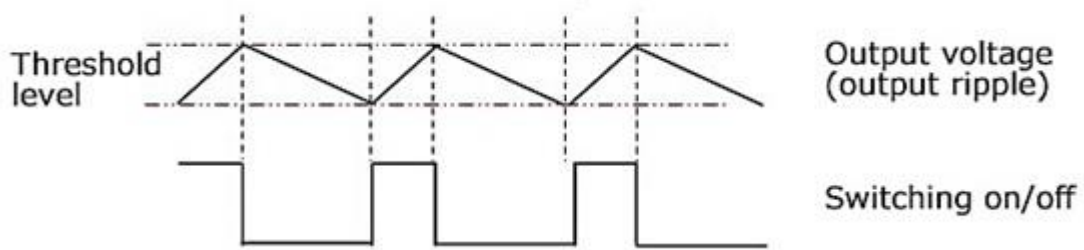


Figure 8. Hysteresis control illustration [10].

This method features extremely fast transient responses due to the direct control exerted by a comparator and the elimination of the need for phase compensation. The method suffers from issues like variable switching frequencies, large jitter, and the need for an output capacitor with a relatively large equivalent series resistor (ESR) for output ripple detection. Indeed, innovations in these areas have advanced, and more and more ICs are incorporating this method.

### • Hysteresis (ripple) control

- ✓ Directly monitors output voltage with a comparator
- ✓ Extremely fast load transient response
- ✓ Highly stable feedback loop
- ✓ Eliminates the need for phase compensation
- ✓ Variable switching frequencies
- ✓ Large jitter
- ✓ Requires a capacitor with a large ESR value to detect ripples

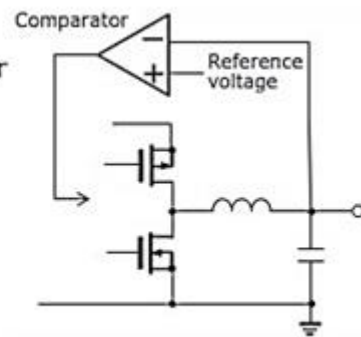


Figure 9. Hysteresis Control, simplified description [10].

Once the state-of-the-art of the current methods have been presented, Section 3 describes the hardware analysis of the integrated circuits employed to implement the prototypes designed in this project.

### **3. Project development:**

The use of a DC-DC converter is essential for the realization of this project. Since developing a DC-DC converter from scratch is unviable in terms of time, the project features a commercial converter as a base.

#### **3.1. Buck converter for LED driver selection**

The criterion to select a Buck converter to implement the LED driver is based on the supported supply voltage range, the maximum power that can handle, the possibility of analog dimming control and a fast control mode.

For the range of supply voltage, we seek the maximum possible, even if it is possible direct connection to 220 V mains.

In terms of maximum power the driver should be able to handle a maximum of 100 W.

The design also requires that the controller supports analog dimming input and, if possible, PWM dimming, too.

Finally, control type determines in some way speed response, so we are looking for the fastest one.

Upon applying all the previous search criteria over the “online search tool” of the main manufacturers, two options outstand:

##### **1- STLUX385 from ST:**

This controller enables a wide variety of configurations as well as programming of specific functions using a ST programming environment. Taking as example the development kit STEVAL-ILL066V1 [11] in Figure 10, its key features are:

- STLUX385A based.
- High efficiency (92%).
- Primary side controlled.
- Up to 100 W (100 V at 1 A or 200 V at 0.5 A).
- Single isolated output suitable for LED connection.
- Wide input voltage range: 90 V to 265 V AC.
- Adjustable LED current and dimming.
- Output resolution: 11-bit equivalent.
- IDLE mode power consumption: < 200 mW.
- Real-time fault detection and protection (e. g.: short- or open circuit).
- Remote control via 0 - 10 V UART.



Figure 10. STEVAL-ILL066V1 board.

## 2- TPS92641 from Texas Instruments:

The TPS92641 is a high-voltage, synchronous NFET controllers for buck-current regulators. Output current regulation is based on valley current-mode operation using a quasi-hysteretic controlled on-time architecture.

Taking as a base TPS92641EVM [12] evaluation kit (Figure 11), it can be configured as a LED power solution providing a single-channel regulated current output to drive 10 LEDs connected in series running at 1 A. This EVM accepts logic level PWM dimming as shown in Table 3. A high-efficiency single-inductor synchronous step-down (buck) converter topology is used.

Parameter		Notes and Conditions <sup>(1)</sup>	Min	Typ	Max	Unit
<b>Input Characteristics</b>						
$V_{IN}$	Input voltage		43	48	53	V
UDIM	UDIM logic high (PWM dimming)	$F_{UDIM} = 200$ Hz	1.3		5.5	V
$I_Q$	Input quiescent current	Device enable, $V_{IN} = 48$ V, $V_{UDIM} = 1$ V, no switching			3	mA
<b>Output Characteristics</b>						
$V_{OUT}$	Output voltage	LED+ (TP5) to GND (TP4) <sup>(2)</sup>	32		33	V
$I_{LED}$	LED current	$R5 = 10$ k $\Omega$ , $R6 = 19.6$ k $\Omega$ , $R10 = 0.2$ $\Omega$	970	1000	1030	mA
<b>Systems Characteristics</b>						
$F_{SW}$	Switching frequency	$R1 = 32.4$ k $\Omega$ , $C6 = 1$ nF, $R7 = 340$ k $\Omega$ , $R8 = 22.6$ k $\Omega$	450		500	kHz

Table 3. TPS92641EVM Electrical and Performance Specifications.



Figure 11. TPS92641EVM board.

### 3.2. TPS92641 specification

Choosing the TPS92641 driver since it allows an easy evaluation from a not very advanced theoretical framework. Also, its documentation seems to be of higher quality than the ST option.

The TPS92641 is a high voltage synchronous NFET controller for buck regulators. Output current regulation is based on valley current-mode operation using a controlled on-time architecture. This control method eases the design of loop compensation while maintaining nearly constant switching frequency. The TPS92641 device includes a high-voltage start-up regulator that operates over a wide input range of 7 V to 85 V. The PWM controller is designed for high speed capability, including an oscillator frequency range up to 1 MHz. The TPS92641 device accepts both analog and PWM input signals, resulting in exceptional dimming control range. Linear response characteristic between input command and LED current is achieved with true zero LED current using low-offset error amplifier and proprietary PWM dimming logic.

The rest of its features are:

- Vin range from 7 V to 85 V.
- Wide dimming range:
  - 500:1 Analog Dimming.
  - 2500:1 Standard PWM Dimming.
  - 20000:1 Shunt Fet Dimming.
- Adjustable LED current sense voltage.
- 2- $\Omega$  1-Apeak MOSFET Gate Drivers.
- Shunt Dimming Gate Driver.
- Programmable Switching frequency.
- Precision voltage reference 3 V  $\pm$ 2%.
- Input UVLO (UnderVoltage LockOut) and Output OVP (OverVoltage Protection).
- Low power shutdown mode and thermal shutdown.

For the purposes of this project, the main features of this driver are the Vin range, which allows for a wide variety of lamps, the analog dimming providing 500 possible levels of adjustable brightness, the 2- $\Omega$  1-A MOSFET Gate Drivers, which enables working with power transistors, and the Programmable Switching frequency to adjust the speed of the control loop.

### 3.3. TPS92641EVM mods

Figure 12 shows the scheme of the TPS92641EVM evaluation board. For this project, the EVM requires some modifications “mods”, listed next.

- **System frequency mod:** Configure the frequency of the system to the maximum established by the manufacturer, 1 MHz, by evaluating the components involved in this parameter as in the datasheet formula (eq. 1).

$$f_{SW} = \frac{(R_{VOUT1} + R_{VOUT2})}{R_{VOUT2}} \times \frac{1}{R_{ON} \times C_{ON}} \quad (\text{eq. 1})$$

Datasheet reference	Schematic reference	Component value
$R_{VOUT1}$	R8	340 k $\Omega$
$R_{VOUT2}$	R7	22 k $\Omega$
$R_{ON}$	R1	32.4 k $\Omega$
$C_{ON}$	C6	1000 pF

*Table 4. Frequency mod involved components.*

$$f_{SW} = \frac{(340 \text{ k}\Omega + 22 \text{ k}\Omega)}{22 \text{ k}\Omega} \times \frac{1}{32.4 \text{ k}\Omega \times 1000 \text{ pF}} = 507.86 \text{ kHz} \quad (\text{eq. 2})$$

For the frequency of 1 MHz, we have the option of modifying  $R_{ON}$  or  $C_{ON}$ , in this case we modify  $C_{ON}$  because the ease of find a generic value. 500 pF which leads us to a 470 pF standard value. We re-do the calculation in eq. 3:

$$f_{SW} = \frac{(340 \text{ k}\Omega + 22 \text{ k}\Omega)}{22 \text{ k}\Omega} \times \frac{1}{32.4 \text{ k}\Omega \times 470 \text{ pF}} = 1.080 \text{ MHz} \quad (\text{eq. 3})$$

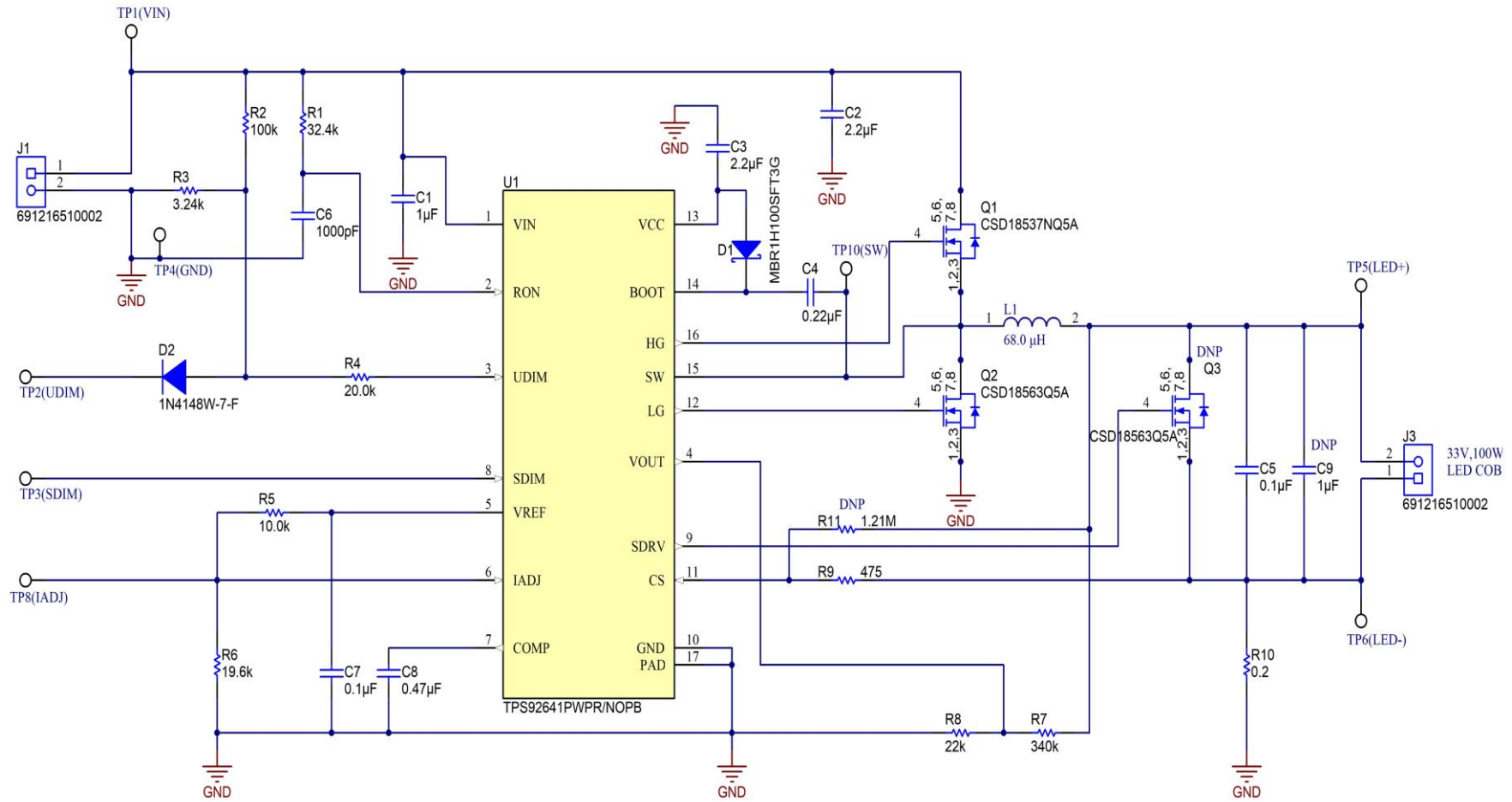


Figure 12. TPS92641EVM Schematic.

- **IADJ control mod:** Evaluation board comes by default configured for a fixed current LED operation which is set by a reference voltage from a resistive divider. To carry out the current control of the LED from an external signal, it is necessary to remove R5 resistor.
- **COMP capacitor mod:** Based on the TPS92641 datasheet, compensation capacitor, corresponding to C8 in the TPS92641EVM, determines control loop response, so we replace default value of 470 nF for the minimum recommended by the manufacturer, 100 nF. Loop response is not characterized by manufacturer, so characterization will be made empirically.
- **MOSFET replacement mod:** In order to maximize the input voltage range according to the TPS92641 specification, and given that the transistors in the evaluation board have a Vds specification of 60 V (NTD3055-150T4G), we replace these for alternative ones with Vds specification of 100 V (FQD19N10L). The rest of external components to the TPS92641 place in the evaluation board which are directly dependent on Vin, supports 100 V nominal voltage.

### 3.4. Hands-on experience with TPS92641EVM

Firstly, referring to  $V_{IADJ}$  pin as the control input, default control to output bandwidth is evaluated. Voltage limitations of the control signal are given by component datasheet, being 2.54 V the maximum voltage value, and having a relationship with the LED current given by eq. 4 and eq. 5:

$$I_{LED} = \frac{V_{CS}}{R_{CS}} \quad (\text{eq. 4})$$

$$V_{CS} = \frac{V_{IADJ}}{10} \quad (\text{eq. 5})$$

$R_{CS}$  corresponds to R10 in the schematic shown in Figure 12 and its value is 0.2  $\Omega$ . Therefore, the maximum current of output is given by eq. 6:

$$I_{LED\_MAX} = \frac{V_{IADJ\_MAX}}{10 \times 0.2} = \frac{2.54}{2} = 1.27 \text{ A} \quad (\text{eq. 6})$$

According to this specification, and in order not to modify the value of  $R_{CS}$ , we use an LED lamp with the specifications shown in Table 4.

<b>Vf – Forward Voltage</b>	32-36 V
<b>If – Forward Current</b>	1 A
<b>Power Rating</b>	36 W

*Table 5 Basic LED specification*

### 3.4.1. Bandwidth measurement

To evaluate the frequency response of the control loop, we make a sweep frequency from 100 Hz to 100 kHz on control input. To imitate the extreme conditions of maximum light level, control signal is established at level corresponding to the 90% average LED current value of the maximum specified in LED specification (table 4), and AC component is configured with an amplitude corresponding to 10% of the maximum current.

Since forward LED current is 1 A, DC component of generated signal is set to 1.8 V and AC component to 200 mV.

Figure 13 shows the configuration of measure equipment. Figure 14 the default response obtained.

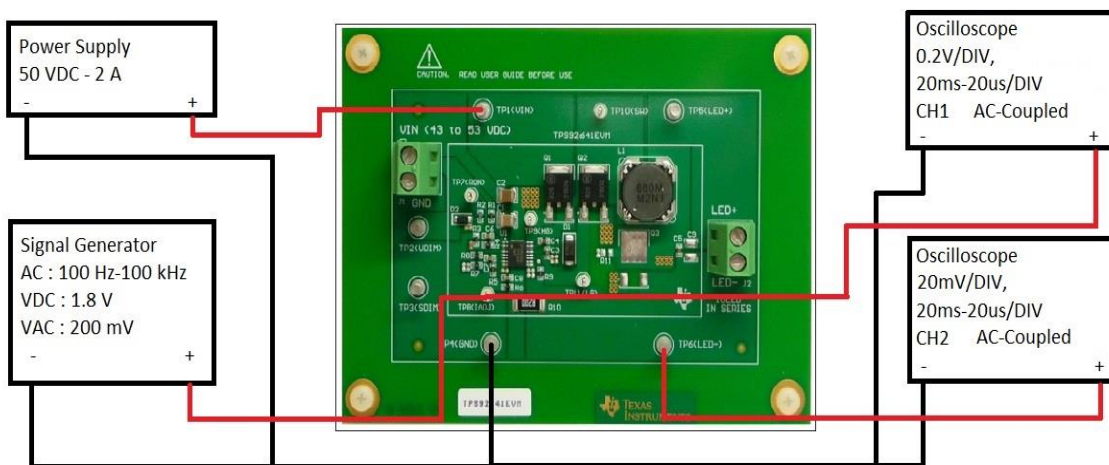


Figure 13. TPS92641EVM AC response measurement connexion diagram.

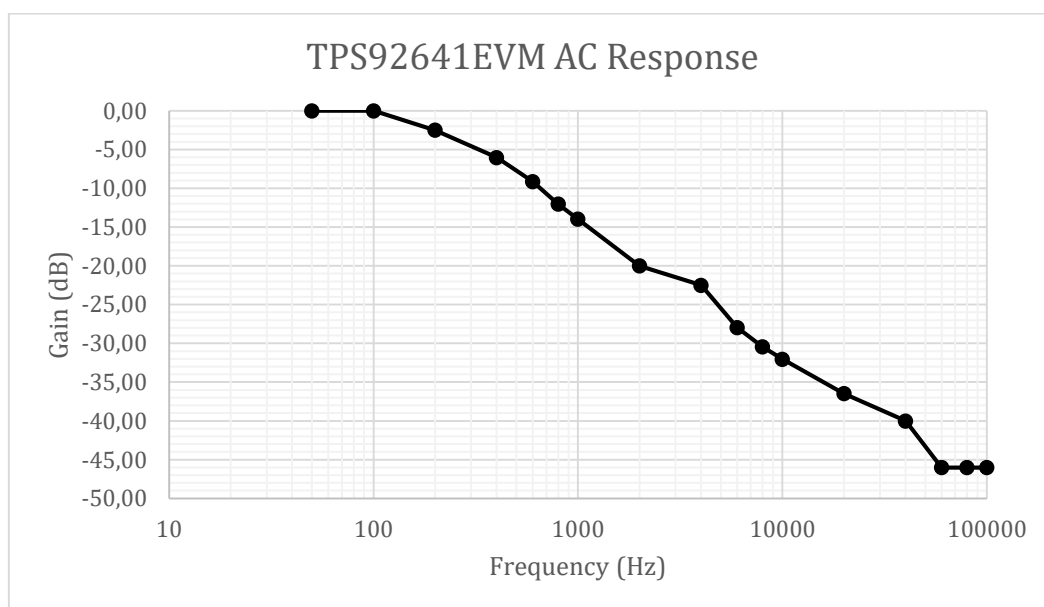


Figure 14. TPS92641 AC Response with  $C_{comp} = 470 \text{ nF}$ .

Figure 14 suggests that the - 3 dB bandwidth is 200 Hz, and we observed an attenuation of 20dB per decade, indicating the presence of a dominant pole over this frequency.

As a first approximation for passband edge frequency ( $\omega_p$ ) , we can set the parameters of the associated pole frequency from a generic RC expression:

$$\omega_p = \frac{1}{R \times C} \quad (\text{eq. 7})$$

Being  $\omega_p$  the value of -3 dB cut-off frequency in rad/s.

$$\omega_p = 2 \times \pi \times f_c = 2 \times \pi \times 200 \text{ Hz} = 1256.6 \text{ rad/s} \quad (\text{eq. 8})$$

In previous equation,  $\omega_p$  value is replaced to obtain  $R$ :

$$R = \frac{1}{\omega_p \times C} = \frac{1}{1256.6 \frac{\text{rad}}{\text{s}} \times 470 \text{ nF}} = 1693.1 \Omega \quad (\text{eq. 9})$$

From obtained  $R$  value, a first approximation is given with  $C_{COMP} = 100 \text{ nF}$ :

$$\omega_p = \frac{1}{R \times C_{COMP}} = \frac{1}{1693.1 \Omega \times 100 \text{ nF}} = 5906.2 \frac{\text{rad}}{\text{s}} \quad (\text{eq. 10})$$

$$f_c = \frac{\omega_p}{2 \times \pi} = \frac{5906.2 \frac{\text{rad}}{\text{s}}}{2 \times \pi} = 940 \text{ Hz} \quad (\text{eq. 11})$$

At this point, we carry out the modification of the compensation capacitor by replacing the 470 nF for a 100 nF one, to the minimum recommended by the manufacturer.

To observe the error magnitude of the approximation just performed, we measure and plot again the bandwidth with  $C_{COMP} = 100 \text{ nF}$ . Figure 15 shows the results obtained, as well as its comparison to  $C_{COMP} = 470 \text{ nF}$  from Figure 14.

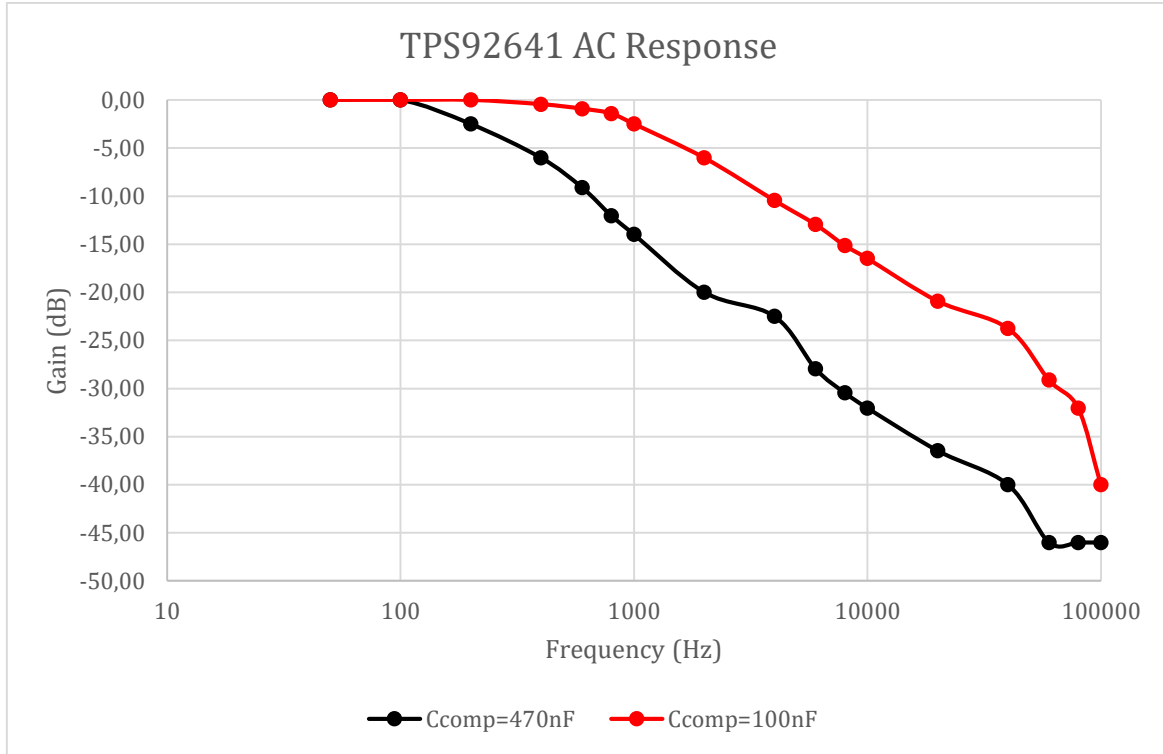


Figure 15. TPS92641 AC response with  $C_{COMP} = 470\text{ nF}$  (black) and  $C_{COMP} = 100\text{ nF}$  (red).

The achieved -3 dB bandwidth with  $C_{COMP} = 100\text{ nF}$  is 1 kHz, so the new approximation offers a good characterization in this case. Again, there is 20 dB/dec attenuation, which means this pole still dominates.

Even if this represents an important improvement, the goal of this project is 100 kHz bandwidth. By recalculating, required  $C_{COMP}$  is 1 nF, a value well below the minimum established by the manufacturer.

In this case, is consulted through the Texas Instruments forum if it is possible to use lower  $C_{COMP}$  values than those listed in component datasheet. The answer was that, in case PWM dimming is not used, this value may be below the 100 nF [15]. Figure 16 shows the corresponding bandwidth measurement for  $C_{COMP} = 1\text{ nF}$ .

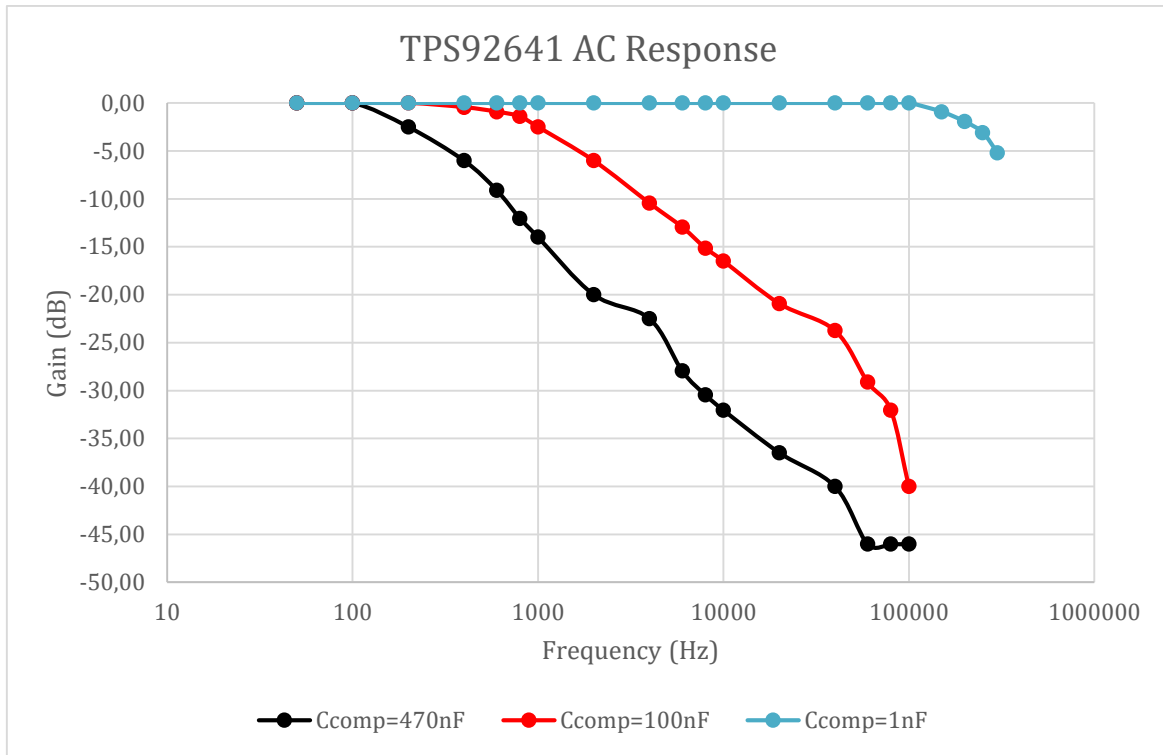


Figure 16. TPS92641 AC response  $C_{comp} = 470\text{ nF}$  (black),  $C_{comp} = 100\text{ nF}$  (red),  $C_{comp} = 1\text{ nF}$  (blue).

Finally, with  $C_{COMP} = 1\text{ nF}$ , we obtain a 100 kHz bandwidth. In this case, it is not possible to assess with certainty the attenuation per decade, since the magnitude of the signal begins to be of the same order as the LED ripple current, by which we cannot determine if the continuous pole being dominant, and thus the stability of the system.

Figure 17 and Figure 18 show LED driver input and output signal using AC and DC coupling respectively.

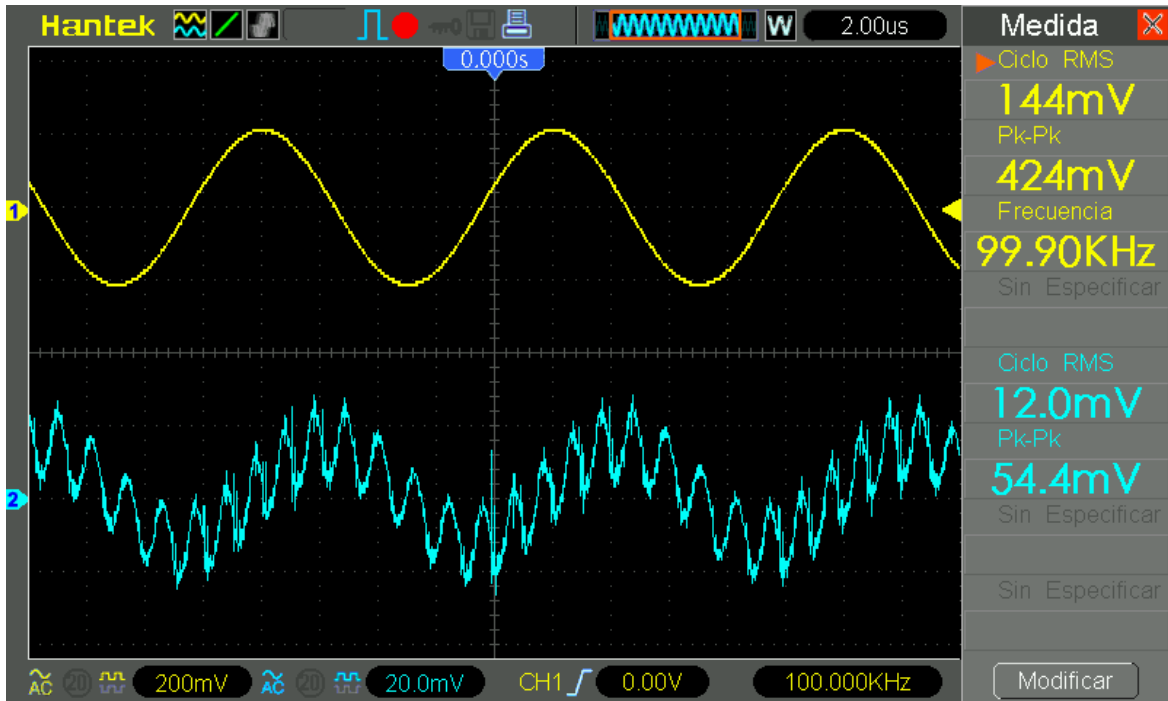


Figure 17. Oscilloscope screenshot with  $V_{in} = 200 \text{ mV}@100 \text{ kHz}$  using Figure 13 equipment configuration AC-coupled.

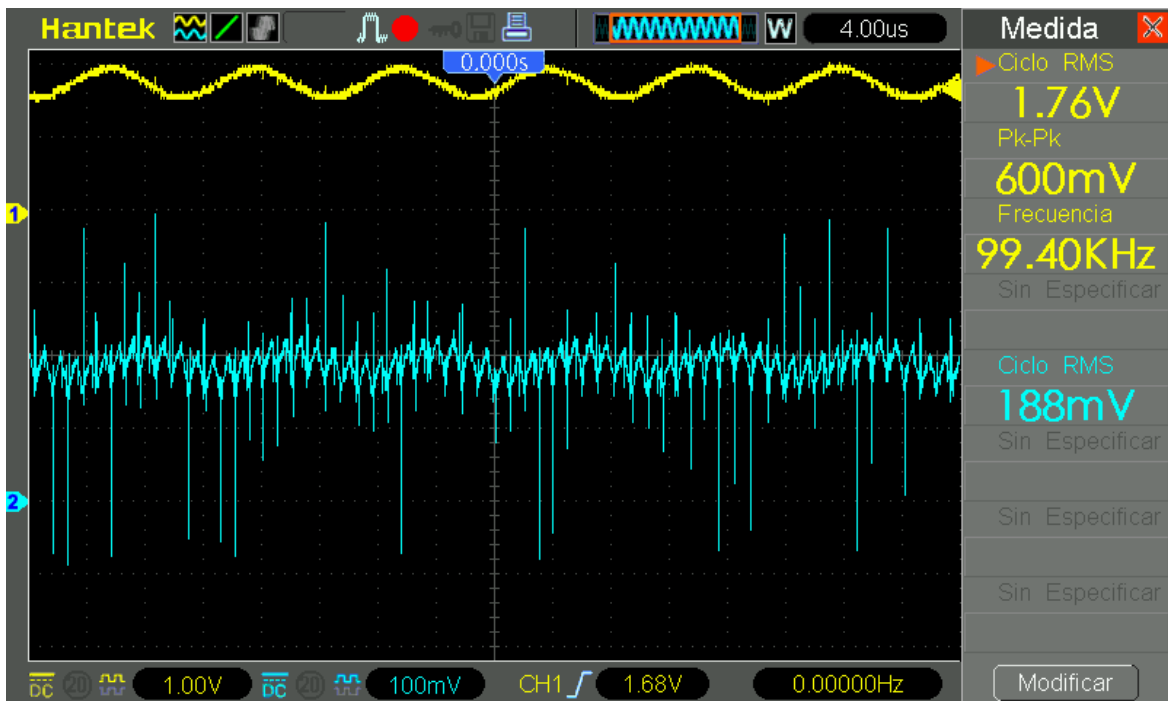


Figure 18. Oscilloscope screenshot with  $V_{in} = 200 \text{ mV}@100 \text{ kHz}$  using Figure 13 equipment configuration DC-coupled.

In Figure 17, channel 2 represents indirect LED current measurement through  $R_{CS}$ . Useful signal (lower frequency) and the LED ripple current due to the switching system are mixed.

The separation between both frequencies is enough to properly filter the useful signal as can be shown in Figure 19.

Figure 18 illustrates the relationship given by the manufacturer (eq. 4 and eq. 5) in datasheet respect to the LED current measured indirectly through  $R_{CS}$  ( $I_{LED}$ ) in function of the control signal ( $V_{ADJ}$ ).

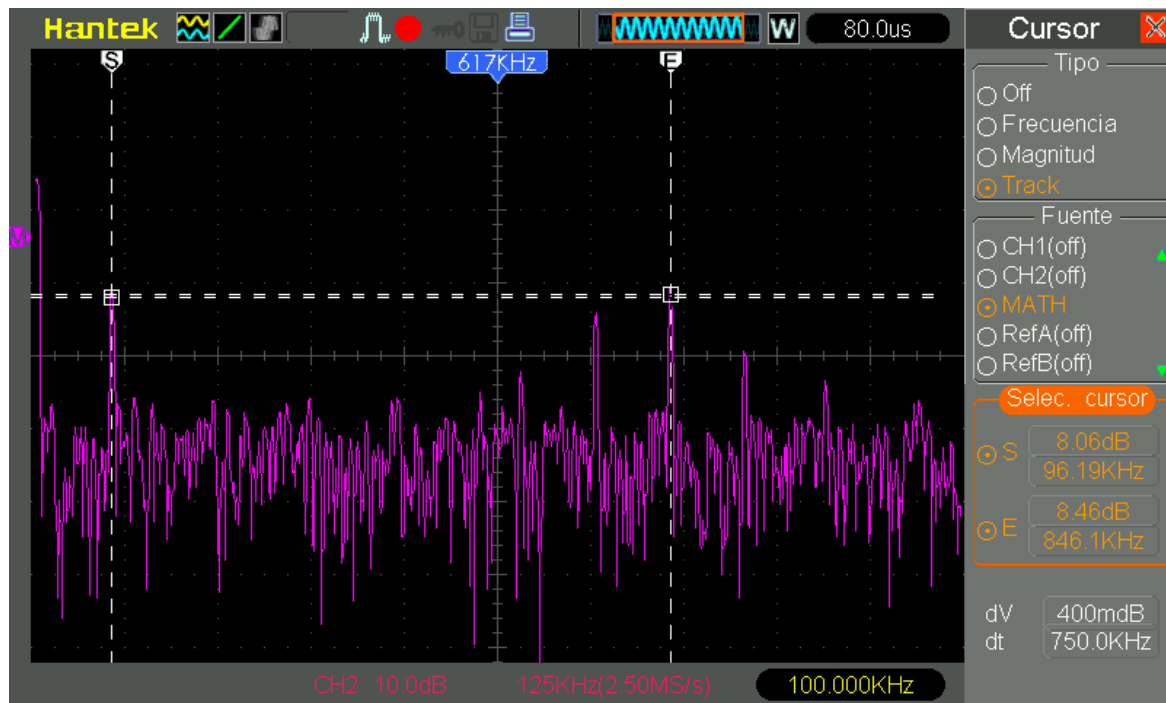


Figure 19. Oscilloscope screenshot with FFT representation of indirect LED current measurement through  $R_{CS}$ . Marker “S” is placed at 96 kHz and marker “E” at 846 kHz.

Figure 19 shows frequency representation of LED current, indirectly measured through  $R_{CS}$ , the 96 kHz spike is related to the control input signal, and 846 kHz to the converter system frequency. Separation between both signals is 750 kHz, related to such frequencies also a decade, so with a passive RC filter should be possible to filter useful signal and attenuate the converter switching frequency at receiver side.

At Figure 19, it is also possible to distinguish two more significant spikes around 846 kHz. In Figure 20, markers are placed over this spikes, 744 kHz and 945 kHz. These frequencies are related to the switching frequency  $\pm$  control signal frequency. This phenomenon can be explained from sampling theorem terms, taking the system frequency as the sampling frequency. In fact, the converter works with On-Off switch states, and some kind of analog to digital conversion is performed from the control input signal.

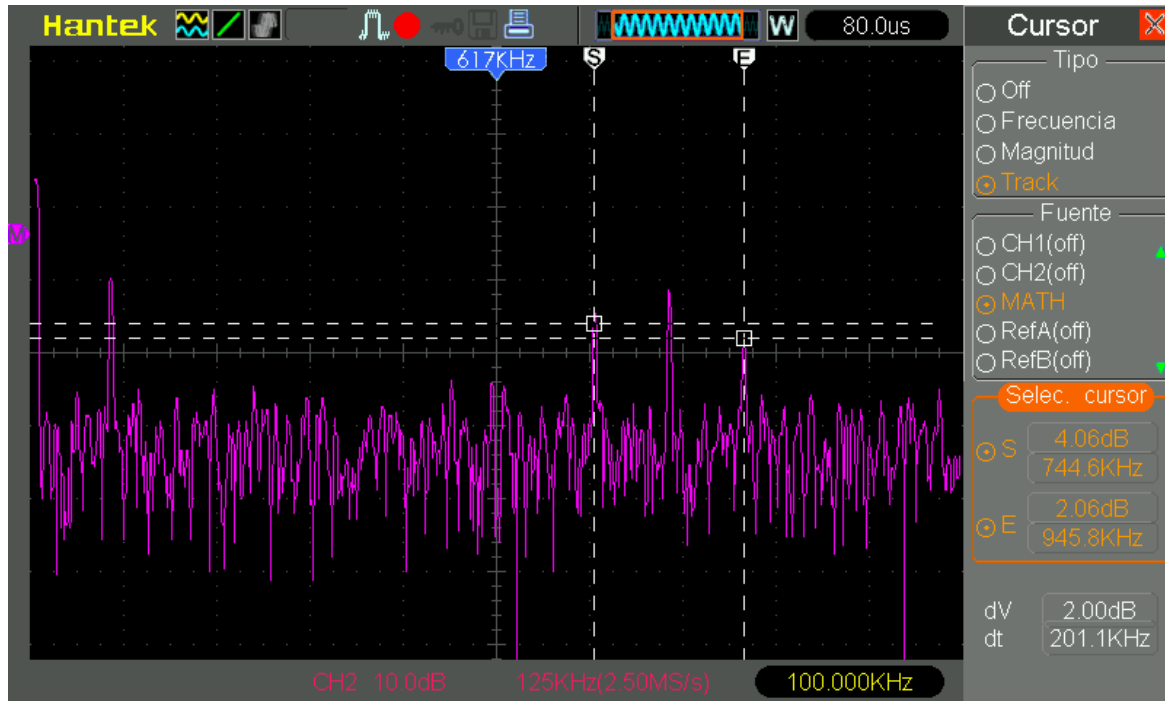


Figure 20. Oscilloscope screenshot with FFT representation of indirect LED current measurement through  $R_{cs}$ . Marker "S" is placed at 744 kHz and marker "E" at 945 kHz.

### 3.4.2. Commercial lamps compatibility test

Along this project, different LED lamp types with different nominal voltage (12 V, 23 V and 48 V) have been tested when operating with the designed LED driver. For such purpose, there is a need to modify certain components on the development kit and make use of a separate power supply. In function of the specific characteristics of the LED lamp, the design criteria followed the following rules:

- **Rated voltage LED lamp:** Nominal lamp voltage sets a minimum of supply voltage. Given the buck topology of the converter, which does not have a 100% efficiency, the power supply voltage will need to be greater than that specified for LED lamp. Datasheet assumes 90% efficiency, which means the minimum voltage must be 10% higher than the LED lamp nominal voltage.

It is a good practice to choose a supply voltage between 30% - 40% higher than the nominal voltage of the LED, since in this way the dynamics of control has more room for manoeuvre respect to duty cycle.

The rated voltage of the components, mainly capacitors connected to the power supply and transistors, must be 20 % greater in terms of voltage specification than the supply voltage. In this case, the evaluation board together with the modifications contemplates the possibility of work with the maximum power supply supported by the TPS92641.

For the correct operation of the converter several external components to the TPS92641 must be configured:

- It requires a voltage of approximately 2.5 V at the  $V_{OUT}$  pin, scaled output voltage feedback, by what you will have to modify the components that affect this parameter, which are  $R_{VOUT1}$  and  $R_{VOUT2}$ , to meet eq. 12.

$$2.5 V = \frac{R_{VOUT1} + R_{VOUT2}}{R_{VOUT2}} \times V_{OUT} \quad (\text{eq. 12})$$

The value of  $R_{VOUT1}$  and  $R_{VOUT2}$  also affects the frequency of the system so collateral effects need to be considered.

- The value of the inductor also is affected by changes in the voltage, specifically regarding  $V_{IN} - V_{OUT}$  relation, so if we maintain this factor constant, we need to calculate the current maximum ripple. The inductance value is obtained from eq. 13.

$$L = \frac{(V_{IN} - V_{OUT}) \times \frac{V_{OUT}}{0.9 \times V_{IN}}}{\Delta I_{L-PP} \times f_{SW}} \quad (\text{eq. 13})$$

- **Current rated LED lamp:** By default, the evaluation board is designed to work with a maximum current of 1.27 A. In case of having less current rating, current regulation dynamic margin is decreased. In case of higher currents, control mechanisms limit the maximum value to 1.27 A.

- In this case, we must check that the maximum current of the transistors and the inductor are at least 20 % higher than nominal LED rated current. Next, we set up the current sense resistor  $R_{CS}$  to maximize the current control dynamic range, from eq. 14.

$$R_{CS} = \frac{I_{LED}}{200 \text{ mV}} \quad (\text{eq.14})$$

Once the operation of the integrated circuits employed in this project has been presented, Section 4 contains the applications developed to test their performance when deployed for VLC purposes.

## 4. Applications

Several applications are developed to evaluate the technology and components developed in this project. This section enumerates and describes each one of them. One of the main requisites is, of course, not altering the original purpose of a lamp, which is being a trustable source of light.

### 4.1. Baseband Audio over VLC

To have a direct perception of the bandwidth performance of the LED driver designed for this project, an application consisting of transmitting an audio signal through VLC is developed.

#### 4.1.1. LED driver control input adaption for baseband audio signal.

The bandwidth of audio signals (20 Hz - 20 kHz) is in the range of the designed LED driver bandwidth (100 kHz). However, to employ audio signal as LED dimming control input, still some modifications need to be done in LED driver control input. Figure 21 shows the diagram of the required control line adaption.

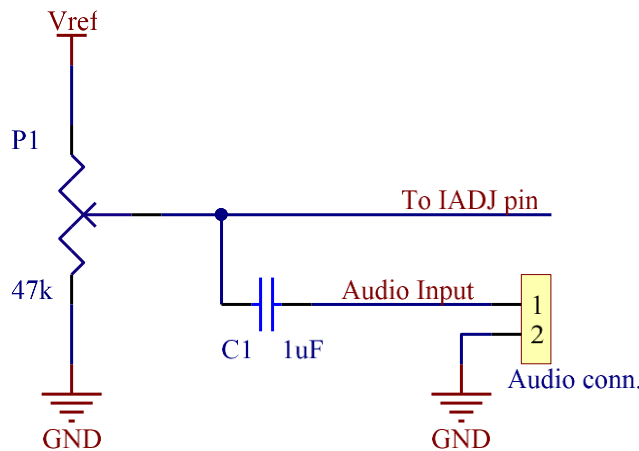


Figure 21. LED driver control input adaptation for audio signal.

Potentiometer  $P1$  adjusts the DC offset voltage, between 0 V and 3 V, corresponding to the LED current mean value (light intensity), and through  $C1$  capacitor audio signal is coupled to the DC offset value.

Potentiometer  $P1$  value is set by considering the TPS92641 reference voltage specifications, which allows you to supply a maximum current of 2 mA. In this case, given that is a reference signal, it is approximately set by considering a 100  $\mu$ A current value in eq. 15.

$$R_{P1} = \frac{V_{REF}}{I_{P1}} = \frac{3V}{100\mu A} = 30k\Omega \quad (\text{eq. 15})$$

We set potentiometer value higher than obtained in eq. 15, concretely 47 kΩ, and the equation is re-evaluated in eq. 16:

$$I_{P1} = \frac{V_{RFF}}{R_{P1}} = \frac{3 V}{47 k\Omega} = 63.8 \mu A \quad (\text{eq. 16})$$

The pair formed by adjusted potentiometer value and capacitor behaves as a high-pass filter, and in function of the potentiometer adjustment, the cut-off frequency is modified.

We assume a minimum adjustment value of 10 kΩ, corresponding to 20% light intensity approximately. With this parameter fixed, the capacitor value is computed using RC filter general expression for a cut-off frequency of 10 Hz in eq. 17.

$$C_1 = \frac{1}{2 \times \pi \times f_c \times R_{P1}} = \frac{1}{2 \times \pi \times 10 \text{ Hz} \times 10 k\Omega} = 1.59 \mu F \quad (\text{eq. 17})$$

Capacitor C1 value is set to a common commercial value of 1 μF.

The frequency response of the circuit in Figure 21 at a potentiometer value of 10 kΩ is shown in Figure 22:

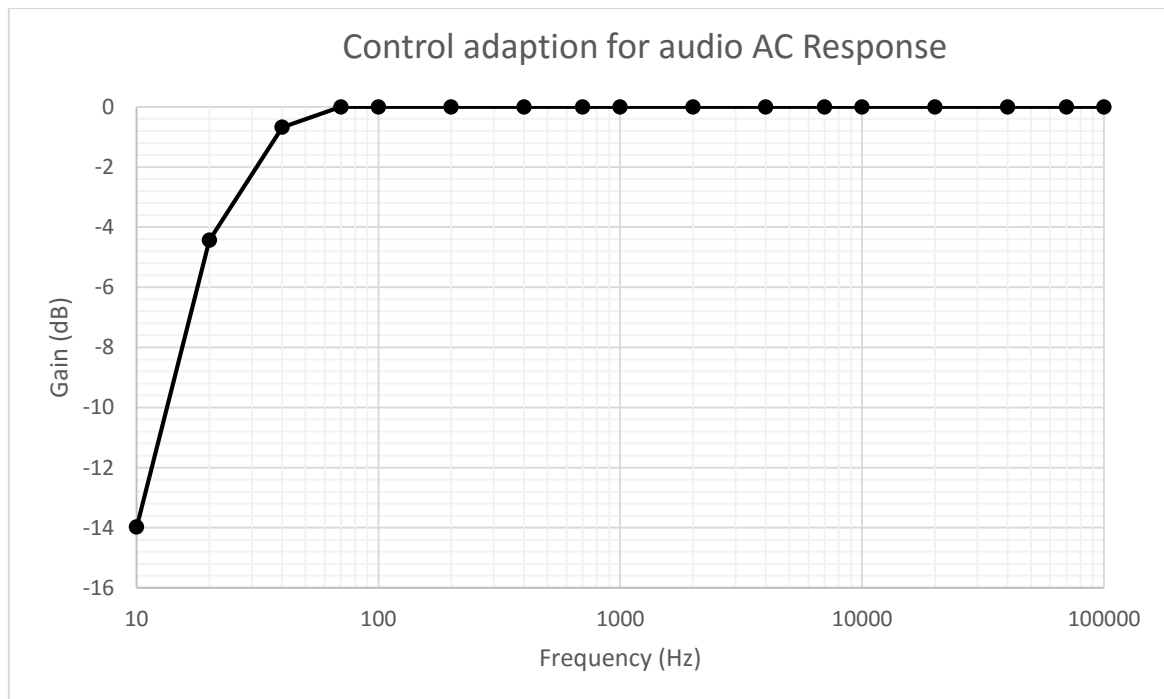


Figure 22. Frequency response of control adaption design for audio signals.

From Figure 22, 20 Hz cut-off frequency is obtained approximately.

As a first test result, in the range of 20 Hz to 50 Hz light flickering is noticeable. A high-pass pre-filtering stage (C2, R1 in Figure 23) is added to take care of this behaviour with established cut-off frequency at 200 Hz to have enough attenuation on the frequencies that generate noticeable light flickering:

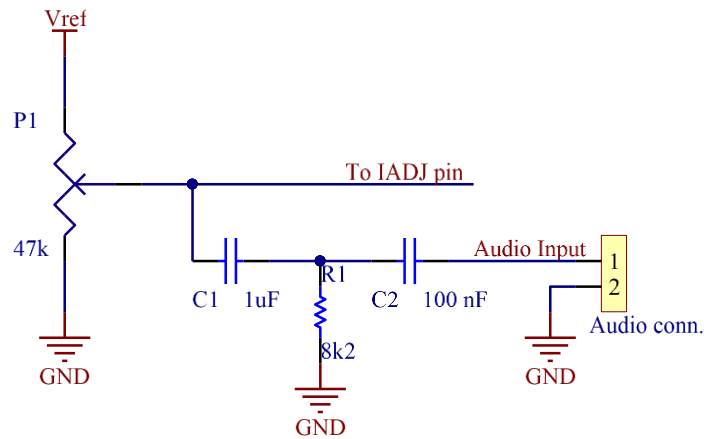


Figure 23. LED driver control input adaptation for audio signal with prefiltering stage added,  $f_c @ 200$  Hz.

Frequency response with the new settings is re-evaluated and the result is shown in Figure 24, which conveniently includes again the previous modification from Figure 23.

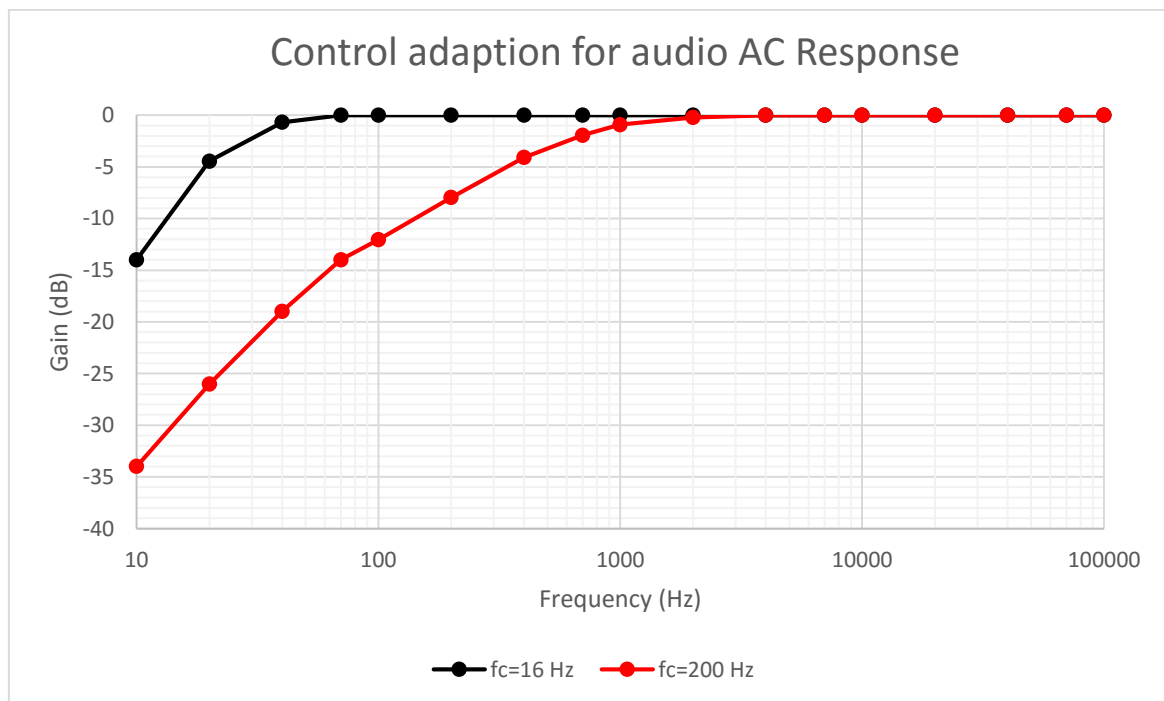


Figure 24. Frequency response of control adaption design for audio signals with no prefiltering (black line) and with it at  $f_c @ 200$  Hz (red line).

Attenuation of approx. 20 dB for frequency of 50 Hz is obtained, which is the maximum flickering frequency noticeable value. When including implemented pre-filtering stage, light flickering is not noticeable anymore in the 20 Hz to 50 Hz frequency range.

Figure 25 shows the TPS92641EVM modified with this control input adaption.

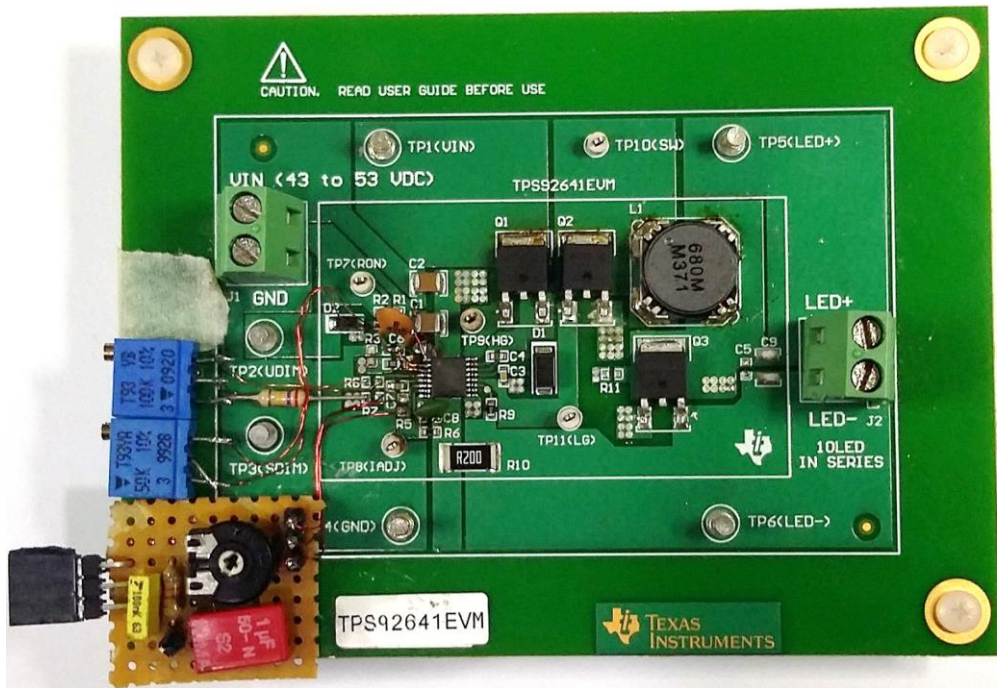


Figure 25. TPS92641EVM with control adaption circuit (prototype board at bottom-left corner of the image).

#### 4.1.2. Baseband Audio over VLC receiver

The receiver is implemented making use of a photovoltaic cell and a generic purpose audio amplifier. The photovoltaic cell frequency is chosen due to its photosensitive behaviour and large sensitive surface. Its frequency response is characterized by an AC sweep from 10 Hz to 100 kHz on control input of implemented LED driver. Such frequency response is shown in Figure 26.

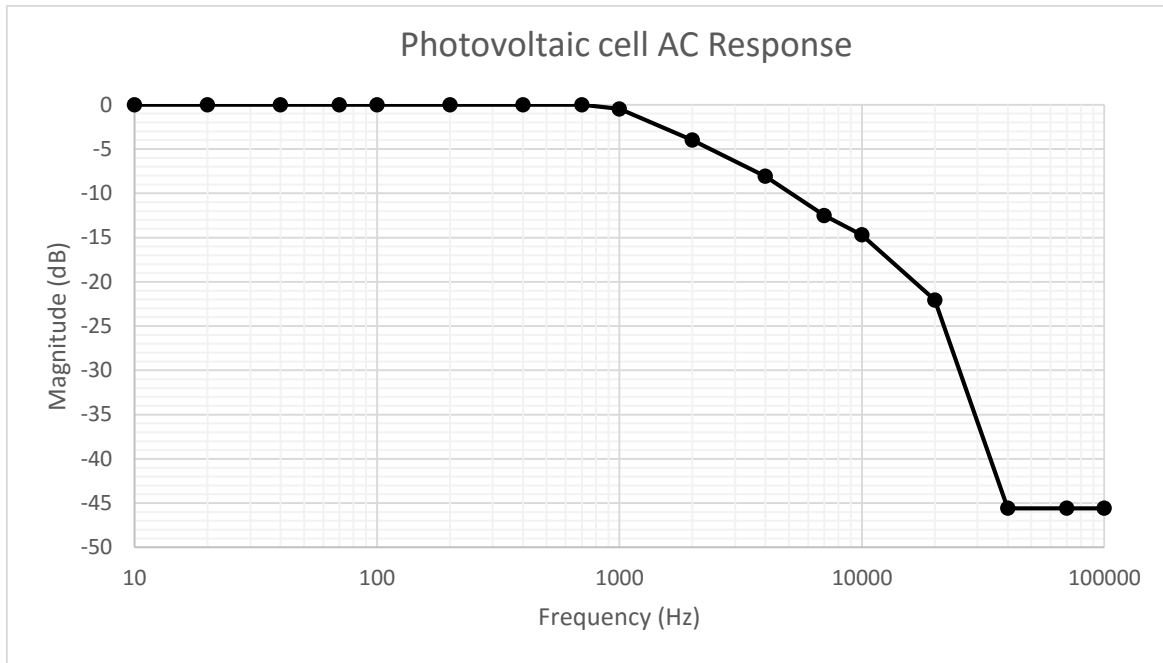


Figure 26. Photovoltaic cell used in this project AC response.

Evaluating the results from Figure 26, a 2 kHz bandwidth is defined for the photovoltaic cell. While such value may seem limited for working with audio signals, for the evaluation of this system is enough to work with mid-band audio frequencies.

Receiver is implemented using the solar cell in combination with an audio amplifier as shown in Figure 27.

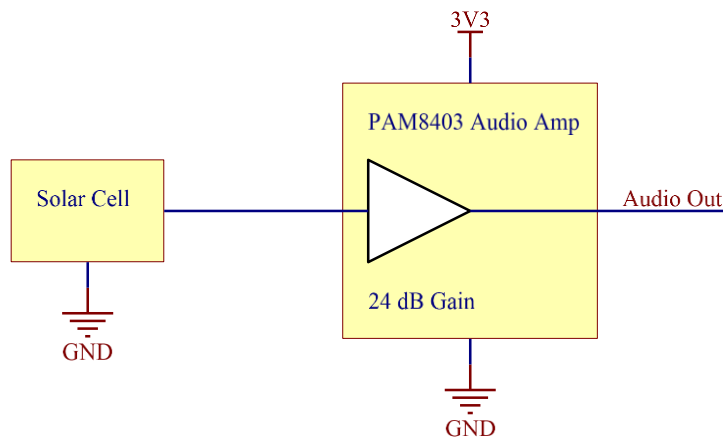


Figure 27. Audio over visible light receiver scheme.

First tests show that the perception of the received audio is clear, although it lacks the low frequencies due to the filtering to avoid light flickering and high frequencies because of the bandwidth offered by the photovoltaic cell as shown in complete system frequency response from Figure 28.

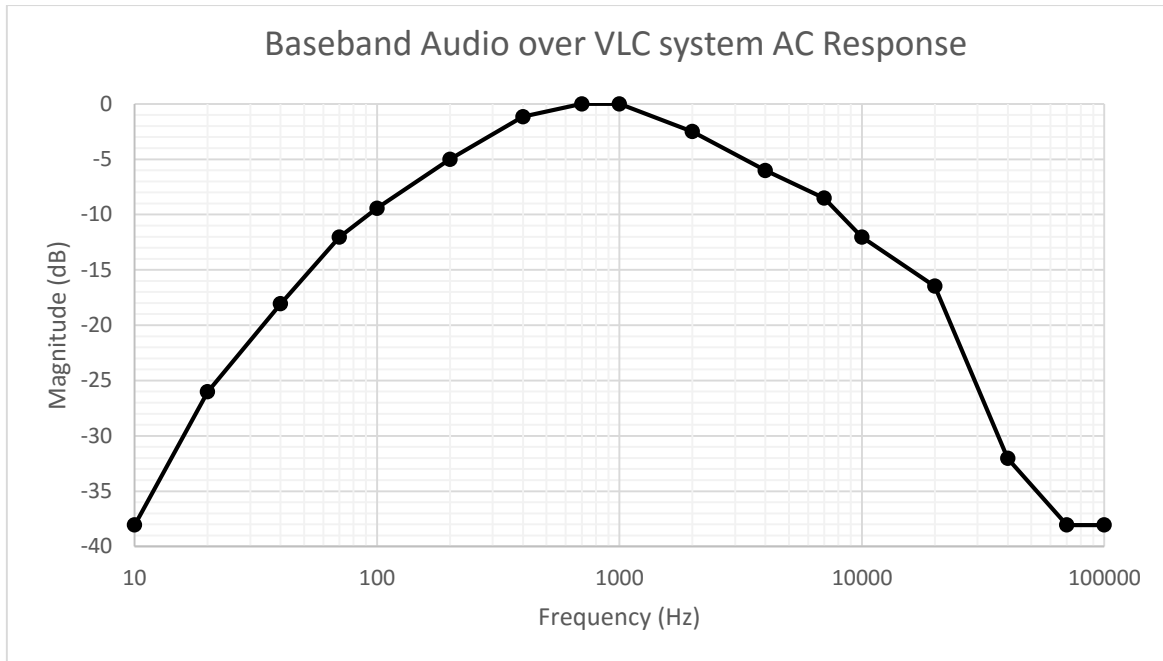


Figure 28. Complete Baseband Audio over VLC system Frequency response.

These tests are performed in a laboratory with interferences from fluorescent lights. Such interferences fluctuate at twice the frequency of the mains voltage and generate a 100 Hz interfering signal which can be clearly noticed in the received audio. Such interference must be further filtered at the receiver.

For such purpose, we use a Twin-T Notch filter configuration with 100 Hz centre frequency, designed using a web application for this purpose [13]. Figure 29 shows the schematic of such filter, while Figure 30 shows its response. Finally, Figure 31 shows its real waveform once captured in the oscilloscope.

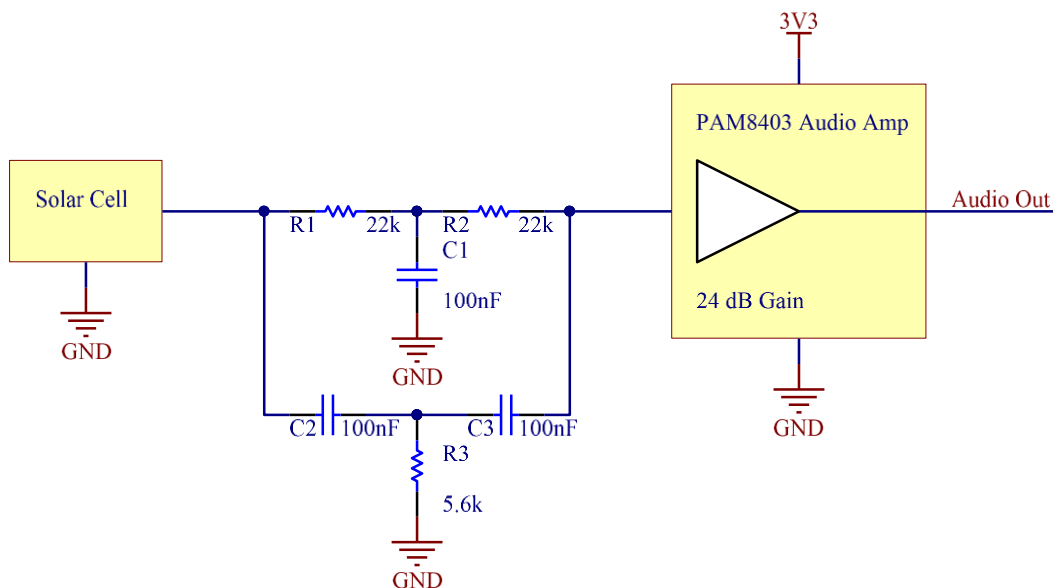


Figure 29. Audio over visible light reception scheme with Twin-T Notch filter.

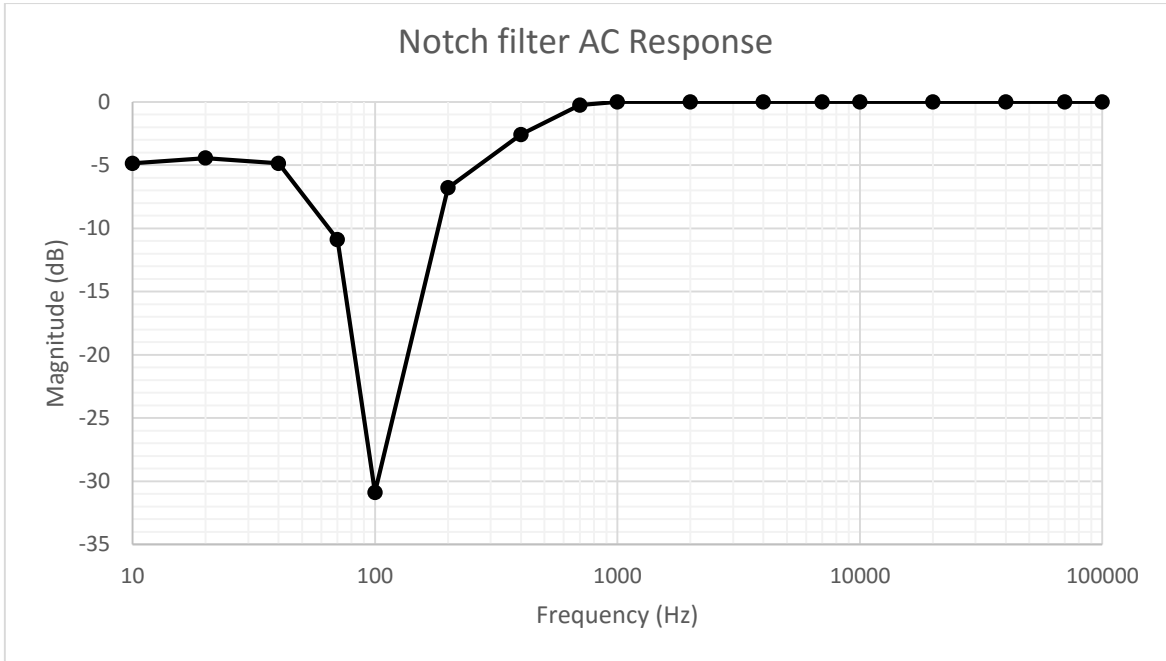


Figure 30. Twin-T Notch filter, configuration implemented in Figure 29 , with center frequency at 100 Hz AC response.

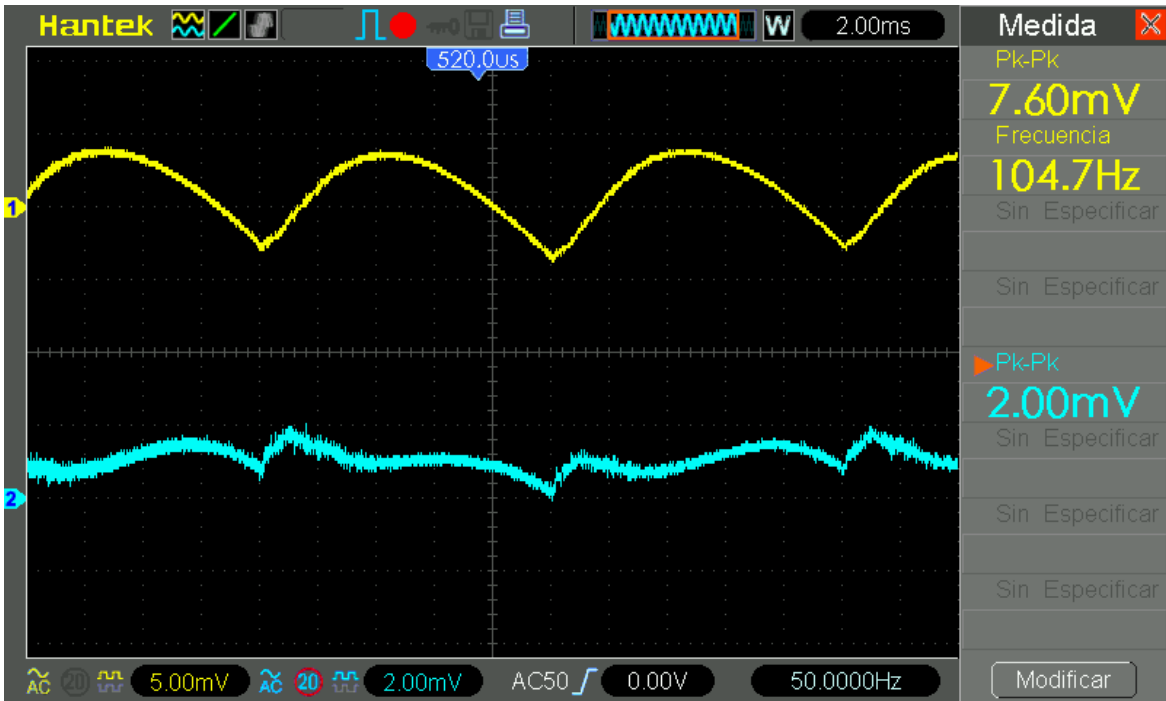


Figure 31. Oscilloscope screenshot measuring fluorescent interference, CH1 received signal on photovoltaic cell, CH2 notch filter output.

Figure 31 shows the aspect of the interfering signal generated by the fluorescents (CH1). It is not a pure sinusoidal waveform as expected from the mains voltage frequency, in fact

it has the aspect of a full rectified waveform. This is because fluorescents, or incandescent lamps, work with both positive and negative half-cycles in the same way. Therefore, a signal rich in harmonics is obtained. Consequently, the result of filtering (CH2) has a peculiar aspect, not being exactly the interfering signal attenuated.

To evaluate the application's throughput, a complete prototype of the system is implemented by using 2 AAA type batteries and shown in the Figure 32.



Figure 32. Audio over visible light receiver prototype.

#### 4.1.3. Conclusions of implemented application

The results are satisfactory, the quality of the sound being equivalent to the one offered by a telephone conversation, as indicated by several test subjects. It is possible to distinguish the received audio signal up to a 5-meter distance. Obviously, for this system, the greater is the distance, the less is the amplitude of the received signal. In the following application, we solve this issue by including Frequency Modulation.

#### 4.2. FM Audio over VLC

To improve the performance of the previous implementation of baseband audio over VLC, modulating audio as in FM is considered as a possible improvement. This should make the system more independent of the distance between the transmitter and the receiver.

Since we have a bandwidth of 100 kHz, the idea is to have a central frequency of 50 kHz, and a deviation of  $\pm 20$  kHz. A generic purpose Phase-Locked Loop (PLL) allows to implement the modulator and demodulator parts.

A PLL is a control system that generates an output signal whose phase is related to the phase of an input signal. The simplest is an electronic circuit consisting of a variable frequency oscillator and a phase detector in a feedback loop. The oscillator generates a periodic signal, and the phase detector compares the phase of that signal with the phase of the input periodic signal, adjusting the oscillator to keep the phases matched.

In this application, we make use of the CD4046B chip for the modulator and demodulator side. Figure 33 shows different internal blocks of the CD4046B. In this application, we will use the Voltage Controlled Oscillator (VCO) block for FM modulation implementation and phase I detector in combination with VCO for the demodulation.

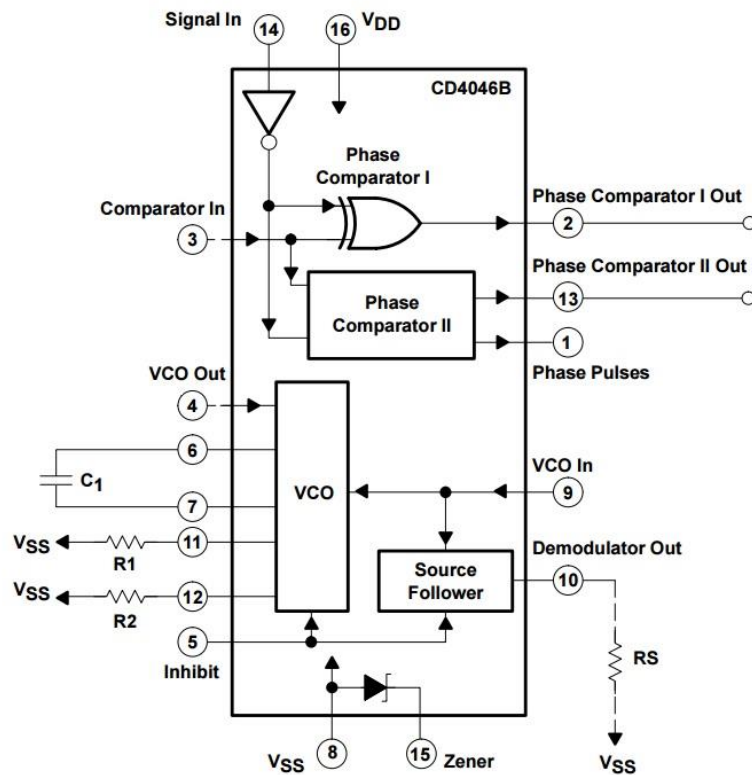


Figure 33. CD4046B internal block diagram.

#### 4.2.1. Frequency modulation implementation

The settings for the FM implementation are as shown in Figure 34.

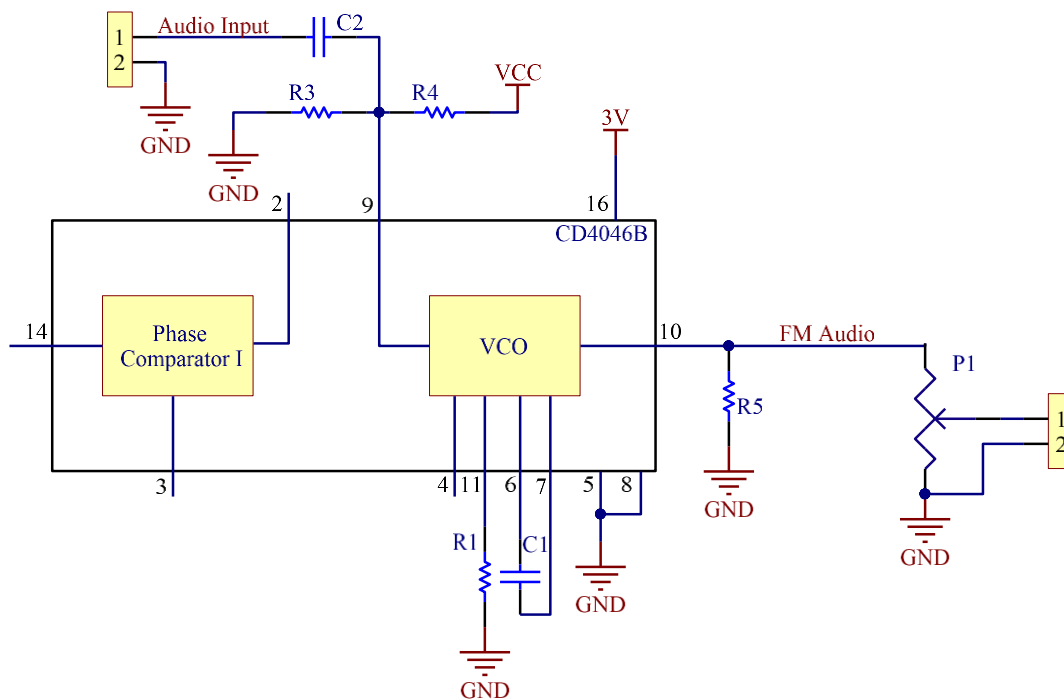


Figure 34. CD4046B diagram for audio FM modulation.

As indicated in the datasheet, the VCO can work at a supply voltage of 3 V. Given its consumption is less than 1 mA, we can make use of the reference voltage provided by the TPS92641 as a voltage source. R1 and C1 set the frequency range of the VCO and they are adjusted to work at 50 kHz when the input voltage of the VCO is half the supply voltage. R3 and R4 sets the half supply voltage at VCO input by which we define  $R3 = R4 = 100 \text{ k}\Omega$ .

Datasheet does not provide a formula to obtain the values of R1 and C1, but these are extrapolated apart from a provided graph. After testing several values, we define the value of  $C1 = 470 \text{ pF}$  and  $R1 = 68 \text{ k}\Omega$ .

The capacitor C2 allows to couple the audio signal on the mean value of VCO input. A value of  $10 \text{ }\mu\text{F}$  is more than enough for the RC network formed by R3, R4 and C2 has less than 10 Hz cut-off frequency. Finally, P1 allows us to adjust the amplitude of the FM signal to adapt it for the LED driver's control input.

We make use of the adaptation circuit implemented in previous application, Figure 23, to interconnect FM modulator and the LED driver.

In order to evaluate the FM modulator behaviour, we make use of equipment configuration shown in Figure 35. The corresponding oscilloscope capture is shown in Figure 36.



Figure 35. Equipment configuration for FM application measurement.

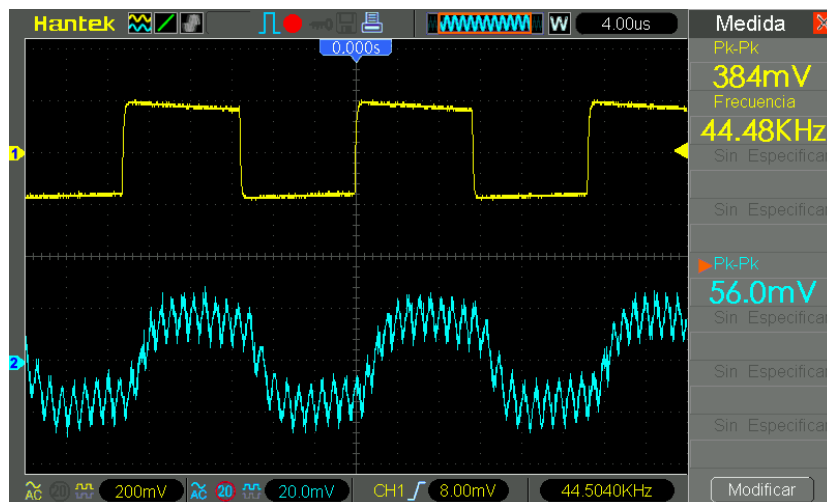


Figure 36. Oscilloscope screenshot, CH1 FM signal, CH2 led current measured through  $R_{cs}$ .

It can be seen in Figure 36, that the measured LED current indirectly from  $R_{cs}$  cannot follow exactly FM signal, due to the high frequencies components of the square-wave signal and its fast rise and fall times. Figure 37 shows the final prototype implementation and the integration with LED driver made for this application.

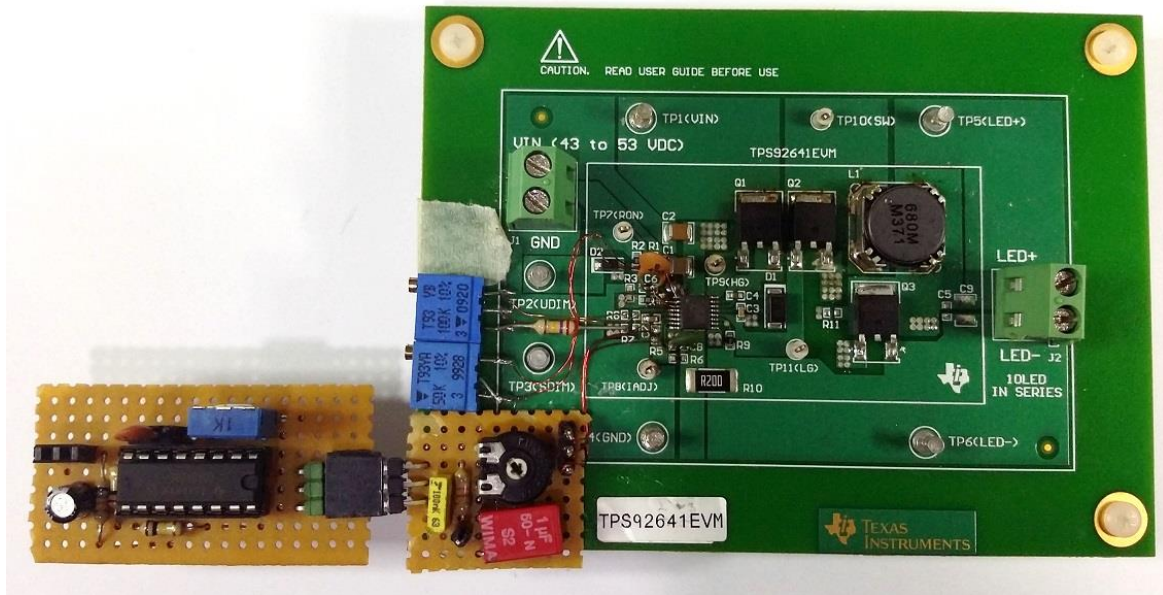


Figure 37. FM implementation and integrated with TPS92641EVM.

#### 4.2.2. Frequency demodulation implementation

For this application, we again need a receiver side capable of managing a bandwidth according to the signals generated by the transmitter. Given the previous analysis of the photovoltaic cell in Section 4.1.2, we discard this component as a possible receiver because it does not provide the necessary bandwidth.

##### 4.2.2.1. VLC receiver

To achieve 100 kHz bandwidth, we opted for the use of a photodiode as a receiver. The OPT101 chip from Texas Instruments is chosen for such purpose.

The OPT101 is a monolithic photodiode with on-chip transimpedance amplifier (TIA). The integrated combination of photodiode and TIA on a single chip eliminates the problems commonly encountered in discrete designs, such as leakage current errors, noise pick-up, and gain peaking due to straight capacitance. Figure 38 shows OPT101 internal block diagram and spectral responsivity.

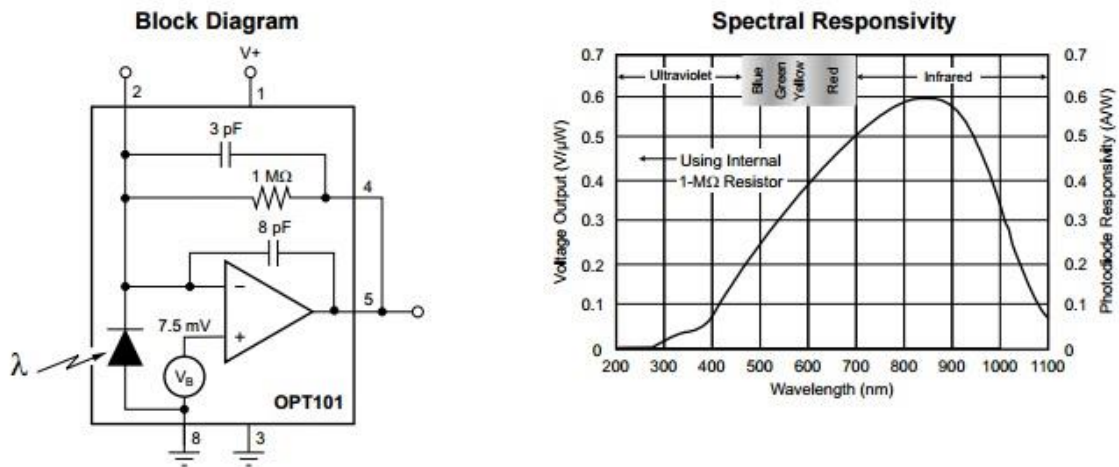


Figure 38. Left, OPT101 block diagram. Right, spectral responsivity.

As seen in Figure 38, the photodiode has a wide spectral response with a maximum peak in the infrared spectrum, and a useable range from 300 nm to 1100 nm. In our case, we want sensitivity over white LED associated wavelength, around 600 nm. The block diagram in Figure 38 shows the mentioned operational amplifier configuration.

The dynamic response of the OPT101 is dominated by the feedback network and op amp combination. Using an internal 1-MΩ resistor, the dynamic response of the photodiode and op amp combination can be modelled as a simple RC circuit with a  $-3$  dB cut-off frequency of approximately 14 kHz. To further improve the frequency response, an external resistor of 100 kΩ is used.

The LED driver is used to characterize the response of OPT101 making an AC sweep from 10 Hz to 100 kHz at control input. The result is shown in Figure 39.

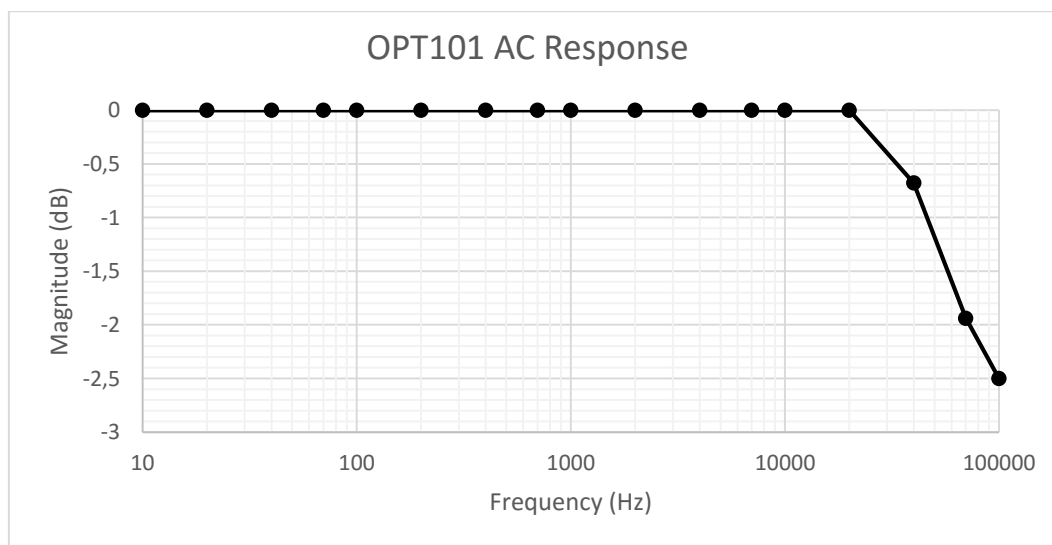


Figure 39. OPT101 AC response with  $R_{ext}=100$  kΩ.

In Figure 39, a 100 kHz bandwidth is achieved successfully. However, as shown in Figure 40, the output voltage level is about 20 mV, not enough to work with. For the demodulator, a second amplification stage is needed.

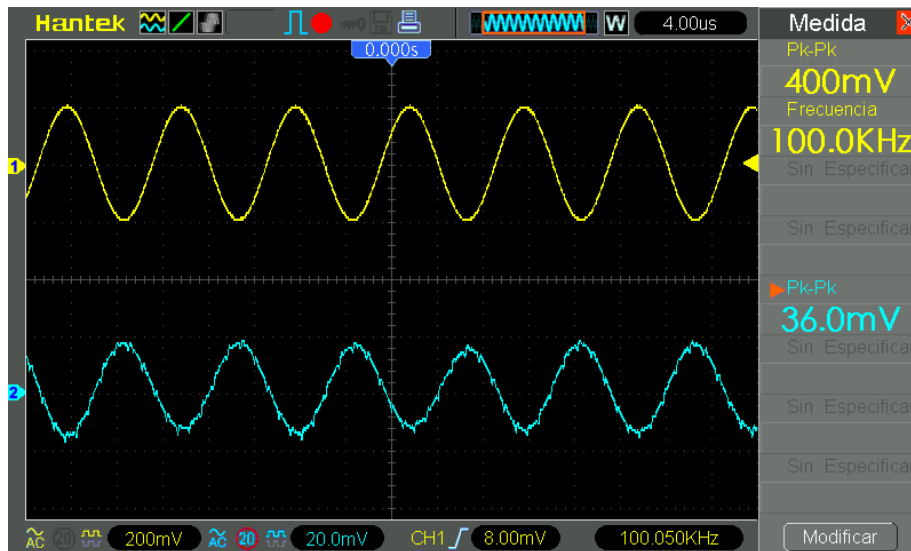


Figure 40. Oscilloscope screenshot, CH1 LED driver control input signal, CH2 OPT101 output signal.

For the second amplification stage, the MAX9814 is used because of featuring an Automatic Gain Control (AGC) to keep the same output level for any distance between transmitter and receiver. The MAX9814 is a low-cost, high-quality microphone amplifier with automatic gain control (AGC) and low-noise microphone bias. The device features a low-noise preamplifier, variable gain amplifier (VGA), output amplifier, microphone-bias-voltage generator, and AGC control circuitry. Figure 41 shows a simplified block diagram of the MAX9814.

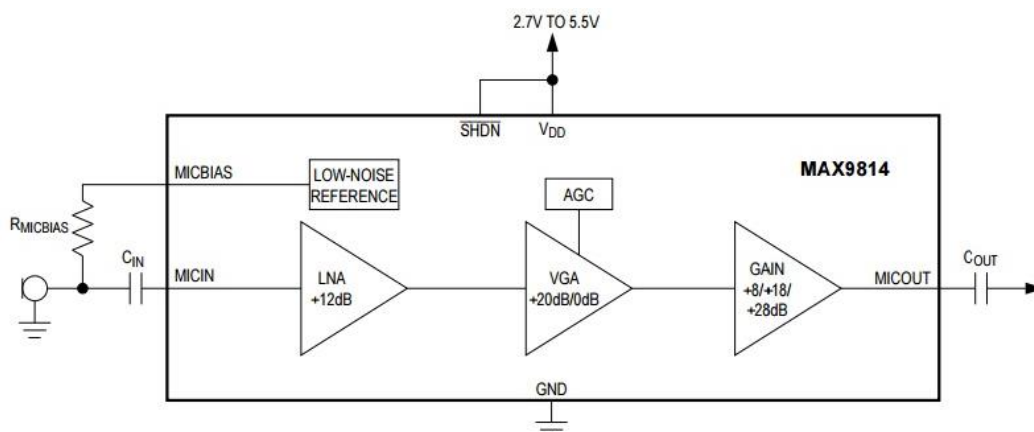


Figure 41. MAX9814 simplified block diagram.

The low-noise preamplifier has a fixed 12 dB gain, while the VGA gain automatically adjusts from 20 dB to 0 dB, depending on the output voltage and the AGC threshold. The output

amplifier offers selectable gains of 8 dB, 18 dB, and 28 dB. With no compression, the cascade of the amplifiers results in an overall gain of 40 dB, 50 dB, or 60 dB. A trilevel digital input programs the output amplifier gain. An external resistive divider controls the AGC threshold and a single capacitor programs the attack/release times. A trilevel digital input programs the ratio of attack-to-release time. The hold time of the AGC is fixed at 30 ms.

The manufacturer doesn't specify a full bandwidth response, so we decide to give it a try. The design criteria for the use of MAX9814 is to configure the overall gain and the attack/release time. For this application, don't have any specific requirement that relates on the attack and release time, which has a direct impact on the AGC stage, so we set a value of 1 ms for the attack time, and 1:4000 attack/release ratio, since we believe that the amplitude of the signal is constant and receiver is placed over a stable surface.

Overall gain is set to 40 dB, 100x gain, so a 2 V output signal amplitude is obtained given a 20 mV input signal amplitude. AGC threshold is set to 1 V to have a good adjustment range.

The figure shows the resulting diagram from the combination of the OPT101 and the MAX9814.

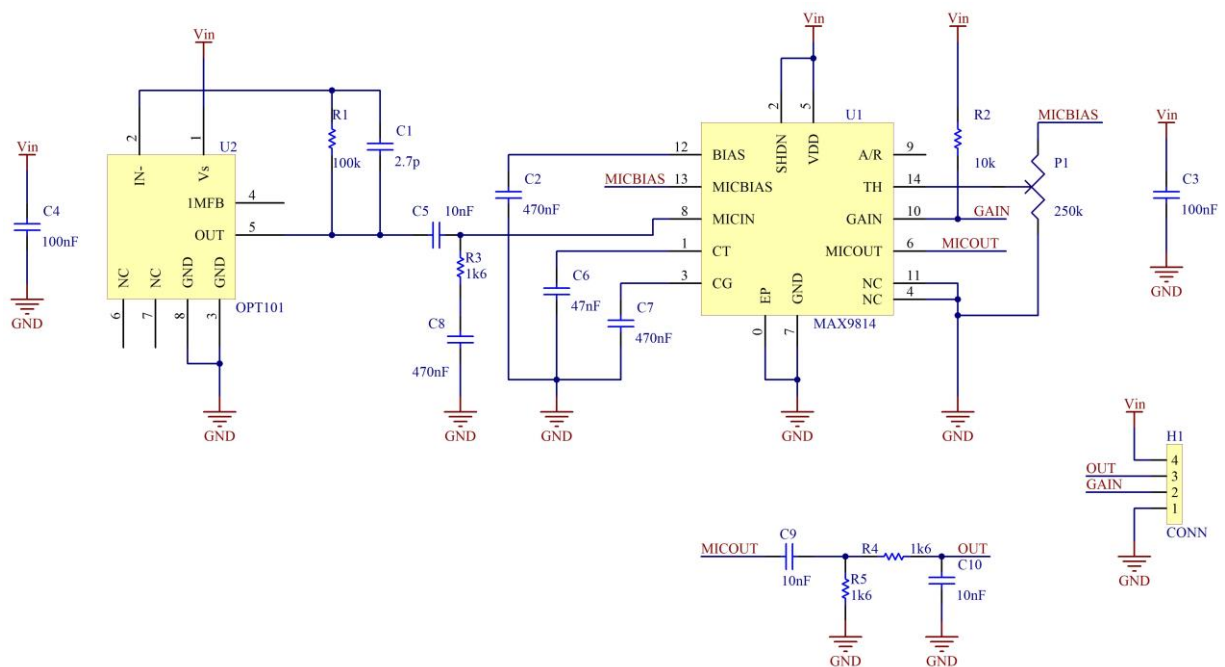


Figure 42. VLC receiver diagram based and OPT101 and MAX9814.

Due to the only available package for MAX9814 is in SMD, a custom PCB design (Figure 43, Figure 44) is made to implement the VLC receiver.

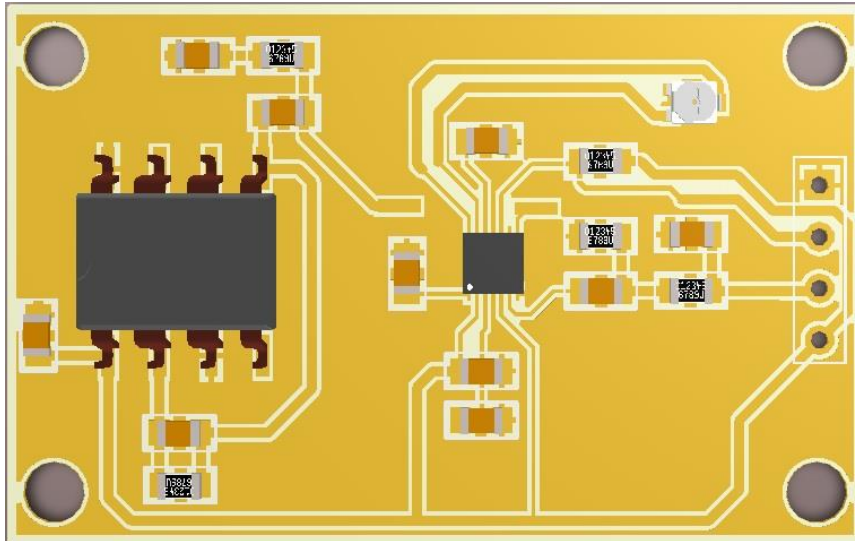


Figure 43. PCB design preview image.

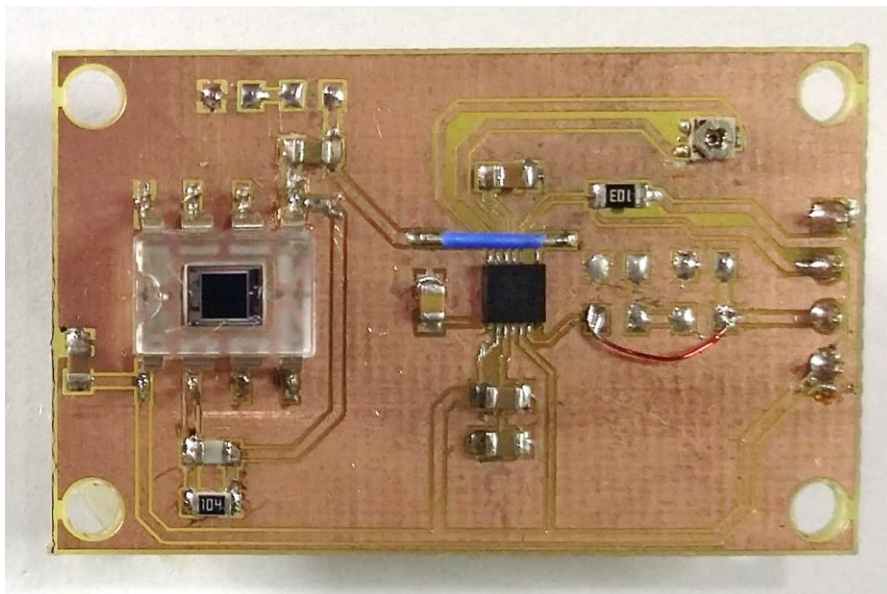


Figure 44. VLC receiver based on OPT101 and MAX9814 prototype.

Tests done at laboratory using the equipment configuration in Figure 45 show that MAX9814 doesn't limit the bandwidth. Thus, 100 kHz bandwidth is defined for this light receiver.



2 meter distance between LED lamp and receiver.

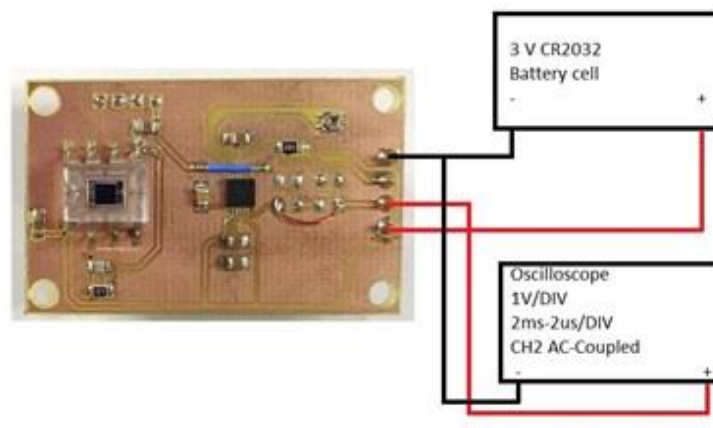


Figure 45. Equipment configuration for receiver evaluation.

Figure 46 shows an oscilloscope screenshot of a measurement with a 100 kHz signal and Figure 47 its FFT representation.

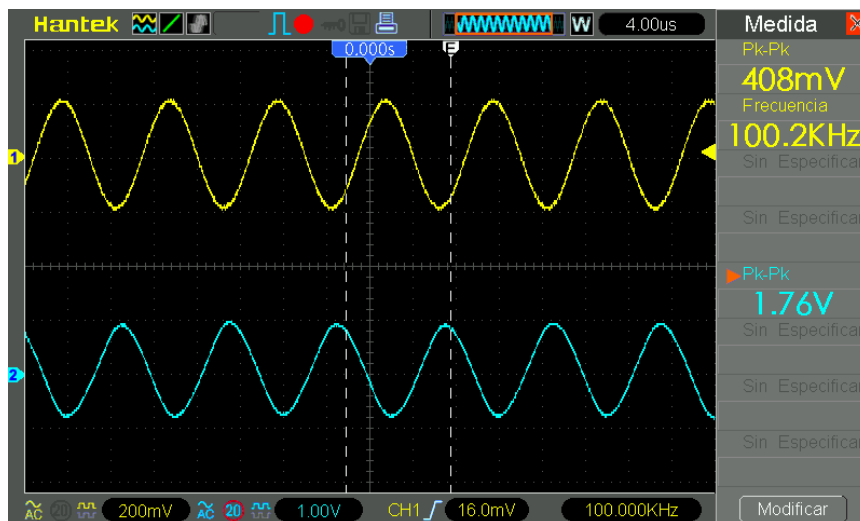


Figure 46. Oscilloscope screenshot, CH1 LED driver control input signal, CH2 Light receiver output signal.

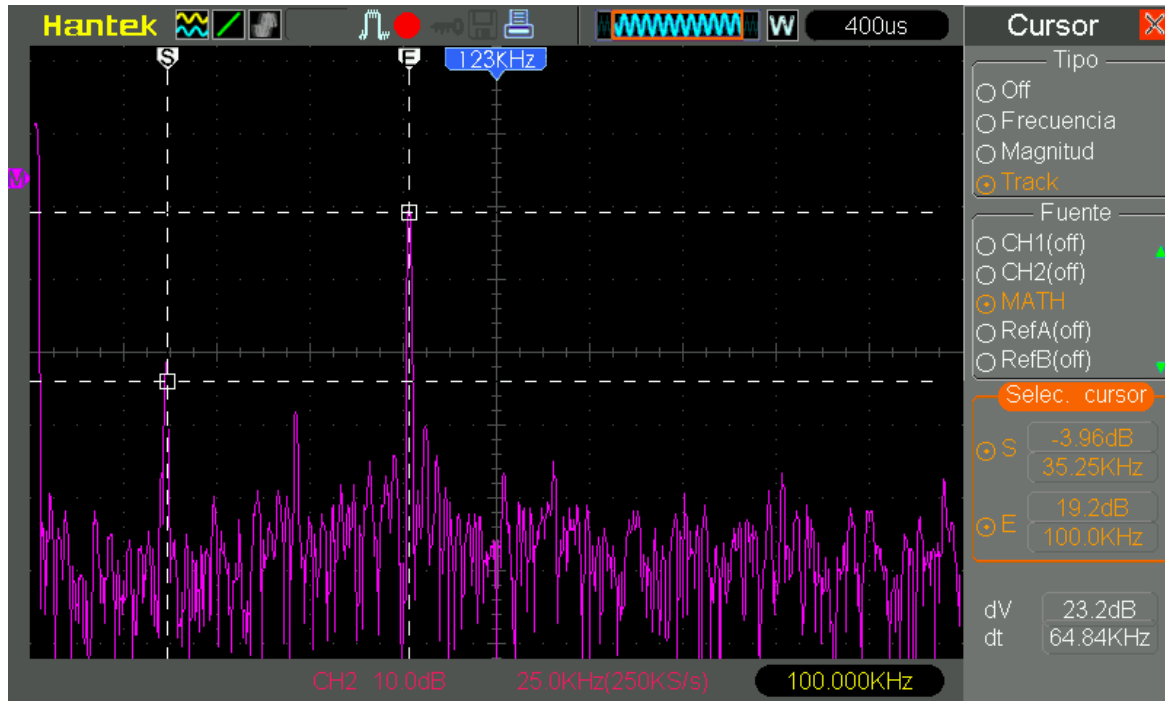


Figure 47. FFT representation of received signal, Figure 46 CH2, Marker “S” is placed at 35 kHz, and “E” at 100 kHz.

The received signal FFT representation from Figure 47 shows frequency components not noticeable at Figure 46 time domain representation. Spike at 100 kHz is due to the LED signal (marker E), and the one at 35 kHz is due to the ambient light, in this case based on LED technology. Because of most ambient light is given by non-modulated LEDs, marker “E” should indicate the switching system frequency of these.

Once the receiver is implemented, we proceed with FM demodulation description.

#### 4.2.3. CD4046B configuration for FM demodulation

Figure 48 shows the diagram of the CD4046B configuration for FM audio signal demodulation.

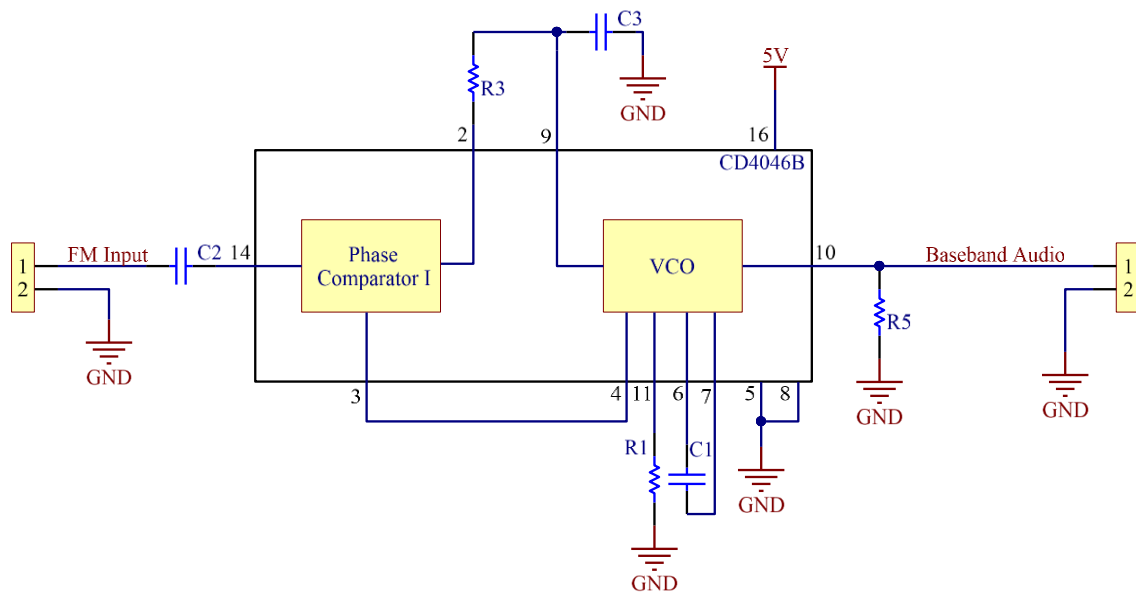


Figure 48. CD4046B diagram for audio FM demodulation.

For the FM demodulation, we used phase comparator I and VCO with feedback loop between both to keep the VCO output locked at input frequency.

In the same way that in the modulator, the centre frequency is configured at 50 kHz, but given that the supply voltage is 5V, the values of R1 and C1 changes respect to the modulator, now being C1 = 1 nF and R1 = 100 kΩ.

The RC network formed by R3 and C3 sets the dynamics of the input frequency tracking control. Since we work with audio signals, we want to allow the loop follows 20 kHz signal. This parameter is called the frequency capture. Starting from the formula that it provides the manufacturer, R3 and C3 are defined:

$$f_c = \frac{1}{2 \times \pi} \sqrt{\frac{2 \times \pi \times f_o}{R_3 \times C_3}} \quad (\text{eq. 18})$$

Where  $f_o$  is the central frequency, in this case 50 kHz.

R3 = 47 kΩ and C3 = 470 pF gives a close value to frequency capture of 20 kHz:

$$f_c = \frac{1}{2 \times \pi} \sqrt{\frac{2 \times \pi \times 50 \text{ kHz}}{47 \text{ k}\Omega \times 470 \text{ pF}}} = 18980 \text{ Hz} \quad (\text{eq. 19})$$

Whole system is evaluated. Figure 49 shows the resulting AC response.

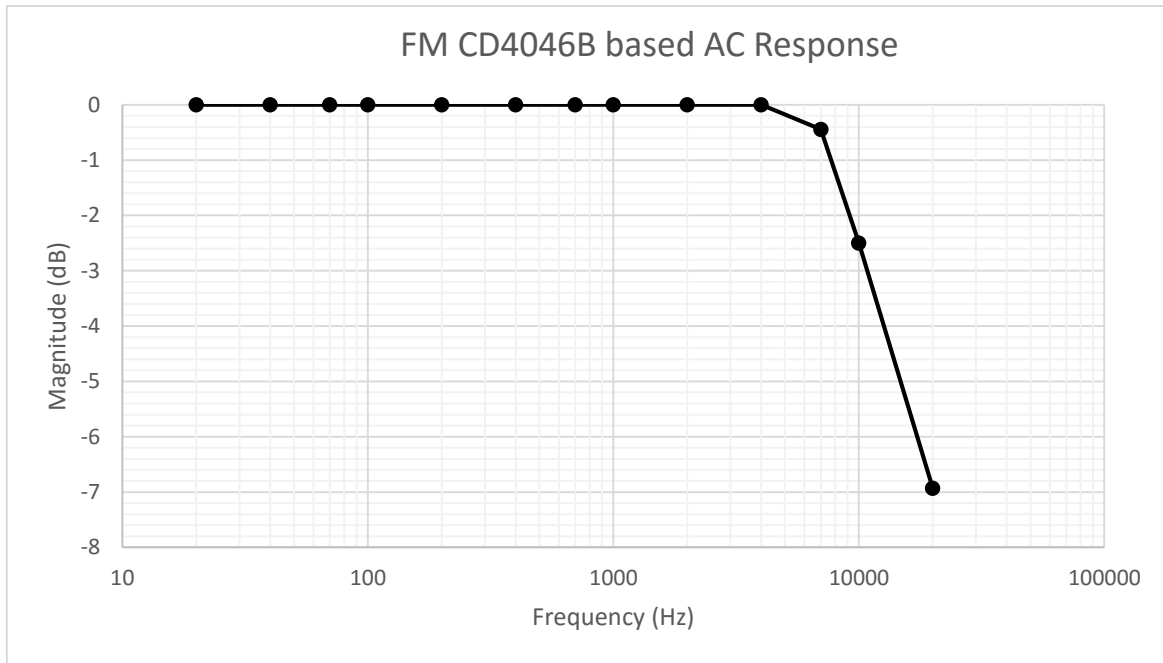


Figure 49. FM audio through light system AC response.

As shown in the Figure 49, the bandwidth is less than 20 kHz, although use case tests carried out give a good result in terms of sound quality. Figure 50 shows the prototype of the receiver next to the one done for the demodulation of FM signal.

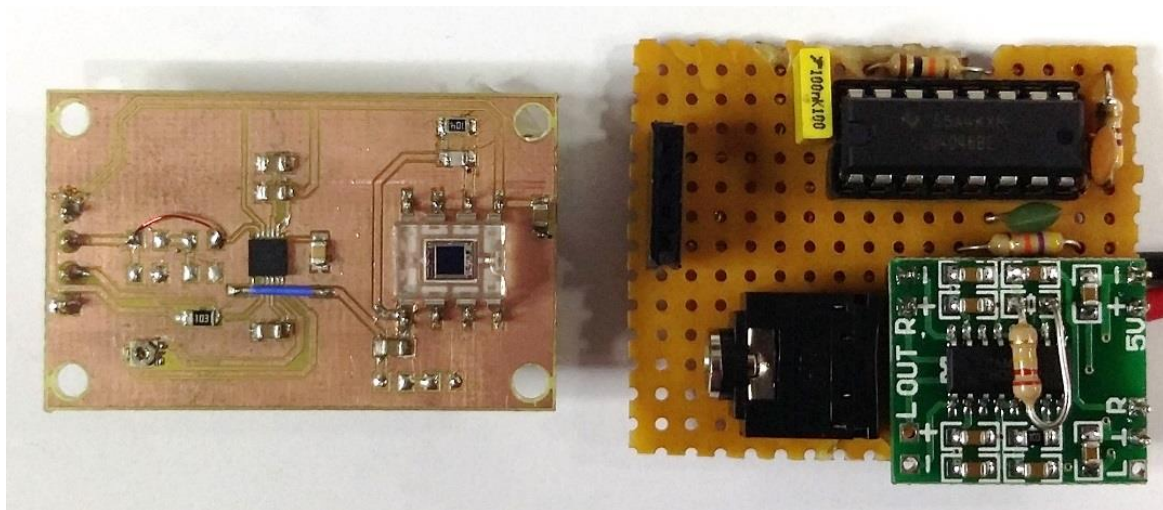


Figure 50. Left, VLC receiver prototype. Right, FM audio demodulation prototype.

#### 4.2.4. Conclusions of implemented application

In relation to the previous implementation of Baseband Audio over VLC, the sound quality improves since it incorporates both the low and high audio frequency components. On the other hand, to achieve a good sound quality it is required that the environment does not have interfering light.

As a curiosity, testing of the earlier application with VLC receiver implemented gives good results improving high frequency band sound quality.

### 4.3. OFDM VLC based system evaluation

This application focuses on evaluating data transmission. We want to check that the LED driver is capable of transmitting signals from analog modulations, specifically ones based on OFDM signals. The idea is to use a commercial OFDM-based modem that works in the range of frequencies that designed VLC LED driver supports. In the search, we find G3-PLC technology and motivation is to combine both technologies, VLC and PLC.

#### 4.3.1. G3-PLC technology

In 2011, several companies including distribution network operators (ERDF, Enexis), meter vendors (Sagemcom, Landis&Gyr) and chip vendors (Maxim Integrated, Texas Instruments, STMicroelectronics) founded the G3-PLC Alliance to promote G3-PLC technology. G3-PLC is the low layer protocol to enable large scale infrastructure on the electrical grid. G3-PLC may operate on CENELEC A band (35 kHz to 91 kHz) or CENELEC B band (98 kHz to 122 kHz) in Europe, on ARIB band (155 kHz to 403 kHz) in Japan and on FCC (155 kHz to 487 kHz) for the US and the rest of the world.

The technology used is OFDM sampled at 400 kHz with adaptive modulation and tone mapping. The required media access control is taken from IEEE 802.15.4, a radio standard. In the protocol, 6LoWPAN has been chosen to adapt IPv6 an internet network layer to constrained environments which is PLC.

G3-PLC has been designed for extremely robust communication based on reliable and highly secured connections between devices, including crossing Medium Voltage to Low Voltage transformers. In December 2011, G3 PLC technology was recognised as an international standard at ITU in Geneva where it is referenced as “G.9903. Narrowband orthogonal frequency division multiplexing power line communication transceivers for G3-PLC networks”.

Table 6 shows the different standards for G3-PLC technology along with the range of frequencies to operate. It can be seen the CENELEC A standard fits into the frequency range supported both by transmitter and receiver.

Band	Number of carriers	First carrier (kHz)	Last carrier (kHz)
CENELEC A	36	35.9375	90.625
CENELEC B	16	98.4375	121.875
FCC	72	154.6875	487.5
ARIB	54	154.6875	403.125

Table 6. MAX79356 frequency bands standard supported.

There are several commercial options to implement this system. We opted for the use of the MAX79356 chip because is the only one that integrates analog front end block by only requiring few outside components to work with a minimal configuration.

#### **4.3.2. MAX79356**

ZENO™ (MAX79356) is a programmable narrowband orthogonal frequency division multiplexing (OFDM)-based PLC modem system-on-chip (SoC) device that provides standards compliant high performance and secured powerline communication in a small package. ZENO integrates two pipelined 32-bit RISC processors to offer high performance and future-proof flexibility which perform dedicated PHY signal processing functions and MAC layer functionality. Figure 51 shows the typical configuration for the MAX79356.

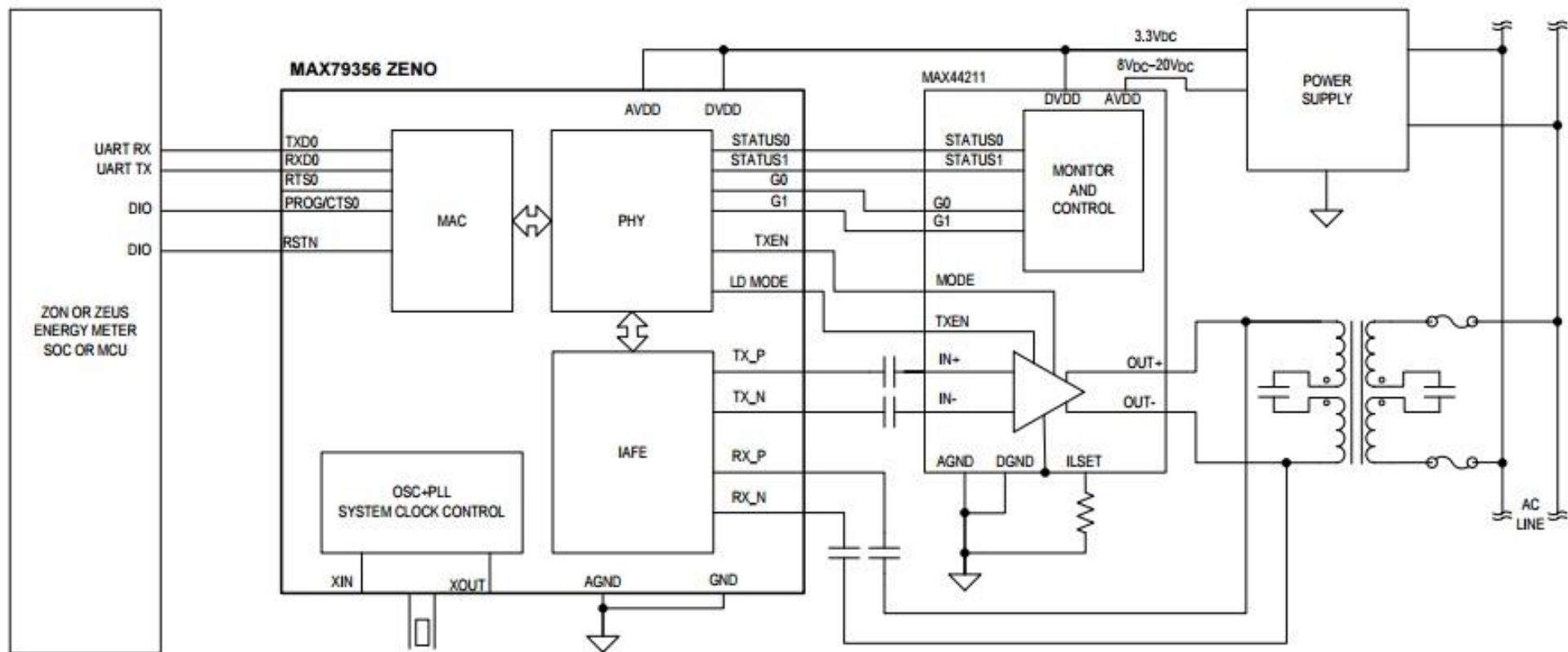


Figure 51. MAX79356 typical configuration.

MAXIM has a Development Board, MAX79356CAEVK1, with the configuration shown in the Figure 51. However, its price (1500 €) is well above the budget allocated for this project. Failing that, we decided to buy the discrete component and make an adaptation board to fit it into a protoboard.

Figure 52 and Figure 53 shows the minimum configuration diagram for the transmitter and receiver respectively.

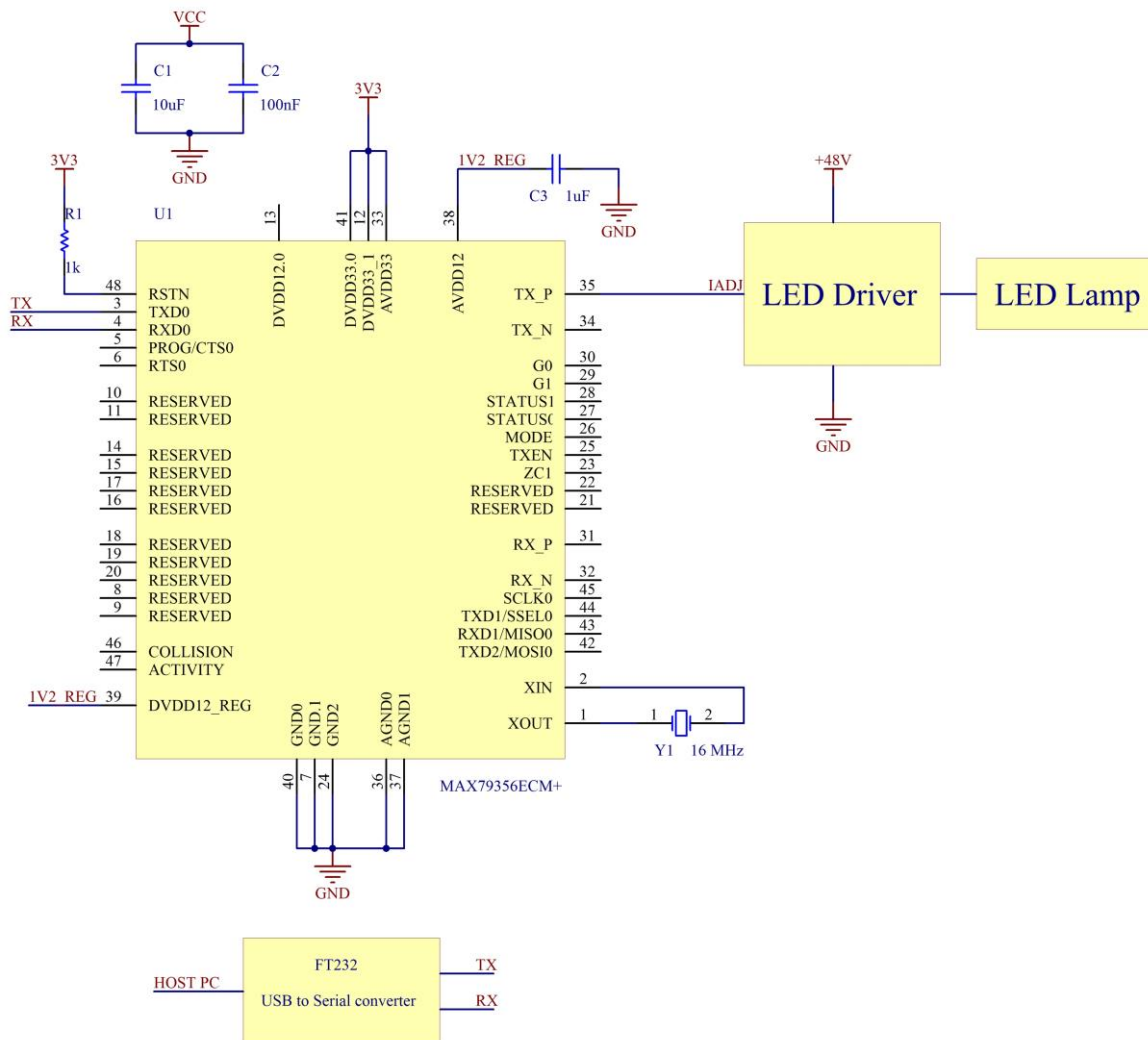


Figure 52. Transmitter diagram with minimum configuration based on MAX79356.

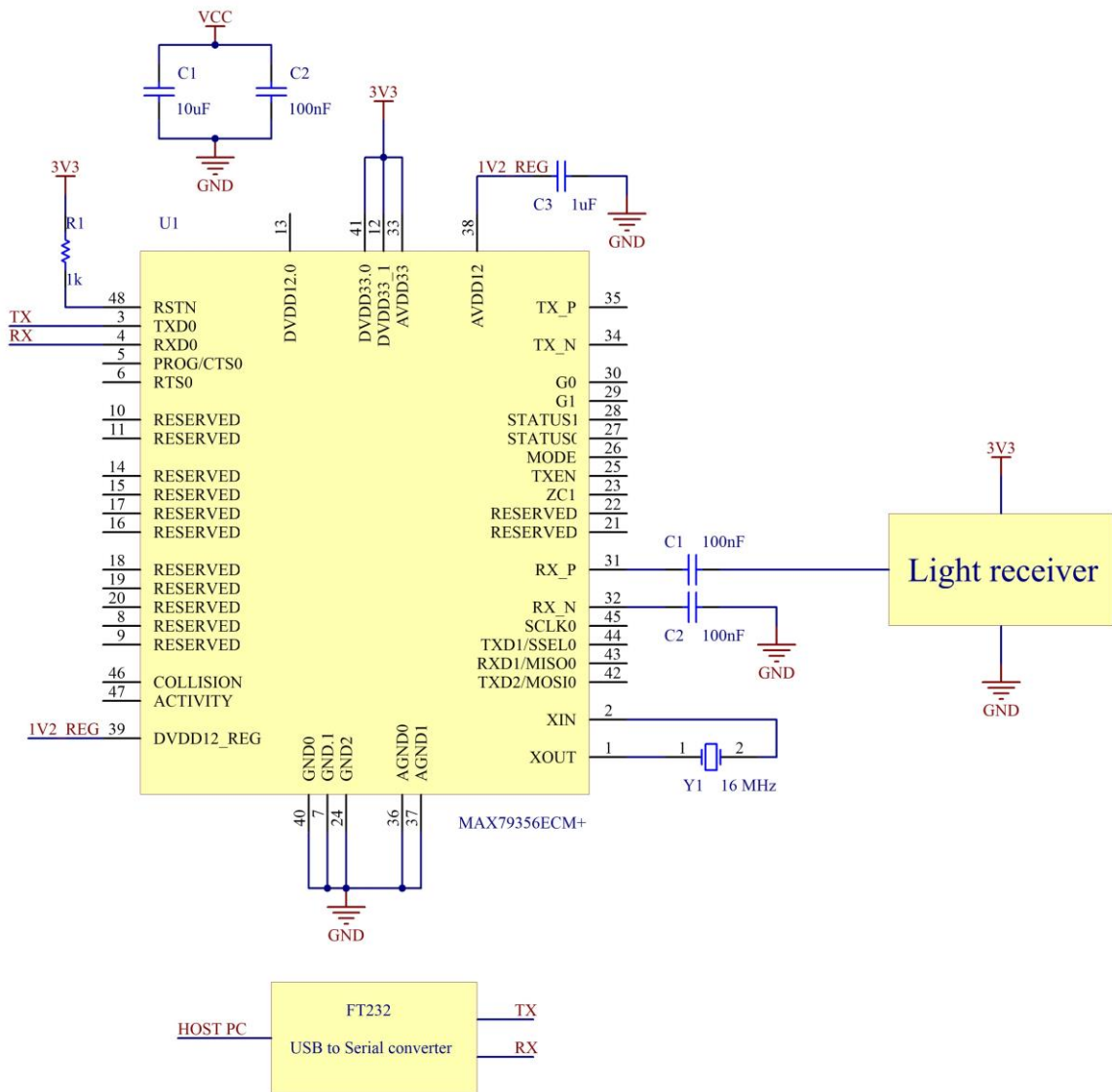


Figure 53. Receiver diagram with minimum configuration based on MAX79356.

Both transmitter and receiver are implemented in hardware as shown in Figure 54 and Figure 55.

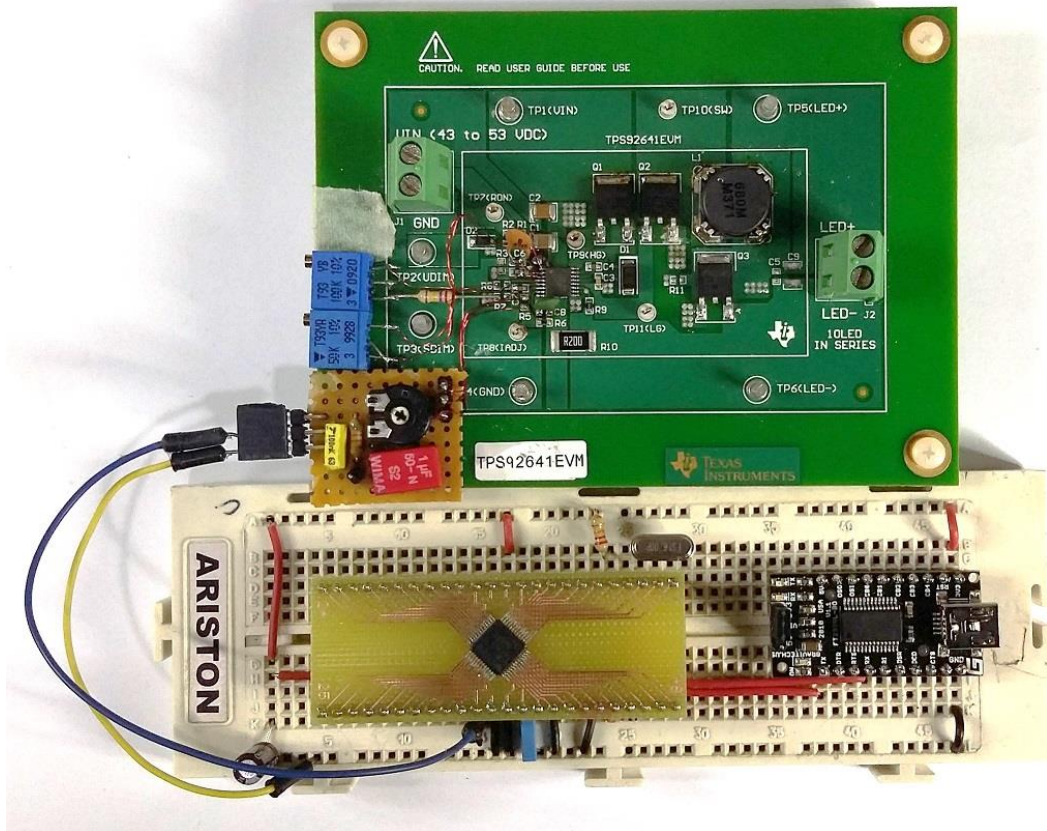


Figure 54. Implemented MAX79356 based transmitter.

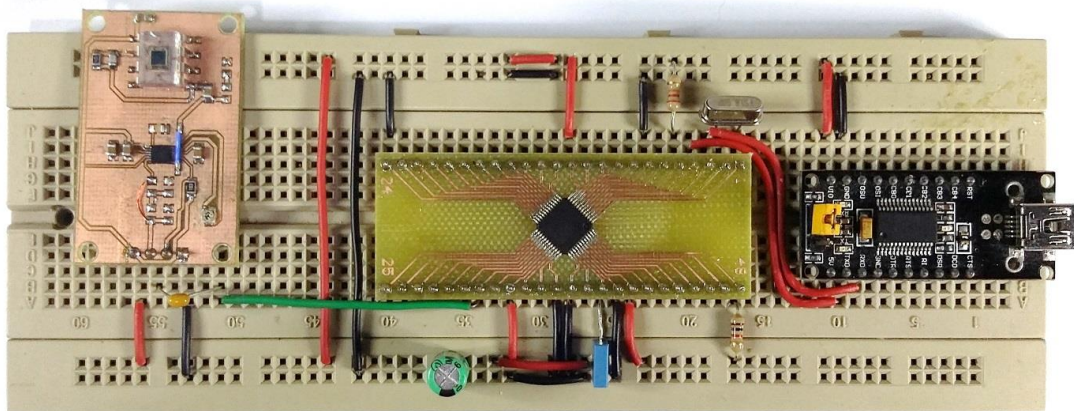


Figure 55. Implemented MAX79356 based receiver.

The MAX97356 purchased by default comes without software, and MAXIM only provides the documentation and necessary files for programming with development kit. After several research and e-mail exchanging with the team in charge of this product, we managed to obtain such documentation and software, and proceed to test the performance of the chip.

The MAX79356 has three different versions of firmware available for use:

- **SimpleMAC Firmware and GUI:** used for testing the PHY and channel in a point-to-point setup. You can select modulation type, packet size, band etc in TX on the evaluation board and check the error rate in RX. The interface to this firmware is through the GUI supplied with the EVKit and you should not use it for your own product.
- **FullMAC Firmware:** G3-standard firmware supporting all features of G3. There are 3 separate certified firmwares for 3 bands plus our latest universal band firmware supporting all bands (recommended). The interface to this firmware is using UART and through a set of primitives described in “G3 PLC Modem Interface Specification Rev 4.3”, available from our FTP site.
- **Transparent UART Master and Slave:** This firmware is very easy to integrate into a solution. It broadcasts all data received in UART of Master to all Slaves. It unicasts all data in UART of each slave to Master only. This can be used in a similar way to RS485. Unlike #2, this firmware only supports point-to-point communication between Master and Slaves and does not including forwarding.

#### 4.3.2.1. Simple MAC firmware evaluation

SimpleMAC is a test FW/GUI that can be used to demonstrate primarily functionality of PHY. Different parameters such as modulation, band, frame length, tone map, among others, can be quickly changed and FER can be measured. To evaluate the Simple MAC firmware performance, we make use of the software provided by maxim, ZENO Simple Connect with the configuration shown in Figure 56.

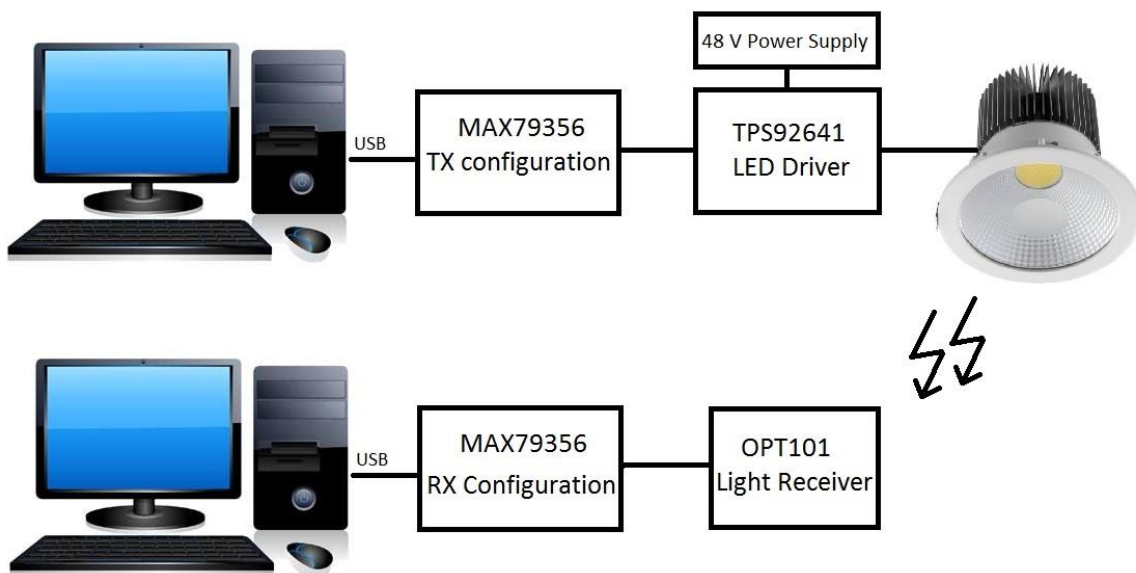


Figure 56. Devices configuration for evaluate Transmitter-Receiver system based on MAX79356.

If the board is properly connected and powered, ZENO Simple Connect software main window should look like Figure 57.

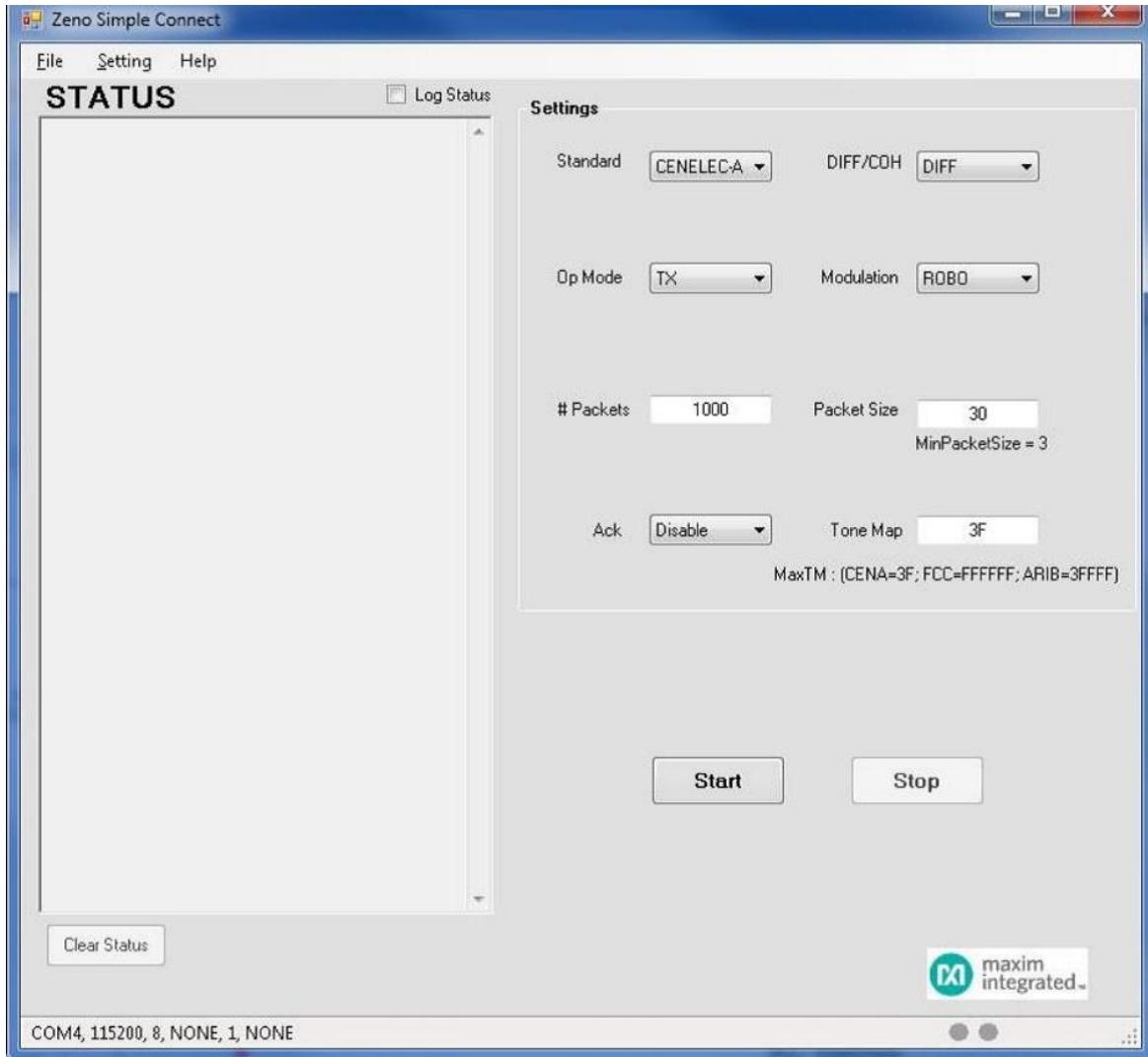


Figure 57. ZENO Simple Connect software main window.

### Transmitter configuration

Select the instance of Simple Connect associated with the evaluation board that is intended to the transmitter. The following items may be configured via drop-down windows or text windows:

- **Standard:** The “Standard” drop-down selects the frequency band to be used (CENELEC-A, FCC, or ARIB)
- **DIFF/COH:** Selects differential or coherent modulation
- **Op Mode:** Selects transmit or receive operation. The Simple Connect software only supports one-way communications.
- **Modulation:** Selects the type of modulation to be use by the transmitter. ROBO, BPSK, QPSK, 8PSK modulation schemes are available.
- **# Packets:** Selects the maximum number of packets to be transmitted when the “Start” button is clicked.
- **Packet size:** Selects the number of bytes per packet. The minimum is 3 bytes/packet

- **Ack:** Enables or disables ACK/NACK handshaking between transmitter and receiver
- **Tone Map:** Allows enabling or disabling specific tones within the tone map defined for the frequency band. Setting a bit to 1 in the hexadecimal value enables the tone in the bitmap corresponding to the position of the bit in the mask value, and clearing a bit disables the corresponding tone. The default setting is that all tones are enabled.

### Receiver configuration

To select and configure the receiver modem, it is only necessary to select an Op Mode of RX and to select the frequency band selected for the transmitter.

To start communication between the two boards, it is only necessary to click the “Start” button for each instance of the Simple Connect software. The transmitter instance will display the number of transmitted frames in the status window.

The receiver instance will display a running count of the number of frames received, the cumulative number of Frame Check CRC (FCHCRC err) errors and packet CRC (CRC err) along with an average data rate (RX Rate).

There are several tests carried out by varying the settings in the transmitter to try to obtain the maximum transfer rate. The configuration with which we get the highest transfer rate, 40000 bps, is:

**Standard:** CENELEC-A

**DIFF/COH:** Differential

**Modulation:** 8 PSK

**Packet size:** 200

**Ack:** disable

**Tone Map:** 3F

Figure 58 shows the result of the performed test.

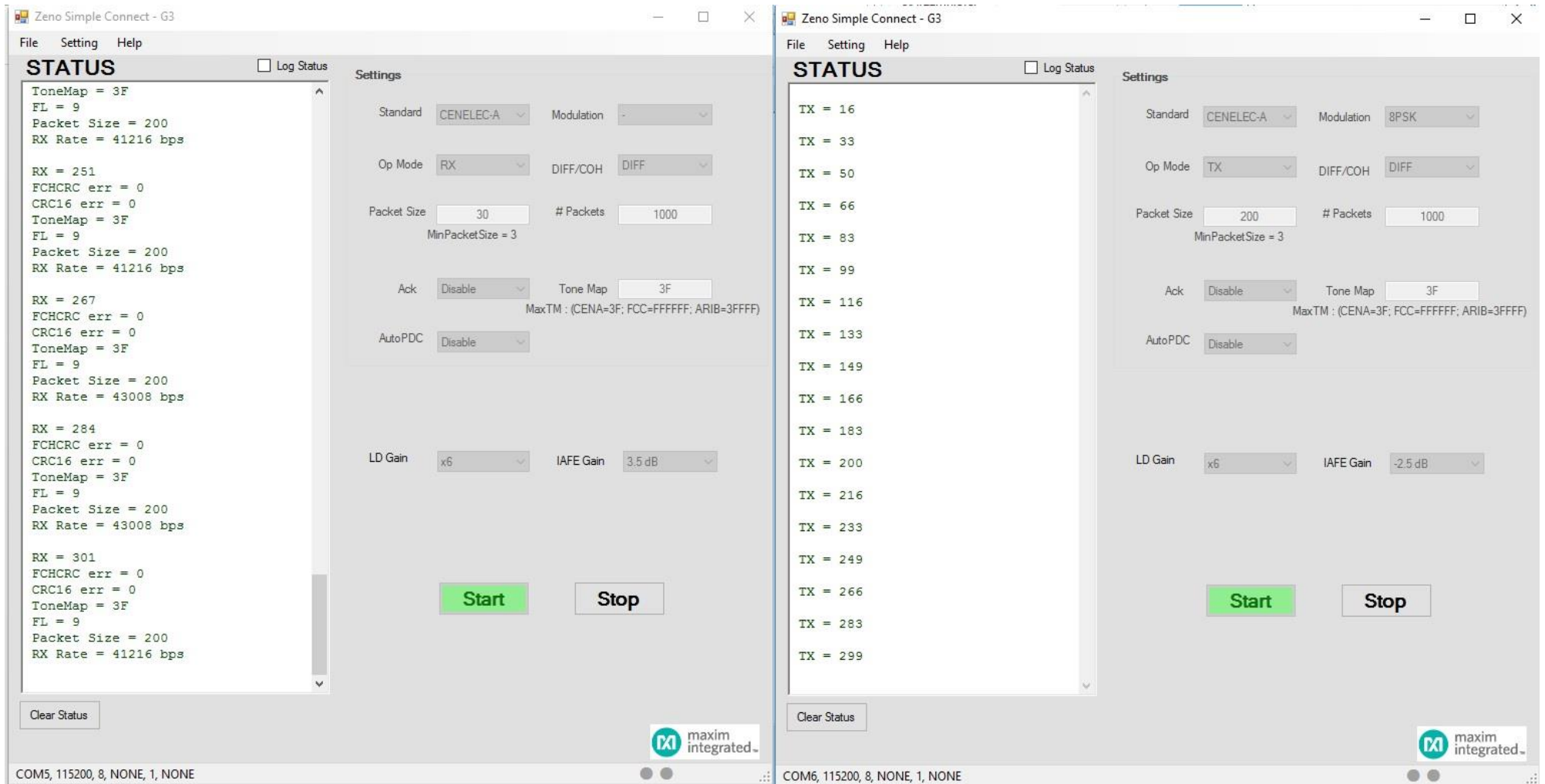


Figure 58. ZENO Simple Connect software screenshot with both transmitter, right side of image, and receiver, left side of image, showing the highest transfer rate achieved.

By observing the transfer rate, we can conclude the main factor that defines it is the used modulation. The Table 7 shows the maximum speed obtained in function of the modulation. Noteworthy is the robustness of the system. Even if the sensor is out of vision line, it continues to operate, this is due to the G3-PLC technology robustness.

<b>Modulation scheme</b>	<b>Data rate</b>
ROBO	5148 bps
BPSK	18952 bps
QPSK	32680 bps
8PSK	43008 bps

*Table 7. Maximum speed obtained in function of used modulation.*

It must be considered that this data rates contemplates error detection and correction mechanism, such Forward Error Correction (FEC), and it means redundancy is added in transmitted data.

Figure 59 shows an oscilloscope screenshot of the signal transmitted and received, using similar configuration as in Figure 45.

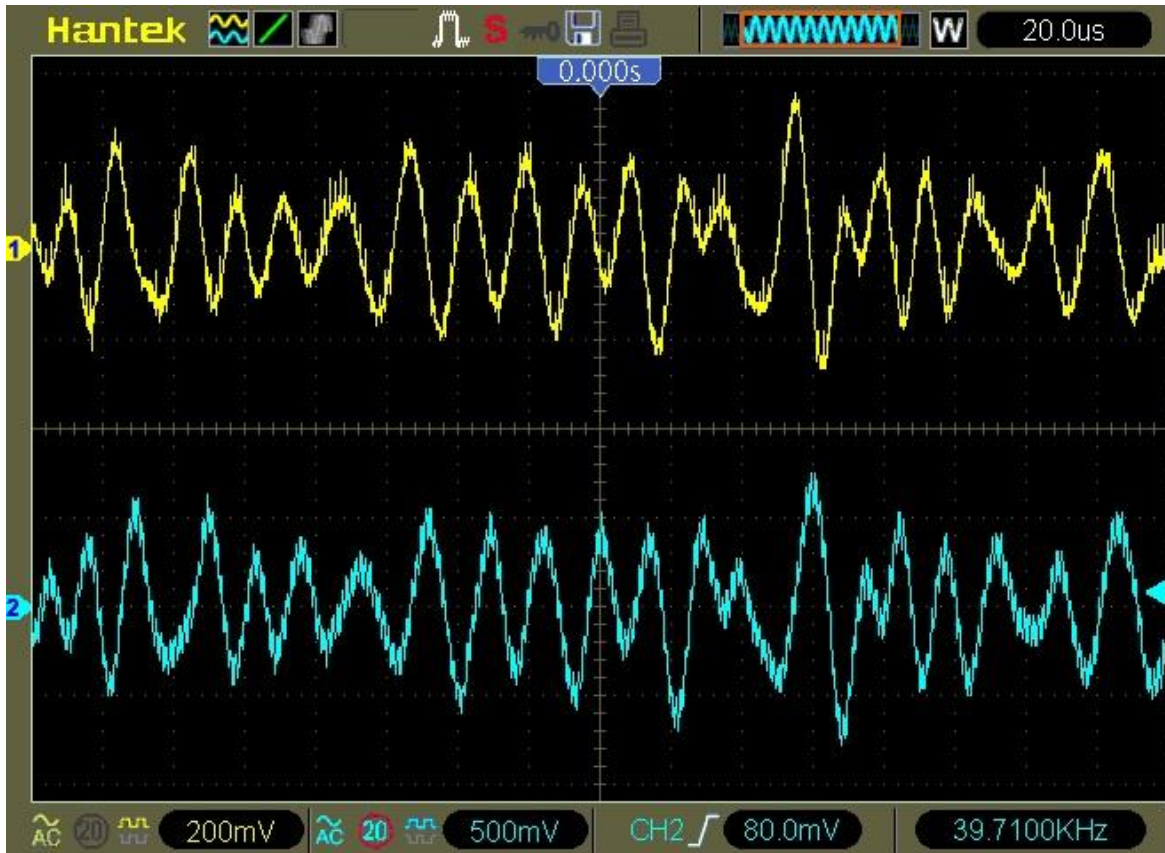


Figure 59. Oscilloscope screenshot, CH1 LED driver signal input, CH2 Light receiver output.

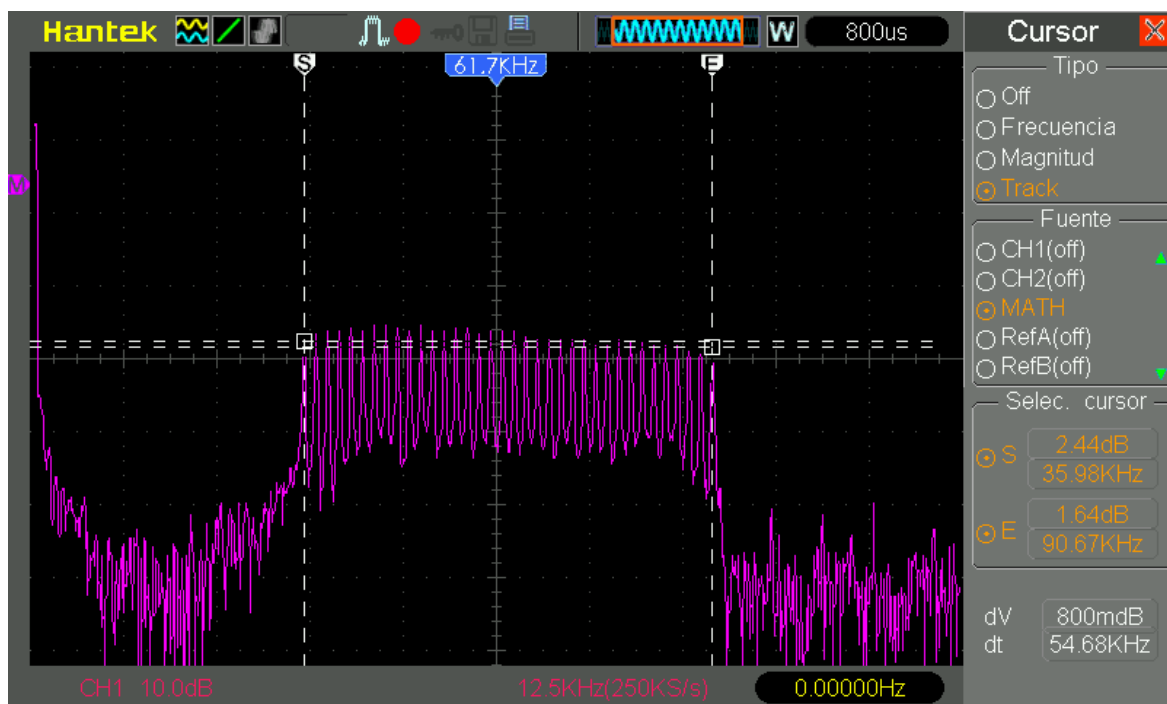


Figure 60. FFT representation of PLC transmission signal at Figure 59. Marker "S" and "E" are placed at first carrier, 35 kHz and last carrier, 90 kHz.

As shown in Figure 60, is represented the FFT of the generated PLC transmission signals. Markers position match with the CENELEC-A frequency specification shown at Table 6, also is possible to distinguish individually each carrier, and the sum of them is 36.

Simple Mac firmware allows to evaluate the physical layer of this component but does not allow the sending of specific data. Full Mac firmware allows a wide range of options, and we focus on the transmission of packets in broadcast mode.

### 4.3.2.2. Full MAC firmware

For Full Mac firmware version, we make use of a different software from the previous one, also provided by maxim, *G3 PLC connect*. Such software includes all the possibilities of the *G3-PLC technology*, and thus a wide variety of configurations. After installing the software, Figure 61 shows the aspect of the first program execution.

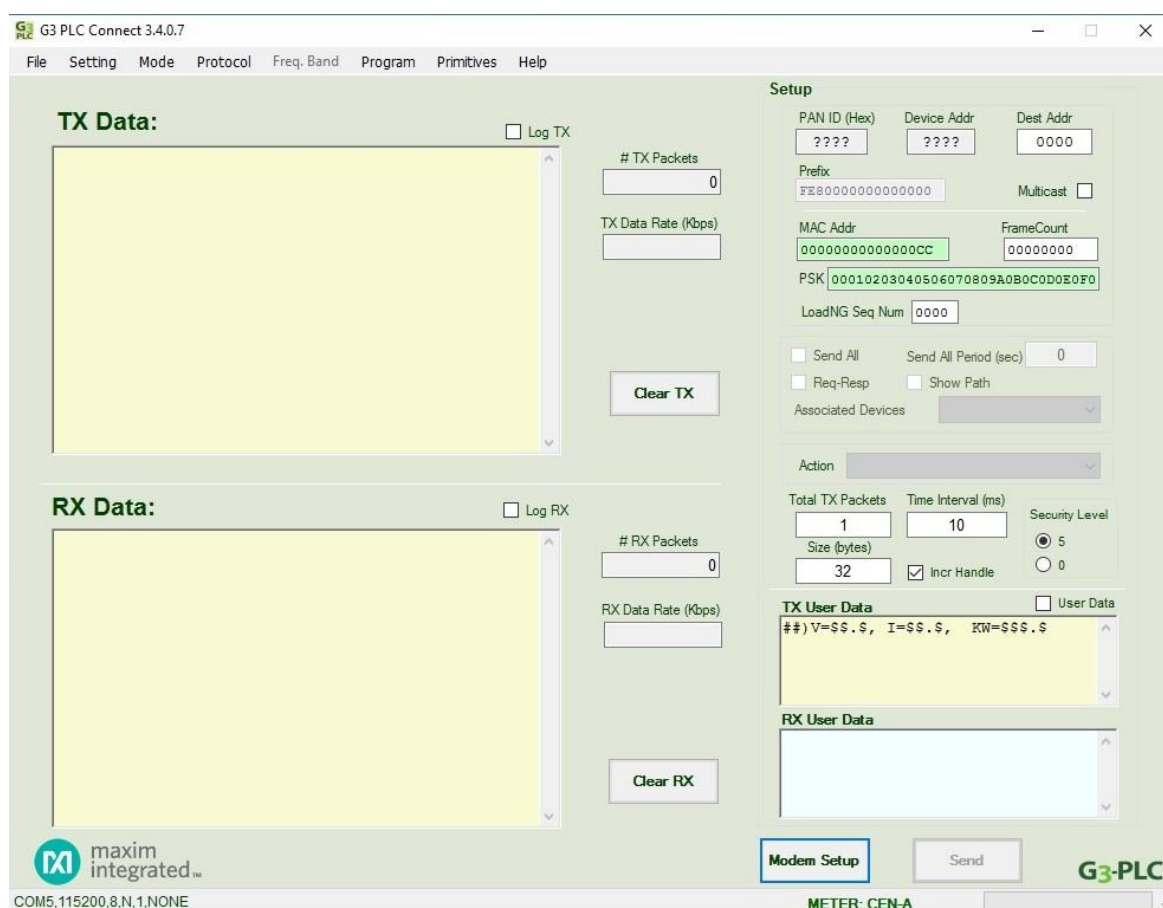


Figure 61. First start of G3 “PLC connect” application screenshot.

We want to evaluate the performance of the system making use of the application layer, and the way is to configure the device for broadcast transmission. At receiver side, is configured to receive such broadcast packets.

For achieve a valid configuration, G3 Modem interface specification has been deeply studied. Using Figure 56 scenario, after setting up the transmitter and receiver, we can establish the communication. The transfer rate decreases down until 1.3 kbps. This is due to the added data by application layer. The simpleMAC firmware shows PHY throughput and does not include overhead of MAC and 6LoWPAN header, segmentation, interframe gap, CSMA, etc.

Figure 62 shows the capture of the software with used configuration after receiving several packets from the transmitter.

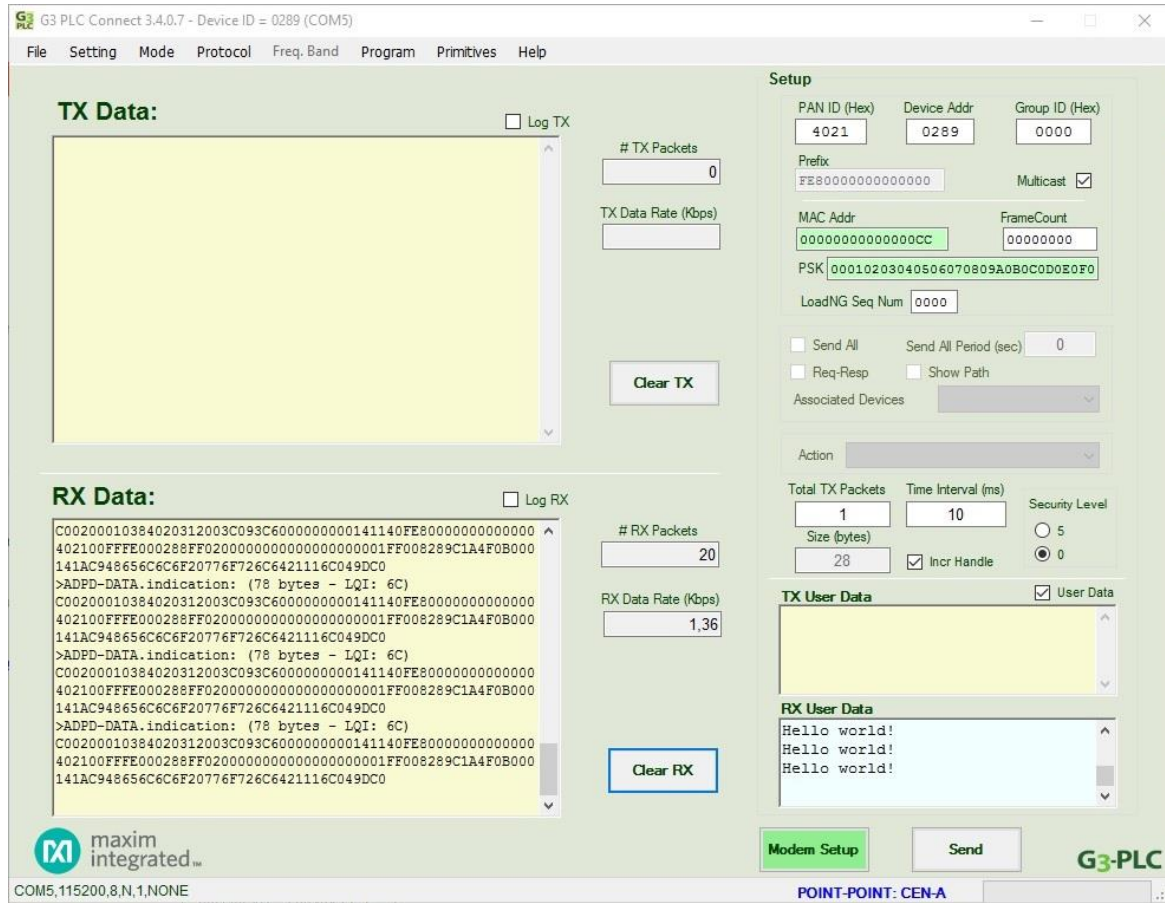


Figure 62. G3 PLC Connect software screenshot after correctly receiving several packets from transmitter.

It is possible to replace the program provided by maxim for another platform as MCU's or Single Board Computers, the only requisite is that they have a serial interface. From here, it is necessary to well known the G3-PLC standard to handle communication correctly.

#### 4.3.2.3. Transparent UART firmware

The Transparent UART firmware cannot be evaluated with the designed transmitter/receiver system, since this requires a two-way channel so it is skipped in this study and considered as a candidate for future work.

#### 4.4. Custom modulation evaluation

Finally, an application aiming to improve the data throughput of the previous application is implemented in a system based on microcontrollers. We want to evaluate transmission performance, in terms of transfer rate, without incorporating error detection/correction mechanism. For this, a custom transmission / reception topology is developed in this application.

#### 4.4.1. Custom modulation transmitter design

The main idea is to get an improved channel performance when compared to FSK or OOK modulation which only can encode 1 bit per symbol. This is carried out setting a symbol table able to encode 2 bits in a single symbol. Table 8 shows our proposed data encoding.

Data	Symbol	Image
00	0	
01	1	
10	2	
11	3	

Table 8. Symbol codification table.

Full period sinusoidal signal is used as a symbol, since the average value of this signal is zero, which ensure no visible light flickering. As the Table 8 shows, the coding consists in modify the phase and amplitude of the sinusoidal signal so that a unique period can encode 2 bits.

Knowing that designed LED driver can work with 100 kHz signals, resulting transmission speed would be over 200 kbps. The transmitter implementation based on the previous coding and according to the previous bit-rate calculation is developed. Figure 63 shows the flow diagram of transmitter operation (see appendix A. for source code).

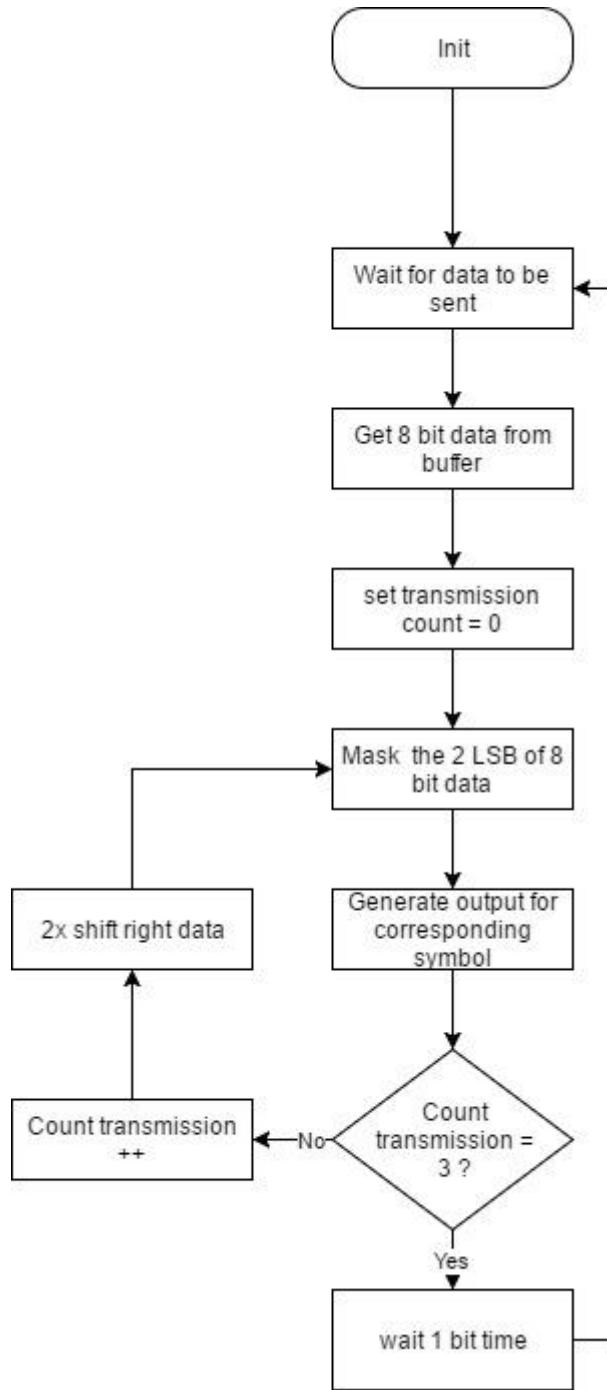


Figure 63. Custom modulation transmitter flow diagram.

Figure 63 flow diagram is implemented in an evaluation board based on the Texas Instruments TMS320F28027 microcontroller unit. Given that this MCU does not include a digital to analog converter able to generate a sinusoidal signal, an 8-bit R2R Ladder DAC as shown in Figure 64 and Figure 65 is implemented. This configuration allows a direct conversion, using only a set of resistors and an operational amplifier.

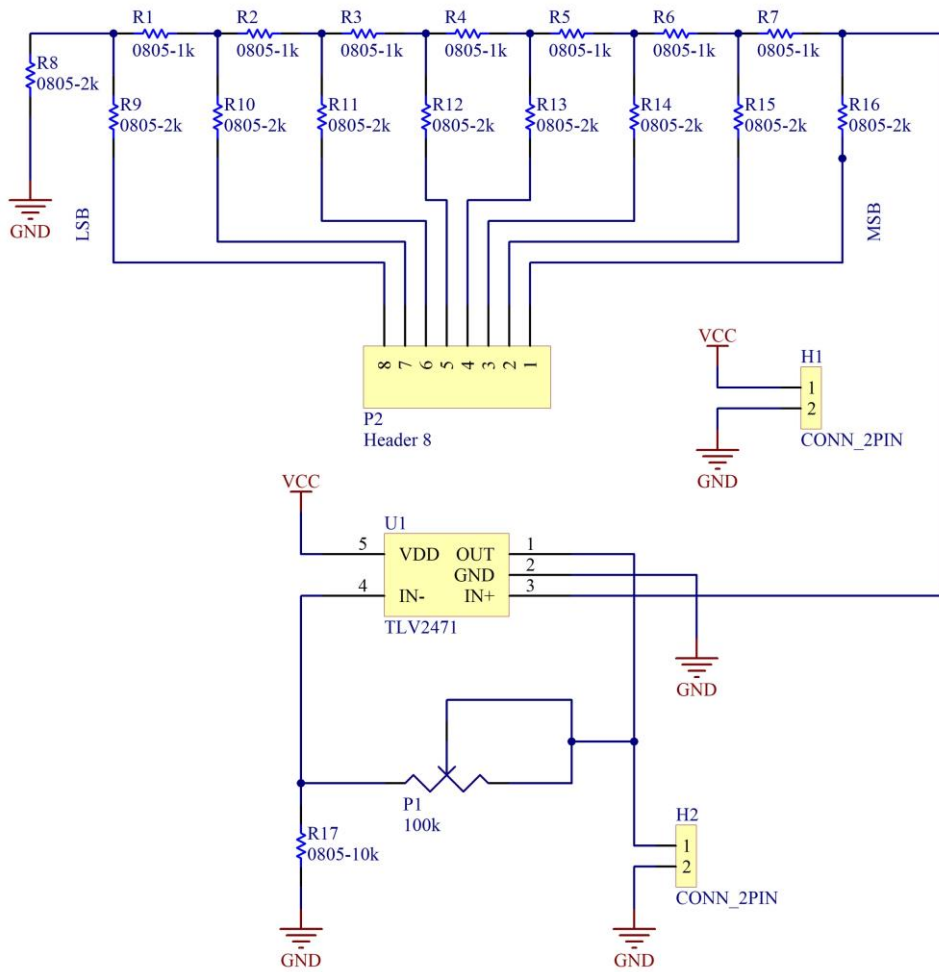


Figure 64. 8 bit R2R ladder DAC converter diagram.

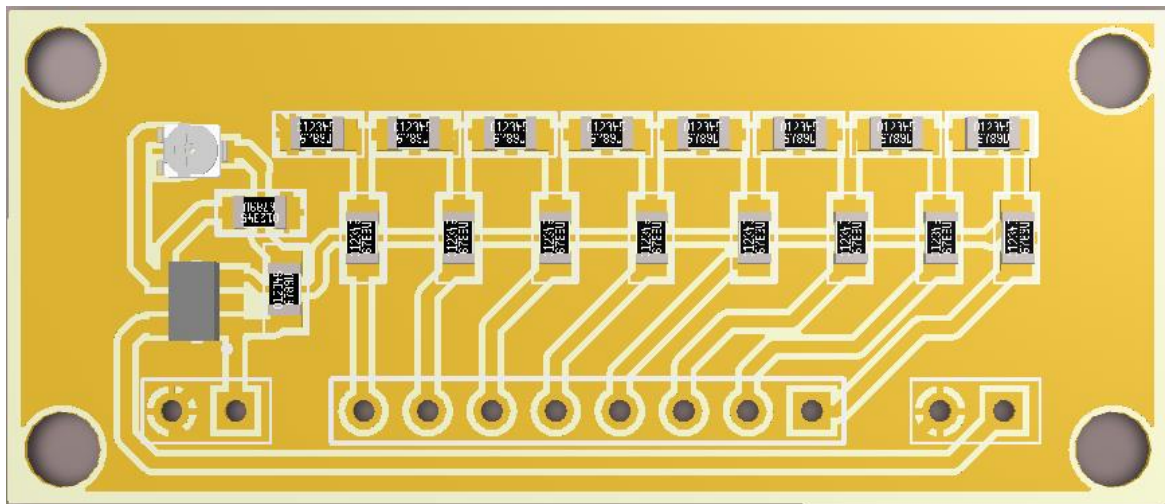


Figure 65. PCB layout of implemented R2R ladder based DAC.

To generate the sine wave signal, a Look Up Table containing 20 evenly samples of a single sine period and with 8-bit resolution for each sample is employed. Each 8-bit sample is generated by the corresponding number of bits from GPIOs of a MCU.

Figure 66 shows the generated signal corresponding to the 4 different symbols defined in Table 8, making use of the MCU and the R2R Ladder based DAC.

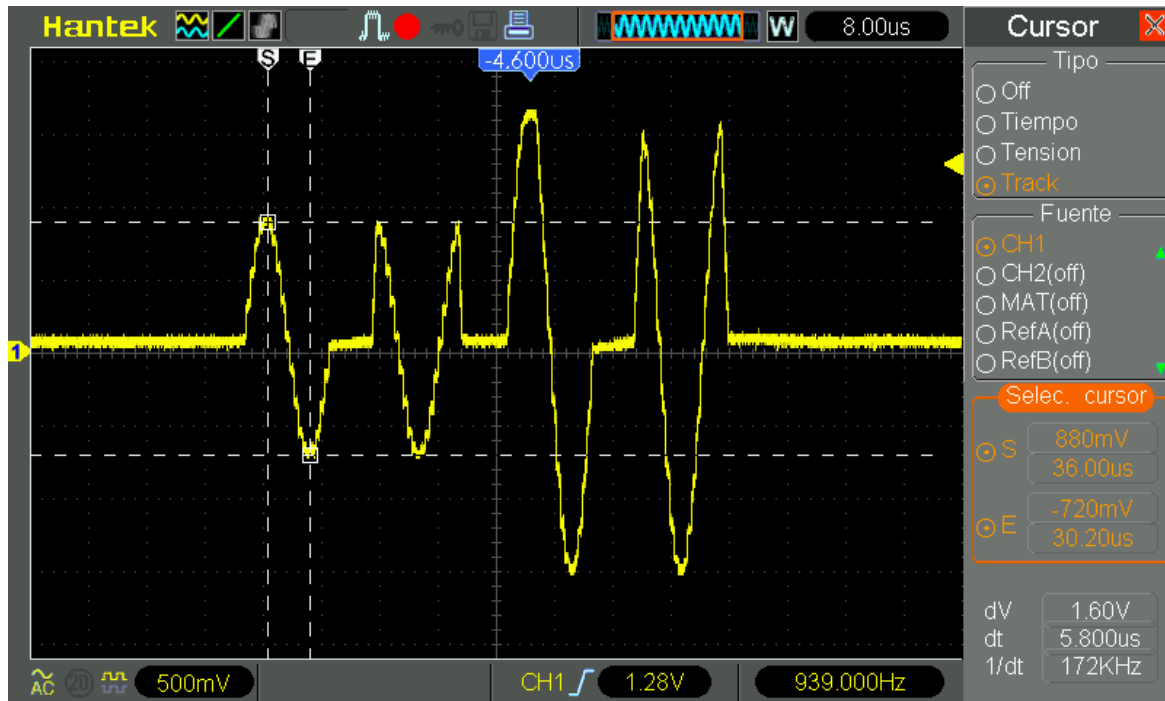


Figure 66. Oscilloscope screenshot measuring R2R ladder based DAC output with the 4 different symbols generated.

To check the integrity of transmitted signal through the LED lamp, we make use of the VLC receiver previously designed for FM Audio over VLC application (Figure 44).

Figure 67 shows both transmitted and received signals.

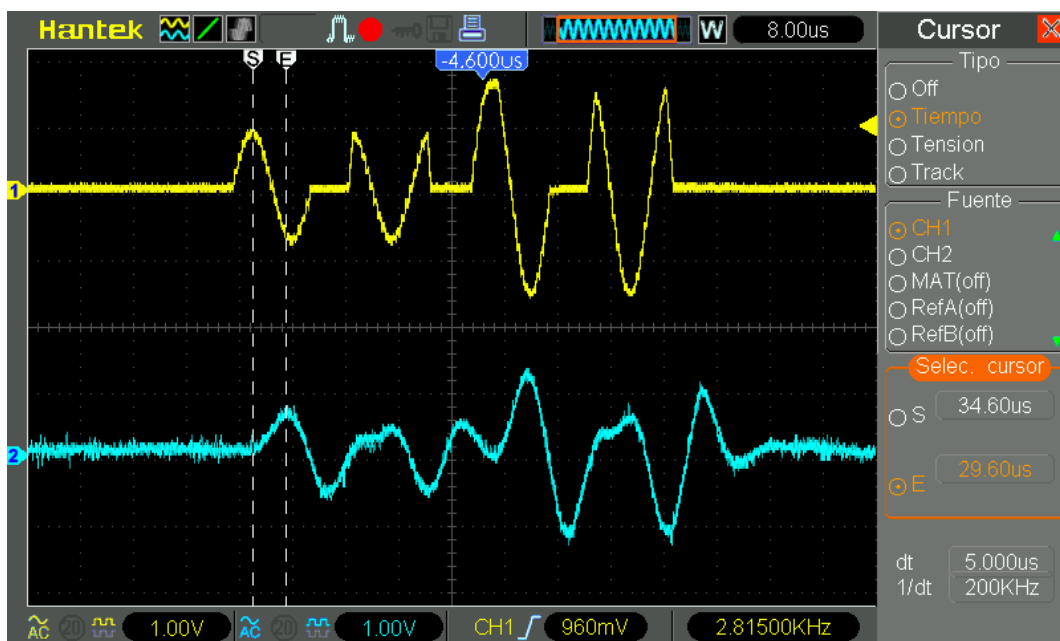


Figure 67. Oscilloscope screenshot with CH1 LED driver control input, CH2 Light receiver output.

We can see in Figure 61 the received signal (CH2) is similar to the transmitted one. Although, the converter cannot follow the abrupt changes in the case of 90° phase symbol due to bandwidth limitations. Figure 68 shows the hardware modulation transmitter implementation.

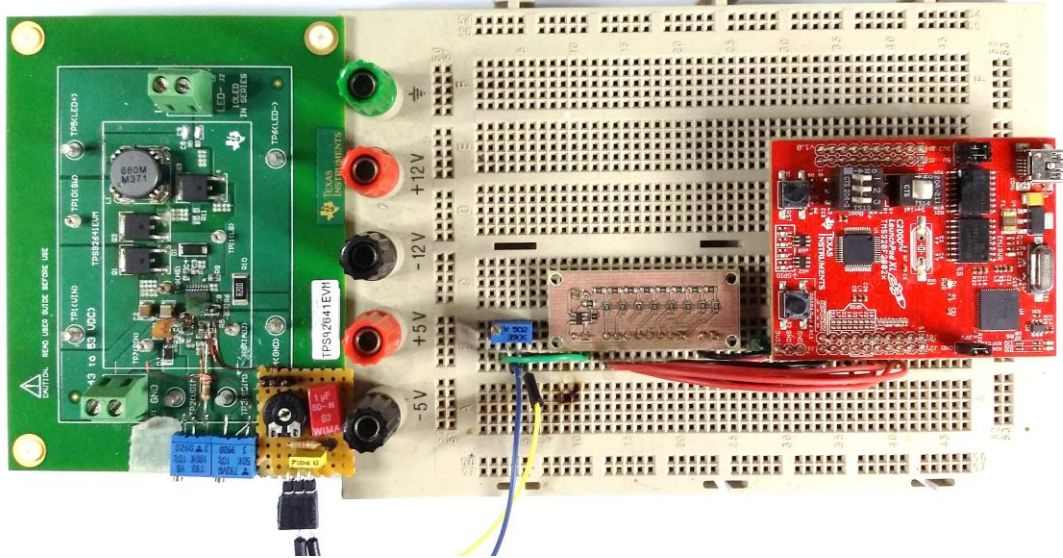


Figure 68. TMS320f28027 transmitter based implementation with R2R ladder and TPS92641 LED driver.

#### 4.4.2. Custom modulation receiver design

On the receiver, we work on time analysis between signal zero-crossing, and setting a threshold for the detection of two possible amplitude levels. In this case, the zero-crossing allows us to both synchronize the receipt of data in respect to the transmitter as well as discretized the phase component. The received signal, goes directly to two comparators inputs, where through a manual adjustment thresholds are set for zero-crossing detection and high level amplitude detection. Figure 69 shows the manual threshold set for zero-crossing detection:

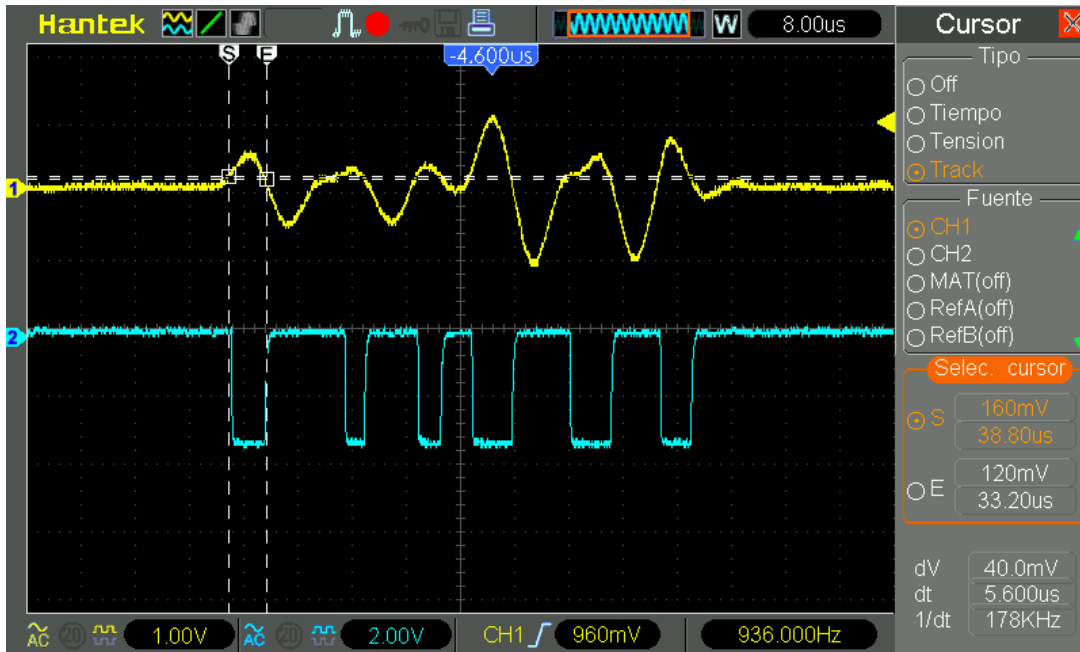


Figure 69. Oscilloscope screenshot, CH1 Received signal, CH2 comparator output, and cursors show the voltage threshold and hysteresis.

As shown in Figure 69, zero crossing threshold setting is set to 120 mV above the average signal value to mitigate false triggers. When performing pulse time analysis, signal above mean value must be equal for all symbols, but distributed in a different way, such in a Pulse Position Modulation. Figure 70 shows comparator threshold setting for the high-level amplitude detection.

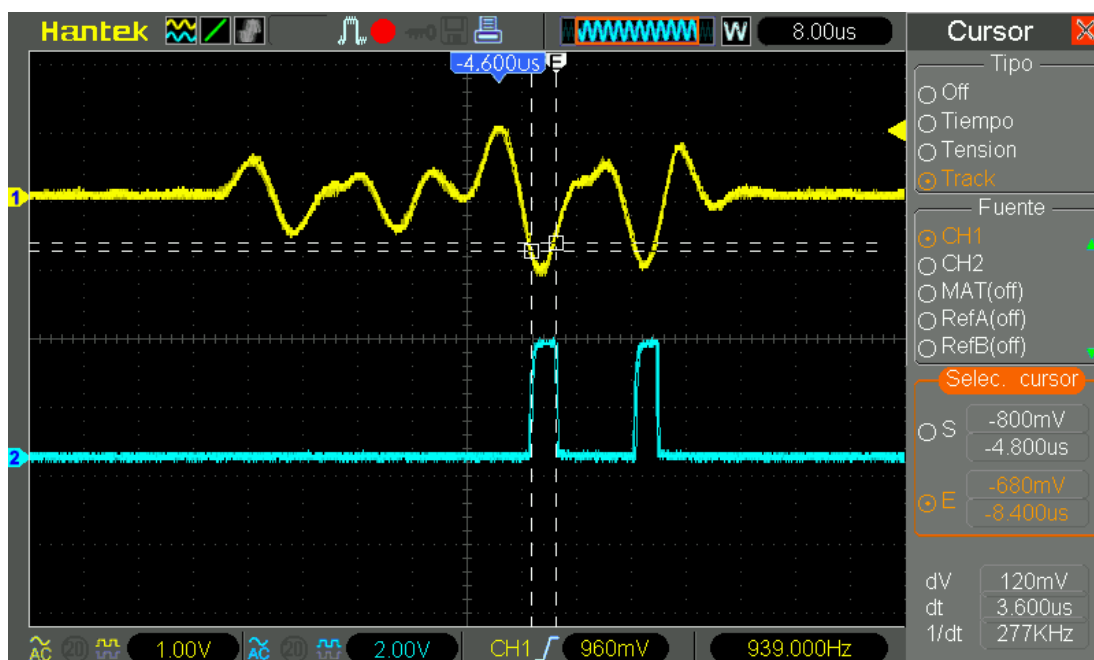


Figure 70. Oscilloscope screenshot, CH1 received signal, CH2 comparator output for amplitude detection, cursor show the threshold configuration.

As shown in Figure 70, for high level amplitude detection, the threshold is established on the negative half-cycle because the difference is clearer. The comparator outputs provide necessary information for different symbols detection, from the duration of generated zero-crossing detection pulses, and the presence or absence of these in the high-level amplitude detection.

The receiver operation follows flow diagram of Figure 71 (see appendix B for source code).

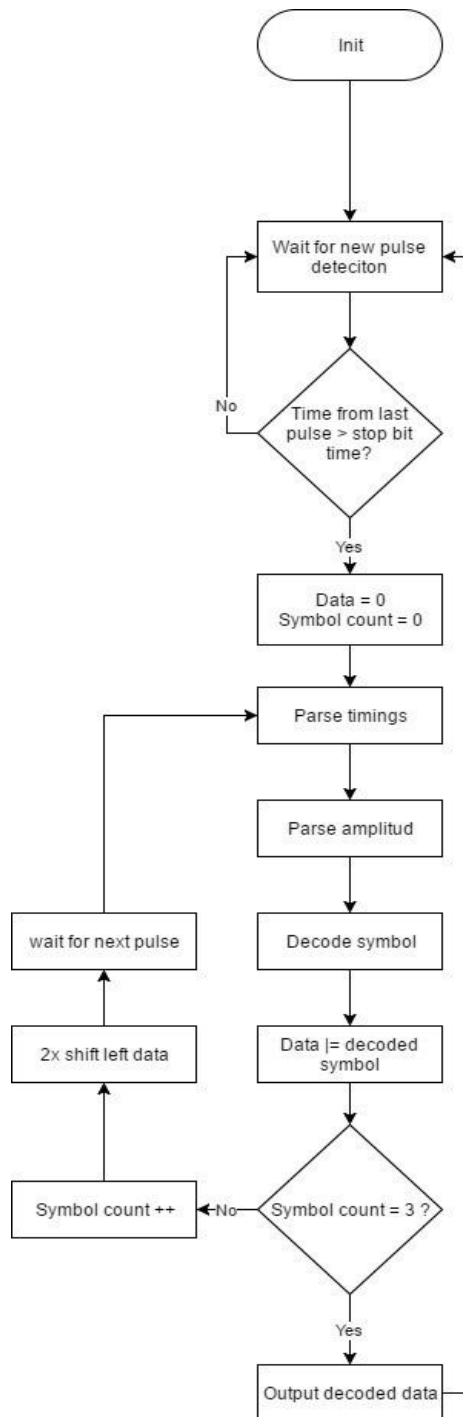


Figure 71. Custom modulation receiver flow diagram

A peripheral inside MCU TMS320f28027 is perfect for our purposes since it enables us to perform pulse duration measurements with 16 ns resolution (appendix C).

To be able to distinguish the different symbols, and since various symbol transitions can generate overlapping pulses, the first symbol is referenced, and once processed its zero-crossing detection pulse after stop time.

The pulses generated by the following symbols are decoded in terms of the previous symbol. Table 9 shows the relation of time in function of the transition between symbols, being  $T_1$  time of half period symbol:

Transition	T value
Silence to Symbol 0 or 2 ( $0^\circ$ )	$T_1$
Silence to Symbol 1 or 3 ( $90^\circ$ )	$T_1/2$
Symbol 0 or 2 ( $0^\circ$ ) to Symbol 0 or 2 ( $0^\circ$ )	$T_1$
Symbol 0 or 2 ( $0^\circ$ ) to Symbol 1 or 3 ( $90^\circ$ )	$T_1/2$
Symbol 1 or 3 ( $90^\circ$ ) to Symbol 0 or 2 ( $0^\circ$ )	$3T_1/2$
Symbol 1 or 3 ( $90^\circ$ ) to Symbol 1 or 3 ( $90^\circ$ )	$T_1$

*Table 9. Possible transitions with associated time values, being  $T_1$  the time equivalent to half period symbol.*

From data shown in Table 9 we can deduce a distance between symbols of  $T_1/2$ , that translated into the numeric value computed in the MCU@60 MHz, establishing  $T_1 = 5.7 \mu\text{s}$ , equals 342 clock cycles, a value that allows setting a decision threshold of 171 units.

Figure 72 shows received signal of one byte transmission, with 0x3C value, between “S” and “E” cursors.

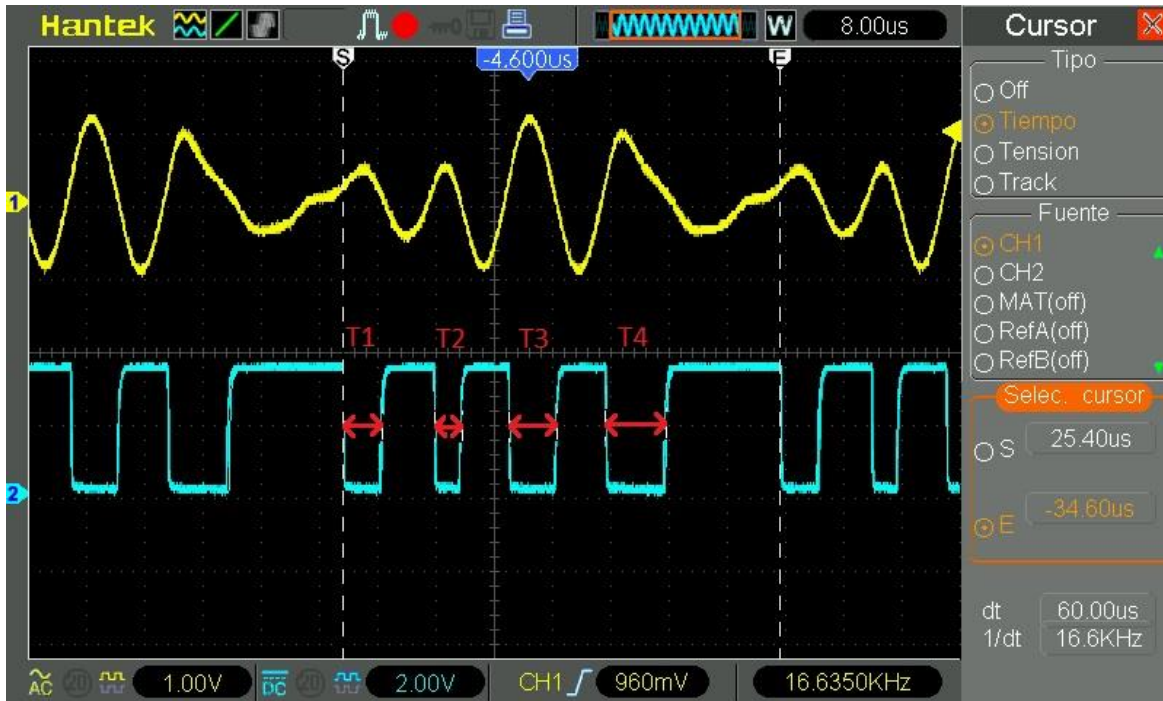


Figure 72. Oscilloscope screenshot CH1 received signal, CH2 zero-crossing detector output. Between “S” and “E” cursors 0x3C byte is transmitted in 60 us. Red markers corresponds to: T1=5.4us, T2=3.4us, T3=6.2us, T4=8.4us

From time measurement between the “S” and “E” cursors, 60 μs, you get 8-bit transmission time. Achieved transfer rate is 133.3 kbps, lower than expected, since some meta-data such as the initial stop bit were initially not considered. Thus, the frequency signal is 87 kHz instead of 100 kHz.

In order to analyse received signal from Figure 72, 0x3C is passed to binary notation, 0b00111100, and the symbol sequence generated by parsing 8-bit data into 2 bits is as follows:

symbol 0 → symbol 3 → symbol 3 → symbol 0

Looking at Figure 72, it is not possible to distinguish visually the fourth symbol in the sequence, but from pulse time analysis it is possible to do it correctly.

For example, we analyse third symbol detection case from Figure 72 with its corresponding pulse time, T3 = 6.2 μs. Given that analysis takes previous symbol as reference, we assume that it is known and is symbol 1.

Based on this information, the decision thresholds from Table 9 allow to decide:

Condition for symbol 0 and 1:

$$T3 > (3T_1/2 - T_1/4) \ \&\& \ T3 < (3T_1/2 + T_1/4)$$

Condition is evaluated with given times from Figure 72:

$$6.2 \ \mu\text{s} > (8.55 \ \mu\text{s} - 1.42 \ \mu\text{s}) \ \&\& \ 6.2 \ \mu\text{s} < (8.55 \ \mu\text{s} + 1.42 \ \mu\text{s}) \ ?$$

$$6.2 \ \mu\text{s} \not> 7.13 \ \mu\text{s} \ \&\& \ 6.2 \ \mu\text{s} < 9.97 \ \mu\text{s}$$

Does not meet symbol 0 and 2 condition.

We confirm that meets condition for symbol 1 and 3.

Symbol 1 and 3 condition:

$$T_3 > (T_1 - T_1/4) \ \&\& \ T_3 < (T_1 + T_1/4)$$

Condition is evaluated with given times from Figure 72:

$$6.2 \ \mu\text{s} > (5.7 \ \mu\text{s} - 1.42 \ \mu\text{s}) \ \text{y} \ 6.2 \ \mu\text{s} < (5.7 \ \mu\text{s} + 1.42 \ \mu\text{s}) \ ?$$

$$6.2 \ \mu\text{s} > 4.28 \ \mu\text{s} \ \&\& \ 6.2 \ \mu\text{s} < 7.12 \ \mu\text{s}$$

Condition for symbol 1 and 3 is met.

The rest of the symbols can be correctly decoded using Figure 72 pulse times values and Table 9 transition times.

Once a symbol is detected in terms of its phase, symbol high level amplitude detection sets the last parameter to finally decode the symbol.

Figure 73 shows the previous 0x3C byte transmission, but in this case with high level amplitude detection signal.

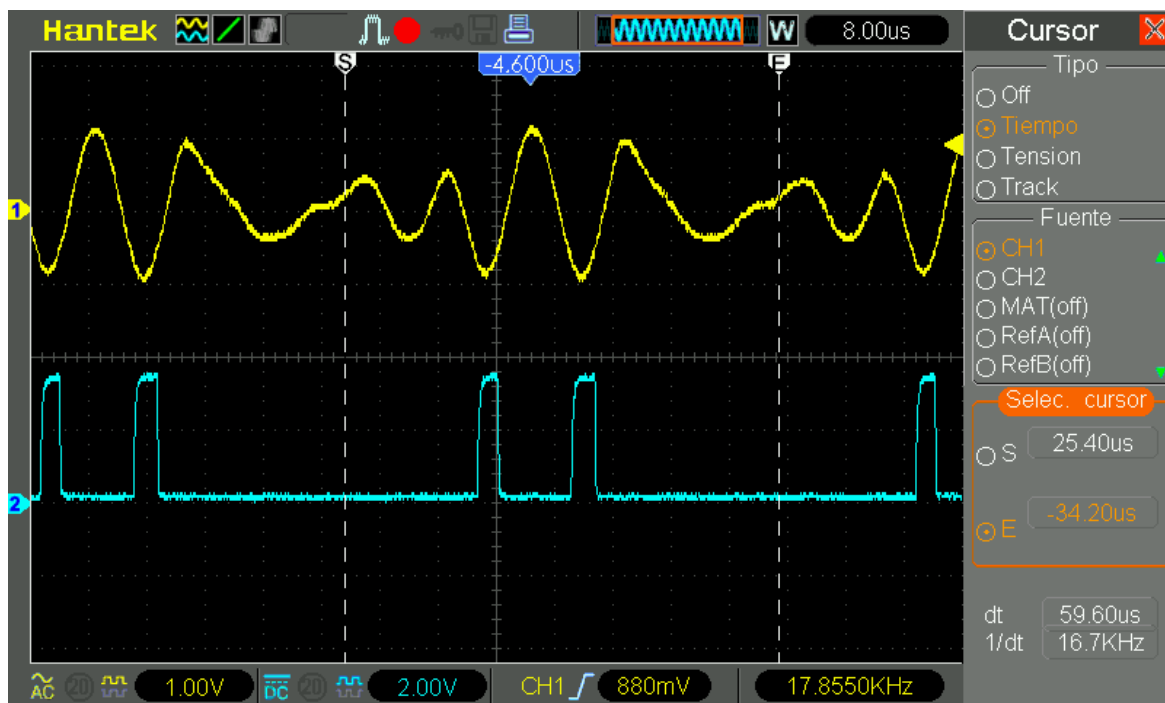
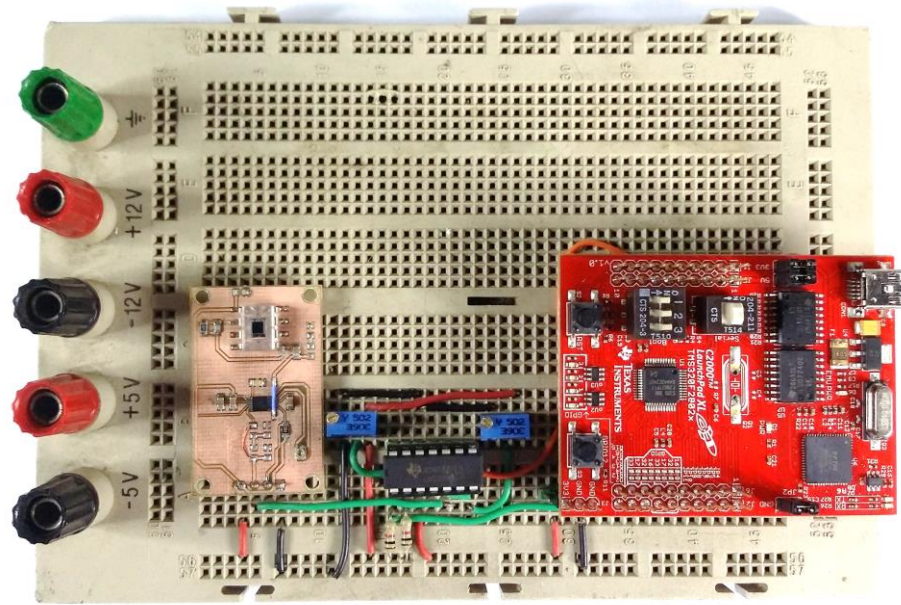


Figure 73. Oscilloscope screenshot, CH1 received signal, CH2 amplitude detector output.

At Figure 73 is seen that only high level amplitude symbols generate a pulse. Figure 74 shows the custom modulation receiver implementation.



*Figure 74. TMS320F28027 receiver based implementation with VLC receiver designed in FM Audio over VLC application*

#### **4.4.3. Conclusions of implemented application**

The implementation in this section demonstrates transmission speeds of 133 kbps without requiring expensive resources. However, the system's immunity from interference or receiver position changes is low, and requires resetting zero-crossing and high level amplitude detection thresholds.

Dedication in this application has been greater respect to the former, since have been worked from scratch with the TMS320F28027 MCU, and the configuration of this to perform the aforementioned operations and also the programming environment is not trivial.

We are currently working in an enhanced version of this system which tries to address these issues in a simple manner.

## 5. Budget

We prepare independent assessment of costs for the development of the VLC LED driver, VLC receiver and the different applications.

For the human resource estimated cost, is supposed a junior engineering hour price of 30 € accounting tax, employer share and indirect costs.

### 5.1. VLC LED driver

Table 10 shows the corresponding VLC LED driver material cost list. Table 11 shows the required tasks as well as their associated time duration and approximate cost estimation. For more detailed information, see Table 1.

Product name	Short description	Unitary Price	Units	Total
TPS92641EVM	LED Driver IC Evaluation Module	46,64 €	1	46,64 €
FQD19N10L	Power MOSFET	0,73 €	2	1,46 €
48 V 100 W PS	LED Power Supply	13,82 €	1	13,82 €
Discrete components	Resistors and capacitors	5,14 €	1	5,14 €
Subtotal				67,06 €
TAX 21%				14,08 €
Total				81,14 €

Table 10. VLC LED driver material cost.

Human resources	Hours
DC-DC converters and VLC technology research	36
VLC compatible LED driver Design	24
VLC compatible LED driver implementation	72
VLC compatible LED driver evaluation	60
Total	192 Hours

Junior engineer approximate cost	5.760 €
----------------------------------	---------

Table 11. VLC LED driver distributed task time and estimated cost.

## 5.2. VLC Receiver

Table 12 shows the corresponding VLC Receiver material cost list. Table 13 shows the required tasks with associated time duration and approximate cost estimation. For more detailed information, see Table 1.

Product name	Short description	Unitary price	Units	Total
OPT101	Photodiode with op-amp	10,33 €	1	10,33 €
MAX9814	Microphone amplifier with AGC	1,39 €	1	1,39 €
Discrete components	Resistors and capacitors	2,58 €	1	2,58 €
Subtotal				14,30 €
TAX 21%				3,00 €
Total				17,30 €

*Table 12. VLC Receiver material cost.*

Human resources	Hours
VLC receiver design	4
VLC receiver implementation	10
VLC receiver evaluation	3
Total	17

Junior engineer approximate cost	510 €
----------------------------------	-------

*Table 13. VLC Receiver distributed task time and estimated cost.*

### 5.3. Baseband Audio VLC application

Table 14 shows the corresponding Baseband Audio VLC application cost, including the designed VLC LED driver as a single unit just considering the material cost. Table 15 shows the required tasks with associated time duration and approximate cost estimation. For more detailed information, see Table 1.

Product name	Short description	Unitary price	Units	Total
VLC LED driver	Compatible VLC LED driver	67,06 €	1	67,06 €
30W-LED-DOWNLIGHT	30 W white LED lamp	39,95 €	1	39,95 €
PAM8403	Audio IC Class-D amplifier	0,91 €	1	0,91 €
SC3726I-8-1	Indoor 3 cm x 2 cm Solar cell	3,17 €	1	3,17 €
AAA battery	1,5 V standard AAA battery	0,72 €	2	1,44 €
Discrete components	Resistors and capacitors	3,42 €	1	3,42 €
Subtotal				115,95 €
TAX 21%				24,35 €
Total				140,30 €

Table 14. Baseband Audio VLC application material cost.

Human resources	Hours
Baseband Audio VLC design	12
Baseband Audio VLC implementation	16
Baseband Audio VLC evaluation	8
Total	36

Junior engineer approximate cost	1.080 €
----------------------------------	---------

Table 15. Baseband Audio VLC application distributed task time and estimated cost.

#### 5.4. FM Audio VLC application

Table 16 shows the corresponding FM Audio VLC application cost, including the designed VLC LED driver and VLC Receiver as a separate single unit considering only the material cost. Table 17 shows the required tasks with associated time duration and approximate cost estimation. For more detailed information, see Table 1.

Product name	Short description	Unitary price	Units	Total
VLC LED Driver	Compatible VLC LED driver	67,06 €	1	67,06 €
30W-LED-DOWNLIGHT	30 W white LED lamp	39,95 €	1	39,95 €
VLC receiver	Compatible VLC receiver	14,30 €	1	14,30 €
CD4046B	PLL integrated circuit	0,46 €	2	0,92 €
5 V Battery	General purpose battery	3,15 €	1	3,15 €
Discrete components	Resistors and capacitors	6,73 €	1	6,73 €
Subtotal				132,11 €
TAX				21% 27,74 €
Total				159,85 €

Table 16. FM Audio VLC application material cost.

Human resources	Hours
FM Audio VLC design	18
FM audio VLC implementation	16
FM Audio evaluation	8
Total	42

Junior engineer approximate cost	1.260 €
----------------------------------	---------

Table 17. FM Audio VLC application distributed task time and estimated cost.

### 5.5. PLC VLC application

Table 18 shows the corresponding PLC VLC application cost, including the designed VLC LED driver and VLC Receiver as a separate single unit considering only the material cost. Table 19 shows the required tasks with associated time duration and approximate cost estimation. For more detailed information, see Table 1.

Product name	Short description	Unitary price	Units	Total
VLC LED Driver	Compatible VLC LED driver	67,06 €	1	67,06 €
30W-LED-DOWNLIGHT	30 W white LED lamp	39,95 €	1	39,95 €
VLC receiver	Compatible VLC receiver	14,30 €	1	14,30 €
MAX79356	PLC based IC	12,56 €	2	25,12 €
FT232	USB to Serial converter	4,58 €	2	9,16 €
Discrete components	Resistors and capacitors	1,76 €	1	1,76 €
Subtotal				157,35 €
TAX				21% 33,04 €
Total				190,39 €

*Table 18. PLC VLC application material cost.*

Human resources	Hours
PLC over VLC design	82
PLC over VLC implementation	24
PLC over VLC evaluation	32
Total	138

Junior engineer approximate cost	4.140 €
----------------------------------	---------

*Table 19. PLC VLC application distributed task time and estimated cost.*

## 5.6. Custom modulation application

Table 20 shows the corresponding Custom Modulation application cost, including the designed VLC LED driver and VLC Receiver as a separate single unit considering only the material cost. Table 21 shows the required tasks with associated time duration and approximate cost estimation. For more detailed information, see Table 1.

Product name	Short description	Unitary price	Units	Total
VLC LED Driver	Compatible VLC LED driver	67,06 €	1	67,06 €
30W-LED-DOWNLIGHT	30 W white LED lamp	39,95 €	1	39,95 €
VLC receiver	Compatible VLC receiver	14,30 €	1	14,30 €
TMS320F28027 Launchpad	Texas Instrument MCU	17 €	2	34 €
TLV2471	Low-Power op amp	2,67 €	1	2,67 €
LM339	General purpose quad comparator	0,68 €	1	0,68 €
Discrete components	Resistors and capacitors	9,32 €	1	9,32 €
Subtotal				167,98 €
TAX 21%				35,28 €
Total				203,26 €

*Table 20. Custom Modulation application material cost.*

Human resources	Hours
Custom modulation design	54
Custom modulation implementation	48
Custom modulation evaluation	30
Total	132

Junior engineer approximate cost	3.960 €
----------------------------------	---------

*Table 21. Custom Modulation application distributed task time and estimated cost.*

**5.7. Summary of total human resource dedication and cost**

<b>Human resouces</b>	<b>Hours</b>
VLC LED driver	192
Baseband Audio over VLC	36
VLC receiver	17
FM Audio over VLC	42
PLC over VLC	138
Custom modulation	132
<b>Total</b>	<b>557</b>

<b>Junior engineer approximate cost</b>	<b>16.710 €</b>
---	-----------------

*Table 22. Total human resource time dedication and estimated cost*

## **6. Conclusions and Future Work**

VLC technology is currently emerging and few commercial options at user-level are available. The absence of commercial products related to this technology gives to understand that it is in a development phase.

This document proposes several proof-of-concept applications requiring low-cost materials which help in having an initial assessment of the VLC technology and its associated benefits and possibilities. This required a considerable amount of laboratory hours for testing and empirically evaluating the performance of different components involved in VLC.

Along the project, special care has been taken with LED driver modifications, given that a minimum fault may cause irreparable damage to the design. It is satisfactory how the project has been successfully finalized with a single LED driver evaluation board.

In general, the obtained results are more than satisfactory. At the personal level, this work allowed to self-evaluate acquired knowledge during previous years and take it to the limit.

As future development, we list next some possibilities:

### **VLC LED driver**

Increase converter control to output signal bandwidth is the main improvement for VLC LED driver.

A future development would be focused on optimizing the dynamic response of the converter by performing faster control topologies or increasing the system's operational frequency.

There is a trade-off increasing system frequency, because that entails a greater power dissipation over switching elements, since it is in state transitions which produces. On the other hand, working with high system frequencies also implies certain restrictions in the LED driver design.

### **Baseband Audio VLC application**

To achieve better sound quality, the use of implemented VLC Receiver already provides improvements respect to the one made in the first instance with the solar cell, although only in the mid-high frequencies reception.

Making use of technics used for turntable audio playback, the RIAA correction [14], should be possible to improve the sound quality of this application by boosting the low frequency audio components. The equalizer curve of the RIAA correction for playback/recording is shown in Figure 75.

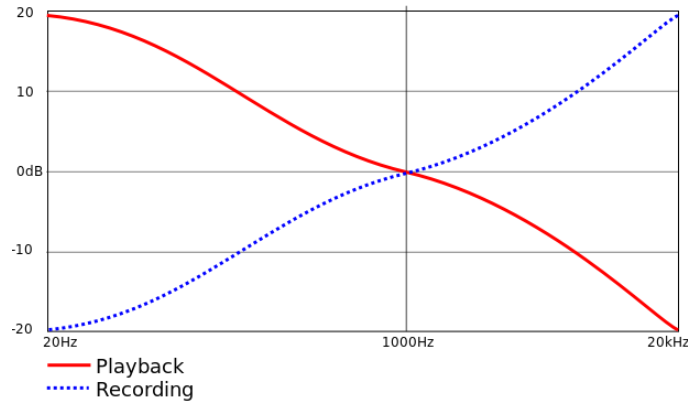


Figure 75 The RIAA equalization curve for playback of vinyl records. The recording curve performs the inverse function, reducing low frequencies and boosting high frequencies [14].

### **VLC Receiver application**

For VLC receiver, achieved bandwidth is 100 kHz, but for high speed communications this number should be greater. The main improvement would be increasing bandwidth and visible light wavelength sensibility.

Both, bandwidth and sensibility, are intrinsic sensor parameters, in this case of the used photodiode. There are available commercial photodiodes that offer better performance than the one used in this project (OPT101). Given that the used photodiode fulfilled with maximum specifications provided by VLC LED driver, a better performance photodiode has not been evaluated in this project.

### **FM Audio application**

The results in relation to the sound quality in this application are satisfactory comparable to any standard music player, not so much in the robustness of the complete system. Future work would intend to work in the received signal filtering to improve this aspect.

Also, even at the cost of reducing sound quality, would be to expand the number of transmitted audio signals, as a generic radio stations transmission system, and take advantage of the whole bandwidth offered by VLC LED driver. This can be implemented using several FM modulators with different carrier frequency forming a single FM signal. At receiver side, a filtering stage should allow to select the proper carrier frequency to demodulate it and obtain its associated audio signal.

### **PLC VLC application**

In this application, maximum transfer rate specified in G3-PLC technology is achieved along with a very good immunity from external interference.

A good improvement for the PLC VLC application would be to elaborate a complete (transmitter / receiver) point to point communication system, from a device connected to the mains and VLC receiver placed near a lamp connected to the same mains. To implement this improvement, would be necessary to implement the typical configuration

shown in Figure 51, for both, transmitter and receiver, and properly configure software device.

### **Custom modulation application**

Plenty of improvements are possible in this application. Existing transmission/reception technics offers excellent performance, such as OFDM, but its implementation is complex. The optimal improvement would be to develop a transmission/reception system based on an existing configuration that offers best performance than the one presented in this application.

## **Bibliography**

- [1] B. Fahs, A. J. Chowdhury and M. M. Hella, "A 12-m 2.5-Gb/s Lighting Compatible Integrated Receiver for OOK Visible Light Communication Links," in *Journal of Lightwave Technology*, vol. 34, no. 16, pp. 3768-3775, Aug.15, 15 2016. doi: 10.1109/JLT.2016.2587598
- [2] Y. Chi, D. Hsieh, C. Tsai, H. Chen, H. Kuo, and G. Lin, "450-nm GaN laser diode enables high-speed visible light communication with 9-Gbps QAM-OFDM," *Opt. Express* 23, 13051-13059 (2015).
- [3] Light-emitting diode. (2017, May 8). In *Wikipedia, The Free Encyclopedia*. Retrieved May 14, 2017, from [https://en.wikipedia.org/w/index.php?title=Light-emitting\\_diode&oldid=779331550](https://en.wikipedia.org/w/index.php?title=Light-emitting_diode&oldid=779331550)
- [4] Wavelength of Visible Light Spectrum. (2016, August 6). In *Buzzle*. Retrieved MAY 14, 2017, from <http://www.buzzle.com/articles/wavelength-of-visible-light-spectrum.html>
- [5] Java Science "LED Frequency Response" [Online] Available: <http://www.iensign.com/Discovery/LEDFrequencyResponse/> [Accessed: 16 April 2017].
- [6] Y. Pei, S. Zhu, H. Yang, L. Zhao, X. Yi, J. Junxi Wang and J. Li, "LED Modulation Characteristics in a Visible-Light Communication System," *Optics and Photonics Journal*, Vol. 3 No. 2B, 2013, pp. 139-142. doi: 10.4236/opj.2013.32B034.
- [7] F. Che, L. Wu, B. Hussain, X. Li and C. P. Yue, "A Fully Integrated IEEE 802.15.7 Visible Light Communication Transmitter With On-Chip 8-W 85% Efficiency Boost LED Driver," in *Journal of Lightwave Technology*, vol. 34, no. 10, pp. 2419-2430, May15, 15. doi: 10.1109/JLT.2016.2535319
- [8] Y. Zhou, J. Zhao, M. Zhang, J. Shi and N. Chi, "2.32 Gbit/s phosphorescent white LED visible light communication aided by two-staged linear software equalizer," *2016 10th International Symposium on Communication Systems, Networks and Digital Signal Processing (CSNDSP)*, Prague, 2016, pp. 1-4. doi: 10.1109/CSNDSP.2016.7573913
- [9] Z. Yu, A. J. Redfern and G. T. Zhou, "Using delta-sigma modulators in visible light OFDM systems," *2014 23rd Wireless and Optical Communication Conference (WOCC)*, Newark, NJ, 2014, pp. 1-5. doi: 10.1109/WOCC.2014.6839942
- [10] Tech Web "Switching Regulator Basics" [Online] Available: <http://micro.rohm.com/en/techweb/knowledge/dcdc/s-dcdc/02-s-dcdc/97> [Accessed: 14 May 2017].
- [11] STEVAL-ILL066V1 Data brief "100 W LED street lighting evaluation board using STLUX385A" [Online] Available: [http://www.st.com/content/ccc/resource/technical/document/data\\_brief/9e/6c/4f/ff/ee/18/4f/24/DM00113865.pdf/files/DM00113865.pdf/jcr:content/translations/en.DM00113865.pdf](http://www.st.com/content/ccc/resource/technical/document/data_brief/9e/6c/4f/ff/ee/18/4f/24/DM00113865.pdf/files/DM00113865.pdf/jcr:content/translations/en.DM00113865.pdf) [Accessed 14 May 2017].
- [12] TPS92641EVM User's Guide [Online] <http://www.ti.com/lit/ug/slvu823/slvu823.pdf> [Accessed: 14 May 2017].
- [13] Twin-T Notch Filter Design Tool [Online] <http://sim.okawa-denshi.jp/en/TwinTCRkeisan.htm> [Accessed 14 May 2017].
- [14] RIAA equalization. (2017, April 5). In *Wikipedia, The Free Encyclopedia*. Retrieved 16:34, May 10, 2017, from [https://en.wikipedia.org/w/index.php?title=RIAA\\_equalization&oldid=773898256](https://en.wikipedia.org/w/index.php?title=RIAA_equalization&oldid=773898256)
- [15] TI E2E Community, "Improving TPS92641 analog dimming AC response" [Online] [http://e2e.ti.com/support/power\\_management/led\\_driver/f/192/p/557104/2040452#2040452](http://e2e.ti.com/support/power_management/led_driver/f/192/p/557104/2040452#2040452) [Accessed 14 May 2017]



## Appendices

### A. Custom modulation transmitter source code

```
//#####  
//  
// File:   VLC_transmitter.c  
//  
// Title:  VLC custom modulation transmitter.  
//  
//!  
//!   This application adapt the serial data received through SCI module  
//!   to be transmitted over VLC  
//!  
//  
//#####  
  
//  
// Included Files  
//  
#include "DSP28x_Project.h"    // Device Headerfile  
  
#include "common/include/clk.h"  
#include "common/include/flash.h"  
#include "common/include/gpio.h"  
#include "common/include/pie.h"  
#include "common/include/pll.h"  
#include "common/include/wdog.h"  
#include "common/include/sci.h"  
  
//global variables  
  
//40 samples of single sine period with phase 0 an 90  
  
const uint8_t sine_0[2][40]={  
{0x80,0x93,0xa7,0xb9,0xca,0xda,0xe7,0xf1,0xf9,0xfd,0xff,0xfd,0xf9,0xf1,0xe7,0xd  
a,0xca,0xb9,0xa7,  
0x93,0x80,0x6c,0x58,0x46,0x35,0x25,0x18,0xe,0x6,0x2,0x0,0x2,0x6,0xe,0x18,0x25,0  
x35,0x46,0x58,0x6c},  
  
{0x81,0x8b,0x94,0x9e,0xa6,0xae,0xb5,0xba,0xbe,0xc0,0xc1,0xc0,0xbe,0xba,0xb5,0xa  
e,0xa6,0x9e,0x94,0x8b,  
0x81,0x76,0x6d,0x63,0x5b,0x53,0x4c,0x47,0x43,0x41,0x40,0x41,0x43,0x47,0x4c,0x53  
,0x5b,0x63,0x6d,0x76}};  
  
const uint8_t sine_90[2][40]={  
{0xff,0xfd,0xf9,0xf1,0xe7,0xda,0xca,0xb9,0xa7,0x93,0x80,0x6c,0x58,0x46,0x35,0x2  
5,0x18,0xe,0x6,0x2,0x0,  
0x2,0x6,0xe,0x18,0x25,0x35,0x46,0x58,0x6c,0x80,0x93,0xa7,0xb9,0xca,0xda,0xe7,0x  
f1,0xf9,0xfd},  
  
{0xc1,0xc0,0xbe,0xba,0xb5,0xae,0xa6,0x9e,0x94,0x8b,0x81,0x76,0x6d,0x63,0x5b,0x5  
3,0x4c,0x47,0x43,0x41,  
0x40,0x41,0x43,0x47,0x4c,0x53,0x5b,0x63,0x6d,0x76,0x81,0x8b,0x94,0x9e,0xa6,0xae  
,0xb5,0xba,0xbe,0xc0}};
```

```

//
// Function Prototypes
//
void delay_loop(void);
void Gpio_config(void);
void Sine_Gen(uint8_t, uint8_t);
void Send_Byte(uint8_t);
void scia_echoback_init(void);
void scia_fifo_init(void);
void scia_xmit(int a);
void scia_msg(char *msg);

#pragma CODE_SECTION(Send_Byte, "ramfuncs");
#pragma CODE_SECTION(Sine_Gen, "ramfuncs");

CLK_Handle myClk;
FLASH_Handle myFlash;
GPIO_Handle myGpio;
PIE_Handle myPie;
SCI_Handle mySci;

//
// Main
//
void main(void)
{
    uint16_t ReceivedChar;
    char *msg;

    CPU_Handle myCpu;
    PLL_Handle myPll;
    WDOG_Handle myWDog;

    //
    // Initialize all the handles needed for this application
    //
    myClk = CLK_init((void *)CLK_BASE_ADDR, sizeof(CLK_Obj));
    myCpu = CPU_init((void *)NULL, sizeof(CPU_Obj));
    myFlash = FLASH_init((void *)FLASH_BASE_ADDR, sizeof(FLASH_Obj));
    myGpio = GPIO_init((void *)GPIO_BASE_ADDR, sizeof(GPIO_Obj));
    myPie = PIE_init((void *)PIE_BASE_ADDR, sizeof(PIE_Obj));
    myPll = PLL_init((void *)PLL_BASE_ADDR, sizeof(PLL_Obj));
    mySci = SCI_init((void *)SCIA_BASE_ADDR, sizeof(SCI_Obj));
    myWDog = WDOG_init((void *)WDOG_BASE_ADDR, sizeof(WDOG_Obj));

    //
    // Perform basic system initialization
    //
    WDOG_disable(myWDog);
    CLK_enableAdcClock(myClk);
    (*Device_cal)();

    //
    // Select the internal oscillator 1 as the clock source
    //
    CLK_setOscSrc(myClk, CLK_OscSrc_Internal);

    //

```

```

// Setup the PLL for x10 /2 which will yield 50Mhz = 10Mhz * 10 / 2
//
PLL_setup(myPll, PLL_Multiplier_12, PLL_DivideSelect_ClkIn_by_2);

//
// Disable the PIE and all interrupts
//
PIE_disable(myPie);
PIE_disableAllInts(myPie);
CPU_disableGlobalInts(myCpu);
CPU_clearIntFlags(myCpu);

//
// If running from flash copy RAM only functions to RAM
//
#ifdef _FLASH
memcpy(&RamfuncsRunStart, &RamfuncsLoadStart, (size_t)&RamfuncsLoadSize);
FLASH_setup(myFlash);
#endif

//
// For this application use the following gpio configuration:
//
Gpio_config();

//
// Setup a debug vector table and enable the PIE
//
PIE_setDebugIntVectorTable(myPie);
PIE_enable(myPie);

scia_echoback_init();           // Initialize SCI for echoback
scia_fifo_init();             // Initialize the SCI FIFO

msg = "\r\n\n\nHello World!\0";
scia_msg(msg);

msg = "\r\nYou will enter a character, and the DSP will echo it \
      back! \n\0";
scia_msg(msg);

//
// Application loop
//
for(;;)
{
    msg = "\r\nEnter a character: \0";
    scia_msg(msg);

    //
    // Wait for inc character
    //
    while(SCI_getRxFifoStatus(mySci) < SCI_FifoStatus_1_Word)
    {
        if (GPIO_getData(myGpio, GPIO_Number_12)==1)
        {

```

```

    }
}

//
// Get character
//
ReceivedChar = SCI_getData(mySci);
//
//Send character throug VLC
//
Send_Byte(ReceivedChar);
//
// Echo character back
//
msg = " You sent: \0";
scia_msg(msg);
scia_xmit(ReceivedChar);

}

}

//
// Send byte: Encodes 2 bit data in a single symbol and
//             generates output signal.
//
void
Send_Byte(uint8_t data)
{
    uint8_t i=0;

    for(i=0;i<4;i++){
        switch ( data&0x03 ){
            case 0:
                Sine_Gen(1,0);
                break;
            case 1:
                Sine_Gen(1,1);
                break;
            case 2:
                Sine_Gen(0,0);
                break;
            case 3:
                Sine_Gen(0,1);
                break;
        }
        data=data>>2;
    }

    ((GPIO_Obj *)myGpio)->GPADAT = 0x000000FF & 0x40;
    DELAY_US(2);
    ((GPIO_Obj *)myGpio)->GPADAT = 0x000000FF & 0x80;
}

```

```

    DELAY_US(3);
}

//
// Sine_Gen: Generates the proper GPIO signals in order to obtain a
//           sine wave signal, with 2 phase and amplitude possibilities.
//           phase = 0 corresponds to 0°
//           phase = 1 corresponds to 90°
//           amp = 0 corresponds to high amplitude
//           amp = 1 corresponds to low amplitude
//
void
Sine_Gen(uint8_t amp, uint8_t phase)
{
    uint8_t i=0;

    switch (phase){
        case 0 :
            for(i=0;i<40;i++)
            {
                ((GPIO_Obj *)myGpio)->GPADAT = 0x000000FF & sine_0[amp][i];
                i++;
            }
            break;

        case 1 :
            for(i=0;i<40;i++)
            {
                ((GPIO_Obj *)myGpio)->GPADAT = 0x000000FF & sine_90[amp][i];
                i++;
            }
            break;

    }

}

//
// Gpio_config -
//
void
Gpio_config(void)
{
    // set the gpios used for DAC as output
    EALLOW;
    ((GPIO_Obj *)myGpio)->GPAMUX1 = 0x00000000;
    ((GPIO_Obj *)myGpio)->GPAMUX2 = 0x00000000;
    ((GPIO_Obj *)myGpio)->GPBMUX1 = 0x00000000;
    ((GPIO_Obj *)myGpio)->GPADIR = 0x000000FF;
    ((GPIO_Obj *)myGpio)->GPBDIR = 0x0000000F;
    EDIS;

    //GPIO config for PushButton
    GPIO_setPullUp(myGpio, GPIO_Number_12, GPIO_PuLLUp_Disable);
    GPIO_setMode(myGpio, GPIO_Number_12, GPIO_12_Mode_GeneralPurpose);
    GPIO_setDirection(myGpio,GPIO_Number_12,GPIO_Direction_Input);
    GPIO_setPullUp(myGpio, GPIO_Number_28, GPIO_PuLLUp_Enable);
    GPIO_setPullUp(myGpio, GPIO_Number_29, GPIO_PuLLUp_Disable);
}

```

```

//GPIO config for SCI module
GPIO_setQualification(myGpio, GPIO_Number_28, GPIO_Qual_ASync);
GPIO_setMode(myGpio, GPIO_Number_28, GPIO_28_Mode_SCIRXDA);
GPIO_setMode(myGpio, GPIO_Number_29, GPIO_29_Mode_SCITXDA);
}

//
// scia_echoback_init - Test 1, SCIA DLB, 8-bit word, baud rate 0x000F,
// default, 1 STOP bit, no parity
//
void
scia_echoback_init()
{
    CLK_enableSciaClock(myClk);

    //
    // 1 stop bit, No loopback, No parity, 8 char bits, async mode,
    // idle-line protocol
    //
    SCI_disableParity(mySci);
    SCI_setNumStopBits(mySci, SCI_NumStopBits_One);
    SCI_setCharLength(mySci, SCI_CharLength_8_Bits);

    SCI_enableTx(mySci);
    SCI_enableRx(mySci);
    SCI_enableTxInt(mySci);
    SCI_enableRxInt(mySci);

    //SCI BRR = LSPCLK/(SCI BAUDx8) - 1
#ifdef CPU_FRQ_60MHZ
    SCI_setBaudRate(mySci, (SCI_BaudRate_e)15);
#elif CPU_FRQ_50MHZ
    SCI_setBaudRate(mySci, (SCI_BaudRate_e)162);
#elif CPU_FRQ_40MHZ
    SCI_setBaudRate(mySci, (SCI_BaudRate_e)129);
#endif

    SCI_enable(mySci);

    return;
}

//
// scia_xmit - Transmit a character from the SCI
//
void
scia_xmit(int a)
{
    while(SCI_getTxFifoStatus(mySci) != SCI_FifoStatus_Empty)
    {

    }

    SCI_putDataBlocking(mySci, a);
}

//

```

```

// scia_msg -
//
void
scia_msg(char * msg)
{
    int i;
    i = 0;
    while(msg[i] != '\0')
    {
        scia_xmit(msg[i]);
        i++;
    }
}

//
// scia_fifo_init - Initialize the SCI FIFO
//
void
scia_fifo_init()
{
    SCI_enableFifoEnh(mySci);
    SCI_resetTxFifo(mySci);
    SCI_clearTxFifoInt(mySci);
    SCI_resetChannels(mySci);
    SCI_setTxFifoIntLevel(mySci, SCI_FifoLevel_Empty);

    SCI_resetRxFifo(mySci);
    SCI_clearRxFifoInt(mySci);
    SCI_setRxFifoIntLevel(mySci, SCI_FifoLevel_4_Words);

    return;
}

//
// End of File
//

```

## B. Custom modulation receiver source code

```

//#####
//
// File:   VLC_receiver.c
//
// Title:  VLC receiver.
//
//!
//! This application enables VLC reception and received data is shown through
//! SCI module.
//!
//! eCAP1 is configured to capture the time between rising
//! and falling edge.
//
//#####

```

```

//
// Included Files
//
#include "DSP28x_Project.h" // Device Headerfile and Examples Include File

#include "common/include/clk.h"
#include "common/include/adc.h"
#include "common/include/flash.h"
#include "common/include/gpio.h"
#include "common/include/pie.h"
#include "common/include/pll.h"
#include "common/include/pwm.h"
#include "common/include/cap.h"
#include "common/include/sci.h"
#include "common/include/comp.h"
#include "common/include/wdog.h"
//
// Function Prototypes
//
__interrupt void ecap1_isr(void);
void InitECapture(void);
uint8_t DecodeSymbol(uint8_t, uint8_t, uint16_t);
void SetSymbolTiming(uint32_t *);
void scia_echoback_init(void);
void scia_fifo_init(void);
void scia_xmit(int a);
void scia_msg(char *msg);
void Adc_Config(void);
void Fail(void);
//
// Globals
//
uint32_t ECap1IntCount;
uint32_t ECap1PassCount;
uint32_t EPwm3TimerDirection;
uint16_t DacRef;

uint8_t frame_init;
uint8_t new_symbol;
uint32_t count_buff;

uint8_t tTrue=1;

volatile struct SymbolTimings
{
    uint32_t Tran_0_To_0;
    uint32_t Tran_0_To_90;
    uint32_t Tran_90_To_0;
    uint32_t Tran_90_To_90;

    uint32_t Error_Offset;
    uint32_t Stop_Bit_Time;
};

CAP_Handle myCap;
ADC_Handle myAdc;

```

```

CLK_Handle myClk;
FLASH_Handle myFlash;
GPIO_Handle myGpio;
PIE_Handle myPie;
SCI_Handle mySci;

//
// Main
//
void main(void)
{
    CPU_Handle myCpu;
    PLL_Handle myPll;
    WDOG_Handle myWDog;

    //
    // Initialize all the handles needed for this application
    //
    myCap = CAP_init((void *)CAPA_BASE_ADDR, sizeof(CAP_Obj));
    myAdc = ADC_init((void *)ADC_BASE_ADDR, sizeof(ADC_Obj));
    myClk = CLK_init((void *)CLK_BASE_ADDR, sizeof(CLK_Obj));
    myCpu = CPU_init((void *)NULL, sizeof(CPU_Obj));
    myFlash = FLASH_init((void *)FLASH_BASE_ADDR, sizeof(FLASH_Obj));
    myGpio = GPIO_init((void *)GPIO_BASE_ADDR, sizeof(GPIO_Obj));
    myPie = PIE_init((void *)PIE_BASE_ADDR, sizeof(PIE_Obj));
    myPll = PLL_init((void *)PLL_BASE_ADDR, sizeof(PLL_Obj));
    mySci = SCI_init((void *)SCIA_BASE_ADDR, sizeof(SCI_Obj));
    myWDog = WDOG_init((void *)WDOG_BASE_ADDR, sizeof(WDOG_Obj));

    //
    // Perform basic system initialization
    //
    WDOG_disable(myWDog);
    CLK_enableAdcClock(myClk);
    (*Device_cal)();
    //CLK_disableAdcClock(myClk);

    //
    // Select the internal oscillator 1 as the clock source
    //
    CLK_setOscSrc(myClk, CLK_OscSrc_Internal);

    //
    // Setup the PLL for x12 /2 which will yield 60Mhz = 10Mhz * 12 / 2
    //
    PLL_setup(myPll, PLL_Multiplier_12, PLL_DivideSelect_ClkIn_by_2);

    //
    // Disable the PIE and all interrupts
    //
    PIE_disable(myPie);
    PIE_disableAllInts(myPie);
    CPU_disableGlobalInts(myCpu);
    CPU_clearIntFlags(myCpu);

    //

```

```

// If running from flash copy RAM only functions to RAM
//
#ifdef _FLASH
memcpy(&RamfuncsRunStart, &RamfuncsLoadStart, (size_t)&RamfuncsLoadSize);
//FLASH_setup(myFlash);
#endif

//
// Initialize GPIO
//
//Led0
GPIO_setPullUp(myGpio, GPIO_Number_0, GPIO_PuLLUp_Enable);
GPIO_setMode(myGpio, GPIO_Number_0, GPIO_0_Mode_GeneralPurpose);
GPIO_setDirection(myGpio,GPIO_Number_0,GPIO_Direction_Output);
//Led1
GPIO_setPullUp(myGpio, GPIO_Number_1, GPIO_PuLLUp_Enable);
GPIO_setMode(myGpio, GPIO_Number_1, GPIO_1_Mode_GeneralPurpose);
GPIO_setDirection(myGpio,GPIO_Number_1,GPIO_Direction_Output);
//Led2
GPIO_setPullUp(myGpio, GPIO_Number_2, GPIO_PuLLUp_Enable);
GPIO_setMode(myGpio, GPIO_Number_2, GPIO_2_Mode_GeneralPurpose);
GPIO_setDirection(myGpio,GPIO_Number_2,GPIO_Direction_Output);
//Led3
GPIO_setPullUp(myGpio, GPIO_Number_3, GPIO_PuLLUp_Enable);
GPIO_setMode(myGpio, GPIO_Number_3, GPIO_3_Mode_GeneralPurpose);
GPIO_setDirection(myGpio,GPIO_Number_3,GPIO_Direction_Output);

//PushButton
GPIO_setPullUp(myGpio, GPIO_Number_12, GPIO_PuLLUp_Disable);
GPIO_setMode(myGpio, GPIO_Number_12, GPIO_12_Mode_GeneralPurpose);
GPIO_setDirection(myGpio,GPIO_Number_12,GPIO_Direction_Input);
//eCAP
GPIO_setPullUp(myGpio, GPIO_Number_5, GPIO_PuLLUp_Enable);
GPIO_setQualification(myGpio, GPIO_Number_5, GPIO_Qual_Sync);
GPIO_setMode(myGpio, GPIO_Number_5, GPIO_5_Mode_ECAP1);
//SCI
GPIO_setPullUp(myGpio, GPIO_Number_28, GPIO_PuLLUp_Enable);
GPIO_setPullUp(myGpio, GPIO_Number_29, GPIO_PuLLUp_Disable);
GPIO_setQualification(myGpio, GPIO_Number_28, GPIO_Qual_ASync);
GPIO_setMode(myGpio, GPIO_Number_28, GPIO_28_Mode_SCIRXDA);
GPIO_setMode(myGpio, GPIO_Number_29, GPIO_29_Mode_SCITXDA);

//
// Setup a debug vector table and enable the PIE
//
PIE_setDebugIntVectorTable(myPie);
PIE_enable(myPie);

//
// Register interrupt handlers in the PIE vector table
//
PIE_registerPieIntHandler(myPie, PIE_GroupNumber_4, PIE_SubGroupNumber_1,
(intVec_t)&ecap1_isr);

//
// Setup peripherals used in this application
//

```

```

InitECapture();
scia_echoback_init();           // Initialize SCI for echoback
scia_fifo_init();              // Initialize the SCI FIFO
Adc_Config();

//
// Initialize global vars
//
frame_init=0;
new_symbol=0;

//
//create local vars
//
uint8_t timing_cal_mode;
uint8_t prev_symbol;
uint8_t symbol;
uint8_t sym_pos_offset;
uint32_t timings[8];
uint8_t t;
uint8_t decoded_data;
uint32_t debug_timings[8];
uint8_t debug_symbols[8];
uint16_t voltage=0;
uint16_t voltage 1=0;
uint16_t fvoltage=0;
uint16_t fvoltage 1=0;
uint16_t delta_volt[8];
uint8_t in_frame;
char *msg;
//
//initialize local vars
//
timing_cal_mode=1;
prev_symbol=0;
symbol=0;
sym_pos_offset=0;
t=0;
in_frame=0;

uint8_t i;

for (i=0;i<8;i++)
{
    timings[i]=0;
    debug_symbols[i]=0;
    debug_timings[i]=0;
    delta_volt[i]=0;
}

//
// Enable CPU INT4 which is connected to ECAP1-4 INT
//
CPU_enableInt(myCpu, CPU_IntNumber_4);

//
// Enable eCAP INTn in the PIE: Group 3 interrupt 1-6
//

```

```

PIE_enableCaptureInt(myPie);

//
// Enable global Interrupts and higher priority real-time debug events
//
CPU_enableGlobalInts(myCpu);
CPU_enableDebugInt(myCpu);

msg = "\r\n\nHello World!\0";
scia_msg(msg);

msg = "\r\nVLC Receiver Test \n\0";
scia_msg(msg);
//check for pushbutton to enter calibration mode
if (GPIO_getData(myGpio, GPIO_Number_12)==0)
{
    timing_cal_mode=1;
}

//   Phase | t
//   -----
//   0      | 1
//   0      | 2
//   90     | 3
//   90     | 4
//   0      | 5

if(timing_cal_mode==1)
{
    while(frame_init!=tTrue)
    {
        __asm("        NOP");
    }
    frame_init=0;
    while(frame_init!=tTrue)
    {
        __asm("        NOP");
    }
    frame_init=0;
    for (i=0;i<5;i++)
    {
        while(new_symbol!=tTrue);
        timings[i]=CAP_getCap2(myCap);
        new_symbol=0;
    }

    SetSymbolTiming(timings);
}

msg = "\r\nCalibration done! \n\0";
scia_msg(msg);

for(;;)
{
    if (new_symbol==tTrue)        //Is there a new symbol available?

```

```

    {
        if(frame_init==tTrue) // if there is a new symbol, is the first
symbol of the frame?
        {
            prev_symbol=0xFF; //set the previos symbol to a known value
for setup correct timings
            sym_pos_offset=0; //reset the cursor position to the first 2
bits

            decoded_data=0;
            frame_init=0; //clear the frame_init flag
            t=0;
            new_symbol=0;
            in_frame=1;

            while(ADC_getIntStatus(myAdc, ADC_IntNumber_1)==0);

            fvoltage = ADC_readResult(myAdc, ADC_ResultNumber_1);
            //
            // Clear ADCINT1 flag reinitialize for next SOC
            //
            ADC_clearIntFlag(myAdc, ADC_IntNumber_1);
        }
        else if (in_frame==1)
        {
            while(ADC_getIntStatus(myAdc, ADC_IntNumber_1)==0);

            voltage = ADC_readResult(myAdc, ADC_ResultNumber_1);
            //
            // Clear ADCINT1 flag reinitialize for next SOC
            //
            ADC_clearIntFlag(myAdc, ADC_IntNumber_1);

            symbol=DecodeSymbol(prev_symbol,CAP_getCap2(myCap), voltage);
            prev_symbol=symbol;
            //set debug variables
            debug_timings[t]=CAP_getCap2(myCap);
            debug_symbols[t]=symbol;
            delta_volt[t]=voltage;
            t++;
            if (symbol==0xFF)
            {
                i++;
            }

            if(sym_pos_offset<6) //Is not the last symbol to complete a
byte?
            {
                decoded_data|=symbol<<(sym_pos_offset); //Make insertion
to the data byte
                sym_pos_offset=sym_pos_offset+2; //update
the new cursor position
            }
            else //affirmation, is the last symbol to complete a byte
            {
                decoded_data|=symbol<<(sym_pos_offset); //make insertion
of the last 2 bits
            }
        }
    }

```

```

        scia_xmit(decoded_data);          //send via SCI decoded
data.
        // reset transmission variables
        sym_pos_offset=0;
        t=0;
        in_frame=0;
    }

    new_symbol=0; //clear the new_symbol flag
}

}
}

//
// InitECapture -
//
void
InitECapture()
{
    CLK_enableEcap1Clock(myClk);

    CAP_disableInt(myCap, CAP_Int_Type_All); // Disable all capture interrupts
    CAP_clearInt(myCap, CAP_Int_Type_All); // Clear all CAP interrupt flags
    CAP_disableCaptureLoad(myCap); // Disable CAP1-CAP4 register loads
    CAP_disableTimestampCounter(myCap); // Make sure the counter is stopped

    //
    // Configure peripheral registers
    //
    CAP_setCapOneShot(myCap); // One-shot
    CAP_setStopWrap(myCap, CAP_Stop_Wrap_CEVT2); // Stop at 2 events

    //
    // Rising edge
    //
    CAP_setCapEvtPolarity(myCap, CAP_Event_1, CAP_Polarity_Falling);

    //
    // Falling edge
    //
    CAP_setCapEvtPolarity(myCap, CAP_Event_2, CAP_Polarity_Rising);

    //
    // Difference operation
    //
    CAP_setCapEvtReset(myCap, CAP_Event_1, CAP_Reset_Enable);

    //
    // Difference operation
    //
    CAP_setCapEvtReset(myCap, CAP_Event_2, CAP_Reset_Enable);

    CAP_enableSyncIn(myCap); // Enable sync in
    CAP_setSyncOut(myCap, CAP_SyncOut_SyncIn); // Pass through
}

```

```

CAP_enableCaptureLoad(myCap);

CAP_enableTimestampCounter(myCap);    // Start Counter
CAP_rearm(myCap);                     // arm one-shot
CAP_enableCaptureLoad(myCap);        // Enable CAP1-CAP4 register loads

//
// 2 events = interrupt
//
CAP_enableInt(myCap, CAP_Int_Type_C EVT2);
}

void
SetSymbolTiming(uint32_t t_value[])
{
    symbol_timings.Tran_0_To_0 = t_value[1];
    symbol_timings.Tran_0_To_90 = t_value[2];
    symbol_timings.Tran_90_To_0 = t_value[4];
    symbol_timings.Tran_90_To_90 = t_value[3];

    symbol_timings.Error_Offset = (symbol_timings.Tran_0_To_0 -
symbol_timings.Tran_0_To_90) / 2 ;
    symbol_timings.Stop_Bit_Time = symbol_timings.Tran_0_To_0 +
symbol_timings.Tran_0_To_0;
}

uint8_t
DecodeSymbol(uint8_t prev_symbol, uint8_t timing, uint16_t volt)
{
    uint8_t symbol_buff=0xFF;

    if (prev_symbol==0xFF)
    {
        if (    timing > (symbol_timings.Tran_0_To_0 -
symbol_timings.Error_Offset) &&
            timing < (symbol_timings.Tran_0_To_0 +
symbol_timings.Error_Offset)) symbol_buff=0x00;
        else if (timing > (symbol_timings.Tran_0_To_90 -
symbol_timings.Error_Offset) &&
            timing < (symbol_timings.Tran_0_To_90 +
symbol_timings.Error_Offset)) symbol_buff=0x01;
    }
    else if(prev_symbol==0x00 || prev_symbol==0x02)
    {
        if (    timing > (symbol_timings.Tran_0_To_0 -
symbol_timings.Error_Offset) &&
            timing < (symbol_timings.Tran_0_To_0 +
symbol_timings.Error_Offset)) symbol_buff=0x00;
        else if (timing > (symbol_timings.Tran_0_To_90 -
symbol_timings.Error_Offset) &&
            timing < (symbol_timings.Tran_0_To_90 +
symbol_timings.Error_Offset)) symbol_buff=0x01;
    }
    else if (prev_symbol==0x01 || prev_symbol==0x03)
    {
        if (    timing > (symbol_timings.Tran_90_To_0 -
symbol_timings.Error_Offset) &&

```

```

        timing < (symbol_timings.Tran_90_To_0 +
symbol_timings.Error_Offset)) symbol_buff=0x00;
        else if (timing > (symbol_timings.Tran_90_To_90 -
symbol_timings.Error_Offset) &&
        timing < (symbol_timings.Tran_90_To_90 +
symbol_timings.Error_Offset)) symbol_buff=0x01;
    }

    if (volt>500) symbol_buff=symbol_buff+2;
    return symbol_buff;
}

//
// scia_echoback_init - Test 1, SCIA DLB, 8-bit word, baud rate 0x000F,
// default, 1 STOP bit, no parity
//
void
scia_echoback_init()
{
    CLK_enableSciaClock(myClk);

    //
    // 1 stop bit, No loopback, No parity, 8 char bits, async mode,
    // idle-line protocol
    //
    SCI_disableParity(mySci);
    SCI_setNumStopBits(mySci, SCI_NumStopBits_One);
    SCI_setCharLength(mySci, SCI_CharLength_8_Bits);

    SCI_enableTx(mySci);
    SCI_enableRx(mySci);
    SCI_enableTxInt(mySci);
    SCI_enableRxInt(mySci);

    //SCI BRR = LSPCLK/(SCI BAUDx8) - 1
#if (CPU_FRQ_60MHZ)
    SCI_setBaudRate(mySci, (SCI_BaudRate_e)194);
#elif (CPU_FRQ_50MHZ)
    SCI_setBaudRate(mySci, (SCI_BaudRate_e)162);
#elif (CPU_FRQ_40MHZ)
    SCI_setBaudRate(mySci, (SCI_BaudRate_e)129);
#endif

    SCI_enable(mySci);

    return;
}

//
// scia_xmit - Transmit a character from the SCI
//
void
scia_xmit(int a)
{
    while(SCI_getTxFifoStatus(mySci) != SCI_FifoStatus_Empty)
    {
    }
}

```

```

        SCI_putDataBlocking(mySci, a);
    }

    //
    // scia_msg -
    //
    void
    scia_msg(char * msg)
    {
        int i;
        i = 0;
        while(msg[i] != '\0')
        {
            scia_xmit(msg[i]);
            i++;
        }
    }

    //
    // scia_fifo_init - Initialize the SCI FIFO
    //
    void
    scia_fifo_init()
    {
        SCI_enableFifoEnh(mySci);
        SCI_resetTxFifo(mySci);
        SCI_clearTxFifoInt(mySci);
        SCI_resetChannels(mySci);
        SCI_setTxFifoIntLevel(mySci, SCI_FifoLevel_Empty);

        SCI_resetRxFifo(mySci);
        SCI_clearRxFifoInt(mySci);
        SCI_setRxFifoIntLevel(mySci, SCI_FifoLevel_4_Words);

        return;
    }
    void
    Adc_Config()
    {
        //
        // Initialize the ADC
        //
        ADC_enableBandGap(myAdc);
        ADC_enableRefBuffers(myAdc);
        ADC_powerUp(myAdc);
        ADC_enable(myAdc);
        ADC_setVoltRefSrc(myAdc, ADC_VoltageRefSrc_Int);

        //
        // Enable ADCINT1 in PIE
        //
        PIE_enableAdcInt(myPie, ADC_IntNumber_1);

        //
        // ADCINT1 trips after AdcResults latch
        //
        ADC_setIntPulseGenMode(myAdc, ADC_IntPulseGenMode_Prior);
    }

```

```

ADC_enableInt(myAdc, ADC_IntNumber_1);           // Enabled ADCINT1

//
// Disable ADCINT1 Continuous mode
//
ADC_setIntMode(myAdc, ADC_IntNumber_1, ADC_IntMode_ClearFlag);

//
// setup EOC2 to trigger ADCINT1 to fire
//
ADC_setIntSrc(myAdc, ADC_IntNumber_1, ADC_IntSrc_EOC1);

//
// set SOC0 channel select to ADCINA4
//
ADC_setSocChanNumber (myAdc, ADC_SocNumber_1, ADC_SocChanNumber_A2);

//
// set SOC0 S/H Window to 14 ADC Clock Cycles, (13 ACQPS plus 1)
//
ADC_setSocSampleWindow(myAdc, ADC_SocNumber_1,
                       ADC_SocSampleWindow_64_cycles);

ADC_setSocTrigSrc(myAdc, ADC_SocNumber_1, ADC_SocTrigSrc_Sw);
}

//
// ecap1_isr -
//
__interrupt void
ecap1_isr(void)
{

//Clear interrupts for let CEVT1 reset de timestamptimer
CAP_clearInt(myCap, CAP_Int_Type_CEVT2);
CAP_clearInt(myCap, CAP_Int_Type_Global);

//
// Acknowledge this interrupt to receive more interrupts from group 4
//
PIE_clearInt(myPie, PIE_GroupNumber_4);

//
// get capture regisers values
//
count_buff=CAP_getCap2(myCap);
uint32_t stop_time = CAP_getCap1(myCap);

//
// compare capture 1 register, which contains
// high level signal time, with stop time
//
if(stop_time > symbol_timings.Stop_Bit_Time &&
   count_buff > (400) &&
   frame_init==0)
{

```

```

        frame_init=1;

    }
    // set new symbol flag
    new_symbol=1;
    ADC_forceConversion(myAdc, ADC_SocNumber_1);

    CAP_rearm(myCap);
}

//
// End of File
//

```

### C. TMS320F28027 eCAP module

The enhanced capture (eCAP) module is used in systems where accurate timing of external events is important.

The so-called eCAP module features the following characteristics:

- Dedicated input capture pin.
- 32-bit time base (counter).
- 4 x 32-bit time-stamp capture registers (CAP1-CAP4).
- 4-stage sequencer (Modulo4 counter) that is synchronized to external events, ECAP pin rising/falling edges.
- Independent edge polarity (rising/falling edge) selection for all 4 events.
- Input capture signal prescaling (from 2-62)
- One-shot compare register (2 bits) to freeze captures after 1 to 4 time-stamp events.
- Control for continuous time-stamp captures using a 4-deep circular buffer (CAP1-CAP4) scheme.
- Interrupt capabilities on any of the 4 capture events.

Figure 76 shows used configuration operation for capture zero-crossing detection pulses in the receiver, called “Time difference (delta) operation Rising and falling edge trigger”.

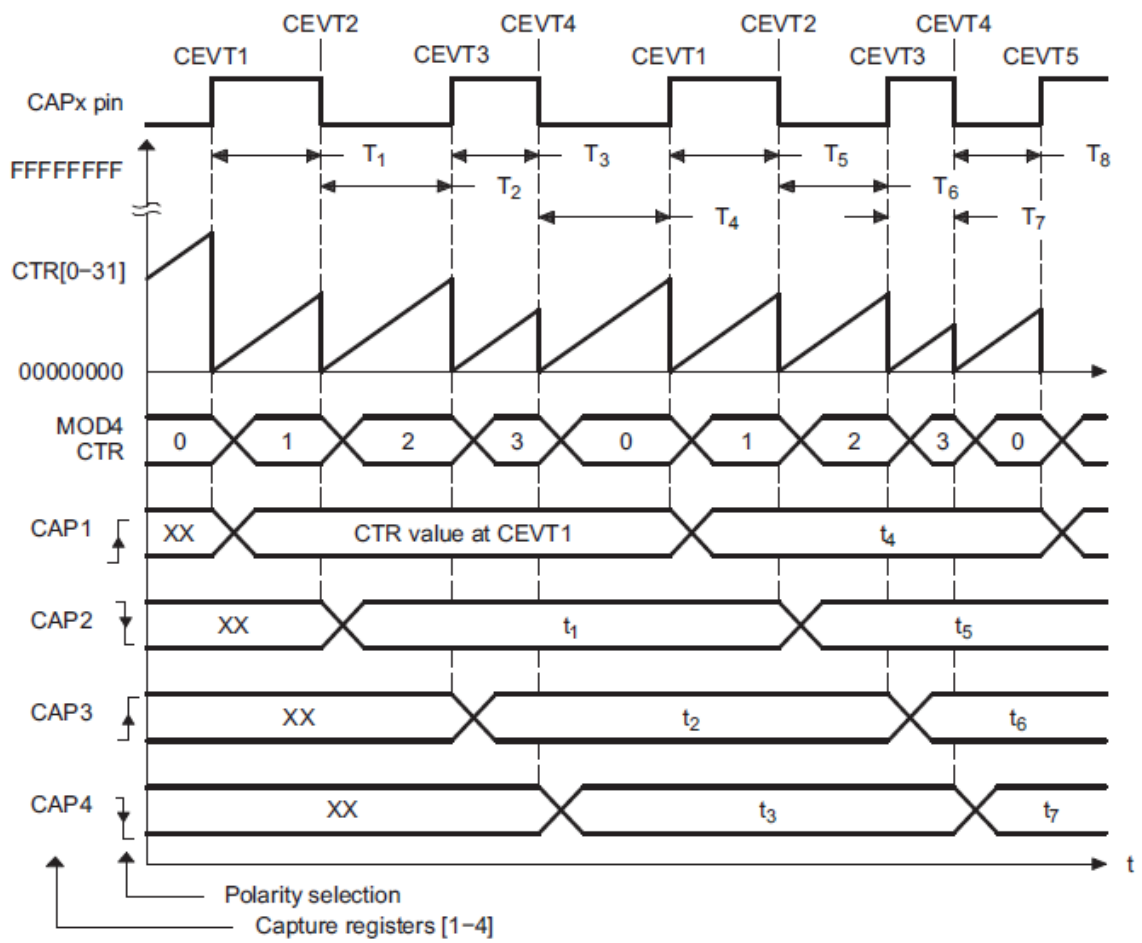


Figure 76 Capture sequence for Delta Mode Time-Stamp With Rising and Falling Edge Detect.

## **Glossary**

**AC** Alternating Current

**ACK** Acknowledgement Packet

**AGC** Automatic Gain Control

**BPSK** Binary Phase Shift Keying

**CPU** Central Processing Unit

**CRC** Cyclic Redundancy Check

**CSMA** Carrier Sense Multiple Access

**DAC** Digital to Analog Converter

**DC** Direct Current

**ESR** Equivalent Series Resistance

**EVM** Evaluation Module

**FEC** Forward Error Correction

**FER** Frame Error Rate

**FFT** Fast Fourier Transform

**FM** Frequency Modulation

**FPGA** Field Programmable Gate Array

**FSK** Frequency Shift Keying

**FW** Firmware

**GPIO** General Purpose Input Output

**GUI** Graphical User Interface

**IC** Integrated Circuit

**LED** Light Emitting Diode

**MAC** Media Access Control

**MCU** Micro Controller Unit

**MOSFET** Metal Oxide Substrate Field Effect Transistor

**NACK** Negative Acknowledgement Packet

**NFET** Negative channel Field Effect Transistor

**OFDM** Orthogonal Frequency-Division Multiplexing

**OOK** On-Off Keying

**PHY** Physical layer

**PLC** Power Line Communication

**PLL** Phase Locked-Loop

**PWM** Pulse Width Modulation

**QAM** Quadrature Amplitude Modulation

**QPSK** Quadrature Phase Shift Keying

**RGB** Red Green Blue

**RISC** Reduced Instruction Set Computer

**SMD** Surface Mount Device

**SoC** System On Chip

**UART** Universal Asynchronous Receiver-Transmitter

**VCO** Voltage Controlled Oscillator

**VGA** Variable Gain Amplifier

**VLC** Visible Light Communication